T.C.
YEDİTEPE UNIVERSITY
INSTITUTE OF HEALTH SCIENCES
DEPARTMENT OF HISTOLOGY AND EMBRYOLOGY

THE EFFECT OF SELENIUM ON THE MORPHOLOGICAL CHANGES IN THE HIPPOCAMPUS AND CEREBRAL CORTEX OF SCOPOLAMINE INDUCED ALZHEIMER'S TYPE DEMENTIA RAT MODEL BY HISTOLOGICAL ANALYSIS

MASTER OF HISTOLOGY AND EMBRYOLOGY

DİLARA BABAN

Istanbul-2021

T.C.
YEDİTEPE UNIVERSITY
INSTITUTE OF HEALTH SCIENCES
DEPARTMENT OF HISTOLOGY AND EMBRYOLOGY

THE EFFECT OF SELENIUM ON THE MORPHOLOGICAL CHANGES IN THE HIPPOCAMPUS AND CEREBRAL CORTEX OF SCOPOLAMINE INDUCED ALZHEIMER'S TYPE DEMENTIA RAT MODEL BY HISTOLOGICAL ANALYSIS

MASTER OF HISTOLOGY AND EMBRYOLOGY

DİLARA BABAN

SUPERVISOR

Assist.Prof.Dr. Alev CUMBUL

Istanbul-2021

THESIS APPROVAL FORM

Institute : Yeditepe University Institute of Health Sciences
Programme : Histology and Embryology
Title of the Thesis : The Effect of Selenium on The Morphological Changes in The Hippocampus and Cerebral Cortex of Scopolamine Induced Alzheimer's Type Dementia Rat Model by Histological Analysis.
Owner of the Thesis : Dilara Baban
Examination Date : 23.08.2021

This study have approved as a Master Thesis in regard to content and quality by the Jury.

	Title, Name-Surname (Institution)
Chair of the Jury:	Assoc.Prof.Aylin Yaba Uçar Yeditepe University Histology and Embryology
Supervisor:	Asst.Prof.Alev Cumbul Yeditepe University Histology and Embryology
Member/Examiner:	Prof.Dr.Süheyla Gonca Kocaeli University Histology and Embryology

APPROVAL
This thesis has been deemed by the jury in accordance with the relevant articles of Yeditepe University Graduate Education and Examinations Regulation and has been approved by Administrative Board of Institute with decision dated ..... and numbered .....

Prof. Dr. Bayram YILMAZ
Director of Institute of Health Sciences

DECLARATION

I hereby declare that this thesis is my work and that, to the best of my knowledge and belief, it contains no material previously published or written by another person nor material which has been accepted for the award of any other degree except where due acknowledgment has been made in the text.

Dilara BABAN
07.09.2021

DEDICATION

This thesis is dedicated to my family; my mother, grandmother, and my beloved father…

ACKNOWLEDGEMENTS

First, I would like to thank my dedicated supervisor Assist. Prof. Dr.Alev Cumbul with all the effort she made and attention paid to this thesis work has been such devotion to me. She has been sincerely giving her support and always there whenever I needed her. For the most part, it is a great honor to be her master's student and I am willing to take our scientific relationship forward.

Moreover, I would like to give my gratitude and thanks to Assoc. Prof. Dr. Aylin Yaba Uçar for her support and everything that she taught me all the time during my education in Histology and Embryology master's.

I am thankful to Prof. Dr. Ece Genç as she helped with locomotor activity tests in the pharmacology department.

I would like to thank Prof Dr. Bayram Yılmaz from physiology department to his consulting for my thesis whenever I need.

Moreover, I have appreciated all the YUDETAM staff for all their help in handling and surviving animals.

Finally, I would like to thank my family, my fiancée Yiğitcan Şengül and my best friend, Deniz Öykü Özen for their love and support.

TABLE OF CONTENTS

LIST OF TABLES

LIST OF FIGURES

LIST OF SYMBOLS AND ABBREVIATIONS

AD	Alzheimer's Disease
Aβ	β-Amyloid Peptide
ACh	Acetylcholine
APOE	Apolipoprotein E
APP	Amyloid Precursor Protein
BACE-1	Beta-site Amyloid Precursor Protein Cleaving Enzyme1
BBB	Blood-Brain Barrier
CA	Cornu Ammonis
Cdk5	Cyclin-Dependent Kinase5
CNS	Central Nervous System
GSK-3	Glycogen Synthase Kinase3
GPx	Glutathione Peroxidase
HNE	Hydroxynonenal
IL	Interleukin
iNOS	Inducible nitric oxide synthase
LPS	Lipopolysaccharide
α2M	α2- Macroglobulins
MAPK	Mitogen-Activated Protein Kinase
MBD	Microtubule Binding Domain
MDA	Malondialdehyde
NFTs	Neurofibrillary Tangles
NOS	Nitric Oxide Synthase
OKA	Okadaic Acid
PBS	Phosphate Buffered Saline

PSEN1	Presinilin1
PSEN2	Presinilin2
RNS	Reactive Nitrogen Species
ROS	Reactive Oxygen Species
SELENOP	Selenoprotein P
STZ	Streptozotocin
TdT	Terminal Deoxynucleotidyl Transferase Enzyme
TLRs	Toll-like Receptors
TNF	Tumor Necrosis Factor
VEGF	Vascular Endothelial Growth Factor

ABSTRACT

Baban, D. (2021). The Effect of Selenium on The Morphological Changes in The Hippocampus and Cerebral Cortex of Scopolamine Induced Alzheimer's Type Dementia Rat Model by Histological Analysis. Yeditepe University, Institute of Health Science, Department of Histology and Embryology MSc Thesis, İstanbul.

Alzheimer's Disease (AD) is one of the neurodegenerative diseases with significant memory loss and it is very common worldwide. Amyloid plaques and neurofibrillary tangles which are important hallmarks of the disease result in progressive neuronal loss in hippocampus and cerebral cortex regions in the brain. In recent years, various studies demonstrates that selenium is one of the important compounds that can be promising effects on AD pathology. Selenium affiliates the active sites of catalytic enzymes which are responsible for the protection of cells from oxidative damage. In this study, the effect of selenium on the hippocampus and cerebral cortex was evaluated in scopolamine-induced Alzheimer's rat model to examine morphological changes. It is hypothesis that selenium has a protective effect in this model.It was observed that the scopolamine substance caused a loss of locomotor movement like Alzheimer's, and it was understood that the selenium substance caused a slight improvement in these movements. Hematoxylin, eosin, cresyl violet and silver staining were used to observe pathological findings, and as expected, less pathological findings were observed in the selenium treatment group compared to the scopolamine group. H-Scores were calculated in iNOS, Amyloid-Beta immunohistochemistry staining, and there are significant differences between the results of the scopolamine and control groups ($p<0.05$, $p<0.05$).Amyloid-Beta immunohistochemistry staining showed intense amyloid plaque formation in the scopolamine group and rare amyloid plaque formation in the test group, but no statistical differences ($p>0.05$) were observed between the groups whose H-Scores were calculated because of VEGF immunohistochemistry staining. Finally, the apoptotic index was calculated with the TUNEL experiment, highest values were obtained in the scopolamine group, second highest in the test group, lowest in the control and selenium groups($p<0.05$). As a result, as anticipated in this study, selenium caused an improvement in Alzheimer's model pathology simulated by scopolamine according to antioxidant role of selenium.

Key words: Alzheimer's Disease, Selenium, Scopolamine, Histology, Amyloid plaques

ÖZET

Baban, D. (2021). Selenyumun Scopolaminle Oluşturulan Alzheimer Tipi Demans Sıçan Modelinde Hipokampüs ve Serebral Korteksdeki Morfolojik Değişiklikler Üzerine Etkisinin Histolojik Olarak İncelenmesi. Yeditepe Üniversitesi Sağlık Bilimleri Enstitüsü, Histoloji ve Embriyoloji ABD, Master Tezi. İstanbul.

Alzheimer hastalığı dünya çapında en çok görülen ciddi bir hafıza kaybına neden olan nörodejeneratif hastalıklardan biridir. Beyindeki hipokampüs ve serebral korteks bölgelerinde amiloid plak ve nörofibrillar düğüm oluşumları devamlı bir nöron kaybına yol açar. Son yıllarda birçok çalışmada selenyum maddesinin Alzheimer hastalığının patolojisine karşı umut verici etkileri olabileceği öne sürülmektedir. Selenyum, görevi hücreleri oksidatif hasardan korumak olan katalitik enzimlerin aktif bölgelerine bağlanır. Bu çalışmada ise skopolaminle indüklenen Alzheimer sıçan modelinde selenyumun hipokampüs ve serebral korteksteki morfolojik değişiklikleri histolojik analizler ile incelemeyi amaçladık ve hipotezimiz selenyumun bu modelde koruyucu etkisi olucağıdır. Lokomotor aktivite testi ile scopolamine maddesinin Alzheimer benzeri bir lokomotor hareket kaybına neden olduğu sonucu gözlemlenmiş olup, selenyum maddesinin ise bu hareketlerde az da olsa iyileşmeye sebep olduğu anlaşılmıştır. Hematoksilen eosin,cresyl violet ve silver boyamaları patolojik bulguları gözlemlemek için kullanılmış olup, beklendiği şekilde selenyum tedavi grubunda scopolamine Alzheimer modeli grubuna göre daha az patolojik bulgu gözlemlenmiştir. iNOS Amyloid-Beta immunohistokimya boyamasında H-score hesaplanmış olup, scopolamine ve kontrol grubu sonuçları arasında belirgin bir farklılık vardır. Amyloid-Beta immunohistokimya boyaması ile ise scopolamine grubunda yoğun, test grubunda ise seyrek amyloid plak oluşumu bulgulanmıştır ($p<0.05$, $p<0.05$). ancak VEGF immunohistokimya boyaması sonucunda hesaplana H-score ile gruplar arasında anlamlı bir farklılık gözlemlenmemiştir ($p>0.05$). Son olarak TUNEL deneyi ile apoptotic indeks hesaplanmış ve scopolamine grubunda en yüksek, test grubunda daha az ve kontrol ve selenyum grubunda en az değerler elde edilmiştir ($p<0.05$). Sonuç olarak, bu çalışmada beklendiği gibi selenium antioksidant rolü ile, skopolamin maddesinin oluşturduğu Alzheimer modeli patolojisinde iyileşmeye neden olmuştur.

Anahtar Kelimeler: Alzheimer Hastalığı, Selenyum, Skopolamin, Histoloji, Amiloid plak

1. INTRODUCTION AND PURPOSE

Alzheimer's Disease (AD) is one of the most common neurodegenerative diseases. It starts with a short-term memory loss and ends up with total cognition loss due to the death of neurons and glial cells especially in the hippocampus and cerebral cortex. (1) Neuronal death occurs owing to some pathological changes in the brain such as amyloid plaques formation, (2) tau hyperphosphorylation. (3) These pathological changes enhance mitochondrial damage, resulting in oxidative stress and neuroinflammation. (4) The pathology of disease progressed by the release of proinflammatory cytokines from microglia, stimulating neurons (5). Likewise, proinflammatory cytokines, reactive oxygen species, and chemokines support cell deaths to initiate AD. (6) While microglia's mediators of inflammation play protective roles in acute activation of astrocytes and neurons, chronic activation of microglia (7) lead to neurotoxic effect to cause neuronal death notably the cholinergic ones (8).

Scopolamine compound creates Alzheimer-like pathology; therefore, it is one of the common neurotoxins to model AD. (9) Scopolamine-induced AD models accomplish blockage of muscarinic receptors of cholinergic neurons with the occurrence of memory and cognitive loss (10). Selenium is one of the substances that is studied to prevent inflammation in AD (11).

Selenium is a trace element that has the antioxidant potential which our body needs. (12) It is found in the active sides of catalyst enzymes which their action on the protection of cells from oxidative damage, so this association is resulting in the prevention of cognitive loss (13). Meanwhile, selenium exists in the structure of selenoproteins which maintain the balance between free radical production and antioxidant action (14). Research demonstrates that selenoproteins are colocalized with neurofibrillary tangles and amyloid plaques in AD(14). Because of that information, it is suggested selenium can prevent amyloid plaque formation and hyperphosphorylation of tau protein (14).

In this study, it is hypothesized that selenium can decrease the pathological effects in neurons at the scopolamine-induced AD rat model. This study aims to investigate the effect of selenium for morphological changes in the hippocampus and cerebral cortex neurons in the scopolamine-induced Alzheimer's Disease model.

2. LITERATURE REVIEW

2.1. Central Nervous System

Central Nervous System (CNS) contains the brain and spinal cord and is made up of about 100 billion neurons and supporting cells called glial cells. The brain can be divided anatomically into three parts; cerebrum, cerebellum, brainstem.(15)

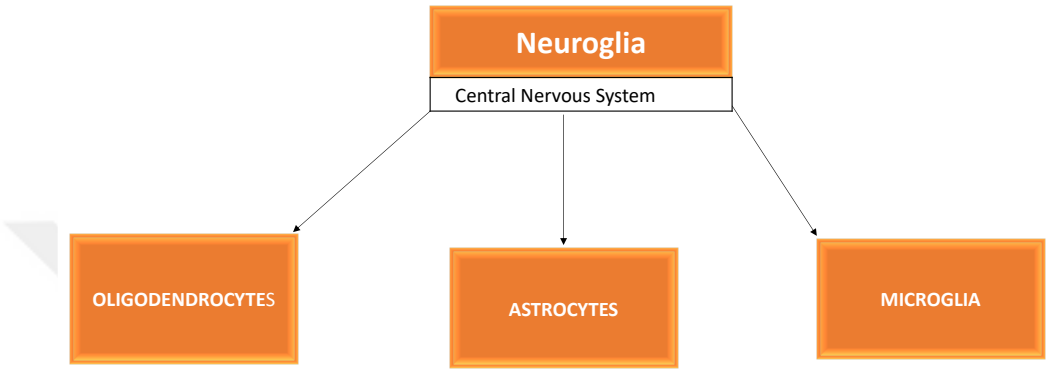

Figure.2.1.1. Glial cell types (15)

2.1.1. The Anatomy of Hippocampus and Cerebral Cortex

Cortex is outermost structure of the brain. The cerebral cortex is the outer covering of gray matter over the hemispheres. This is typically 2- 3 mm thick, covering the gyri and sulci. Certain cortical regions have different functions. These include areas directly receiving sensory input (vision, hearing, somatic sensation) or directly involved in production of limb or eye movements. The association cortices subserve more complex functions. Regions of association cortex are adjacent to the primary cortices and include much of the rostral part of the frontal lobes also regions encompassing areas of the posterior parietal lobe, the temporal lobe, and the anterior part of the occipital lobes. These areas are important in more complex cortical functions including memory, language, abstraction, creativity,emotion, and attention. They are also involved in the synthesis of movements (16) . Most of the cerebral cortex is neocortex. It contains between 10 and 14 billion neurons. Somatosensory, visual, auditory, motor, and prefrontal cortex are the other parts of cerebral cortex. Nerve cell arranges in three cortical layers that are contains different neuronal shapes, sizes, and density as well as different organizations of nerve fibers.

Hippocampus is a small complex extension of brain embedded deep into temporal lobe. It has a major role in learning and memory. Dentate gyrus, the subiculum and cornu ammonis (CA) regions constitute hippocampus.

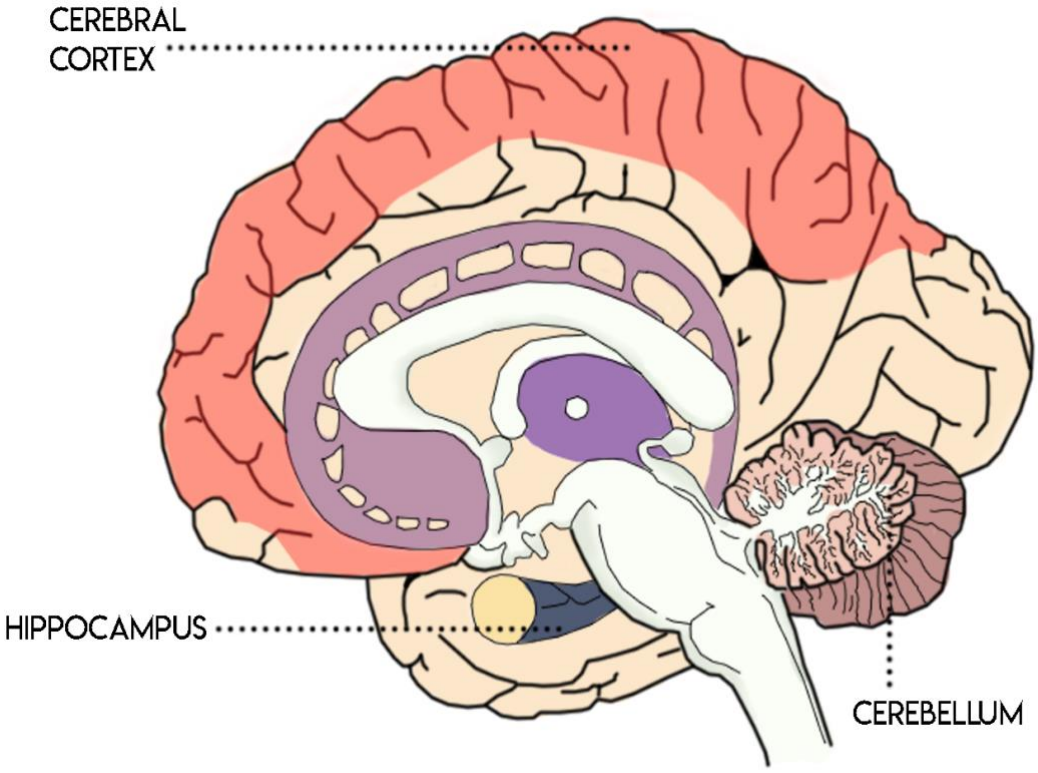

Figure 2.1.2. Anatomy of Brain (16)

2.1.2. The Histology of Hippocampus and Cerebral Cortex

There are several identifiable cell types in the cerebral cortex. Gray matter contains molecular layer, purkinje cell layer and granuler cell layer. While molecular Layer contains Stellate cells and Basket cells; Purkinje cell Layer; contains Purkinje cells and Granule cell Layer; contains Granule cells, Golgi cells, Lugaro cells and Unipolar Bushy cells. Finally, regions of the cerebral cortex are tied together by bundles of fibers which forms white matter(medulla) (16)

Moreover, in the hippocampus, the dentate gyrus receives inputs from Entorthinal cortex whereas the CA regions have pyramidal neurons which functions as synaptic input transformation. Cornu ammonis subdivided into four groups as C1, C2, C3, C4. (17). It is a plastic and vulnerable structure that gets damaged by a variety of stimuli (18). Studies

have shown that it also gets affected in a variety of neurological and psychiatric disorders (19).

2.1.3. Neurons

Neurons are nervous system signaling cells that are involved in producing the action potential and the transmitting of nerve impulses across the body. Nerve cells are specialized cells with structural features which are dendrites and axons in order to conduct electrochemical signaling. Dendrites and axons are attached to the cell body called soma. While axons have long tail-like structures, dendrites have short branch-like structures. Not all but some axons are covered with myelin sheath which is a special feature for electrochemical signaling. Small terminal buttons exist in the ends of axons electrochemical signals move from one axon terminal to another neuron's dendrite via synapses (18). Action potential is generated across the membrane by the changes of sodium and potassium ions concentrations between outside and inside of the neuron. Neurotransmitters are released from the terminals of the axons into the synapse. These nerve cells are called presynaptic neurons. Neurotransmitters in the synapse trigger the next neuron called the postsynaptic neuron. In conclusion, neurons are mainly responsible for transmitting electrochemical signals from one cell to another (20).

2.1.4. Glial Cells

Besides the neurons, there are supporting cells in the CNS called glial cells. Even though they are not part of the electrical signaling, they modulate neuronal activity and brain function. They support and protect neurons in order to maintain their signaling abilities (7). Other than the functional differences from neurons, there are also structural distinctions. Glial cells are mostly smaller than neurons, and they don't have any axons and dendrites. The main functions of glial cells can be told as; neurotransmitter uptake controlling, scaffold providing for neural development, and preventing or recovering neural injury. There are three types of glial that exist in CNS: astrocytes, microglia, and oligodendrocytes. Oligodendrocytes are the cells that are responsible for the production of myelin sheets of neurons in the CNS. Myelin sheath provides speed for action potential conduction in neurons (48).

2.1.4.1. Microglia

Microglia are the glial cells that derive from the bone marrow. It can be said that they are the phagocytes that exist in the brain and spinal cord. They inspect the microenvironment in the brain and produce the factors that affect surrounding astrocytes and microglia (46). In physiological conditions, microglia stay inactive situation. Although the presence of a pathogen or damaged tissue it becomes activated and produces anti-inflammatory factors. Normally, the production of anti-inflammatory factors is stopping when the tissue is repaired or the infection is eradicated. If this production won't stop and continues then the pathological condition occurs (24).

2.1.4.2. Astrocytes

Astrocytes are one of the other kinds of glial cells. Astrocytes are responsible from communication between the neurons, secretion of neurotransmitters, ion homeostasis. Also, they contributed to the formation of the blood-brain barrier. During the inflammation, they are stimulated by cytokines which are secreted by microglia. They proliferate and increase in size due to these stimulations. After all, they stimulate neurons with proinflammatory signals (24).

2.1.5. Blood-Brain Barrier

In the CNS, vessels are continuous, but they are specialized to maintain exchanges of molecules, ions, and cells between blood and CNS. The blood-brain barrier (BBB) is a term that is used for this specialized vessel barrier found in CNS. BBB is highly significant to the regulation of CNS homeostasis, proper neuronal function, and protection of neurons from toxins, pathogens, inflammation, injuries, and diseases. When BBB is broken down and lost its special functions due to the occurrence of some diseases such as neurodegenerative diseases; (25)harmful blood components, aberrant transport and clearance of molecules and cellular infiltration leads to neuronal dysfunction and degeneration. BBB consist of endothelial cells, vascular smooth muscle cells, and pericytes but the specialization of BBB occurs with the interactions of glial cells and neurons of the CNS. Besides the benefits of BBB restriction, it becomes an obstacle for drug delivery to the CNS (51). Nowadays, studies have been made to overcome this obstacle to deliver therapeutic treatments for CNS (52).

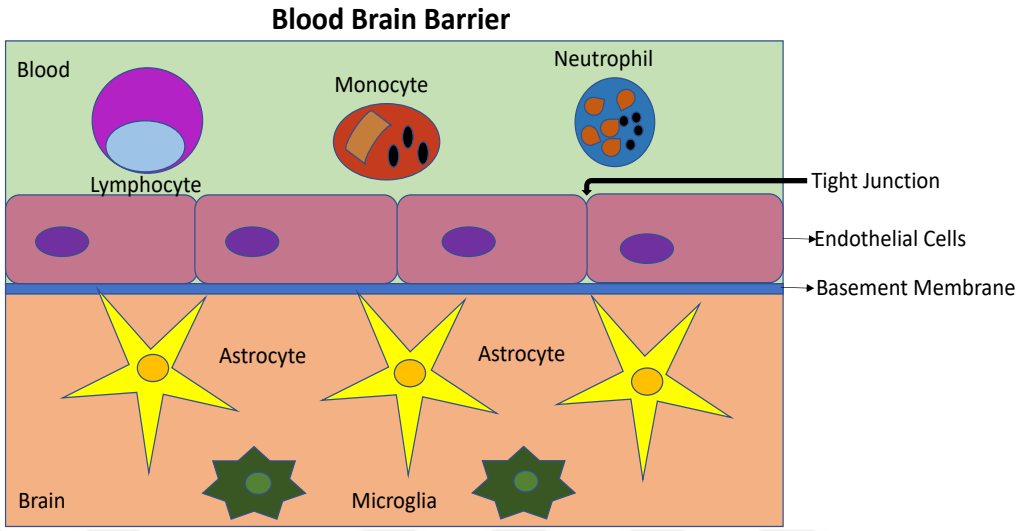

Figure 2.1.3. Blood Brain Barrier (28)

2.2. Alzheimer's Disease

2.2.1. General Introduction of Alzheimer's Disease

Alzheimer's Disease (AD) is one of the neurodegenerative diseases that start with temporary memory loss and ends up with total cognitive loss. Worldwide,44 million people are suffered from the disease, and it is assumed that will be 135.5 million people by 2050. According to Turkish Statistical Instute's statistics, 600.000 people have AD in our country. Because of the cognitive loss, not only patients but also relatives of the patients are affected. Nowadays, there are many therapeutic approaches to provide symptomatic relief but there is not any promising therapeutic cure (29).

AD can be classified into two types according to the reason that occurs. Rare, familial, autosomal-dominant type of AD caused by mutations in the Amyloid Precursor Protein (APP), presinilin1(PSEN1), or presinilin2(PSEN2) genes. Moreover, Sporadic AD occurs due to multifactorial genetic and environmental risk factors (29).

2.2.2. Pathology of AD

As the most important pathological hallmarks of AD, amyloid plaques and neurofibrillary tangles (NFTs) can be given. Amyloid plaques occur with the composition of extracellular amyloid filaments and β-amyloid (Aβ) peptides. Aβ peptides form from APP via proteolytic cleavage by secretase. Microtubule-associated tau proteins become

highly phosphorylated and form NFTs. Protein tau accumulates in soma and dendrites and affects the activities of protein kinases and phosphatases in AD patients. These pathological hallmarks lead to inflammation in the brain which results in the death of neurons and glial cells. Inflammatory mediators secreted from microglia stimulates astrocytes and neurons leads to a progression of AD. Proinflammatory cytokines, reactive oxygen metabolites, and chemokines play the important role in the occurrence of AD due to the promotion of the apoptosis of neurons and glial cells (4).

2.2.2.1. Processing of Amyloid Precursor Protein

β peptides consist of 36 to 43 amino acids and occur naturally. Amyloid precursor protein undergoes proteolysis by sequential enzymatic actions of beta-site amyloid precursor protein–cleaving enzyme 1 (BACE-1), a β-secretase, and γ-secretase, a protein complex with presenilin 1 and results in Aβ peptides. Aβ started to accumulate due to unbalanced production and clearance. This excess amount of Aβ may be considered as an initiation factor in AD. Aβ can arrange themselves to form insoluble amyloid plaques (1)

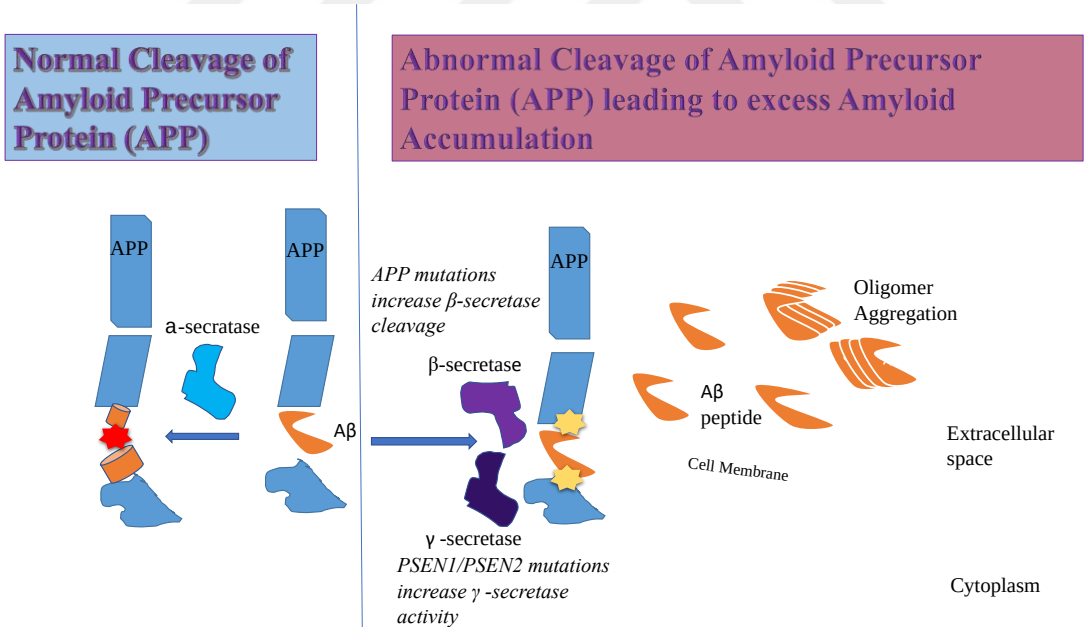

Figure.2.2.1. Normal and abnormal cleavages of Amyloid Precursor Protein(30)

2.2.2.2. Neurofibrillary Tangles

Tau protein is a soluble protein found in axons and responsible for assembly promotion, transportation of vesicles, and stability of microtubules. On the other hand, hyperphosphorylated tau is not soluble and their aggregated forms are the major

component of NFTs. Those abnormal tau proteins are cytotoxic. According to experimental evidence, Aβ accumulation stimulates tau aggregation. The microtubule-binding domain (MBD) of tau is made up of four repeat sequences (R1-R4). In normal phosphorylation of tau, glycogen synthase kinase 3 (GSK-3β), cyclin-dependent kinase (cdk5) and its activator subunit p25, or mitogen-activated protein kinase (MAPK) phosphorylate the serine and threonine residues. Hyperphosphorylated tau occurs by excessive kinase, reduced phosphatase activities, or both. Hyperphosphorylated sites tend to flank to MBD in Alzheimer's disease (31).

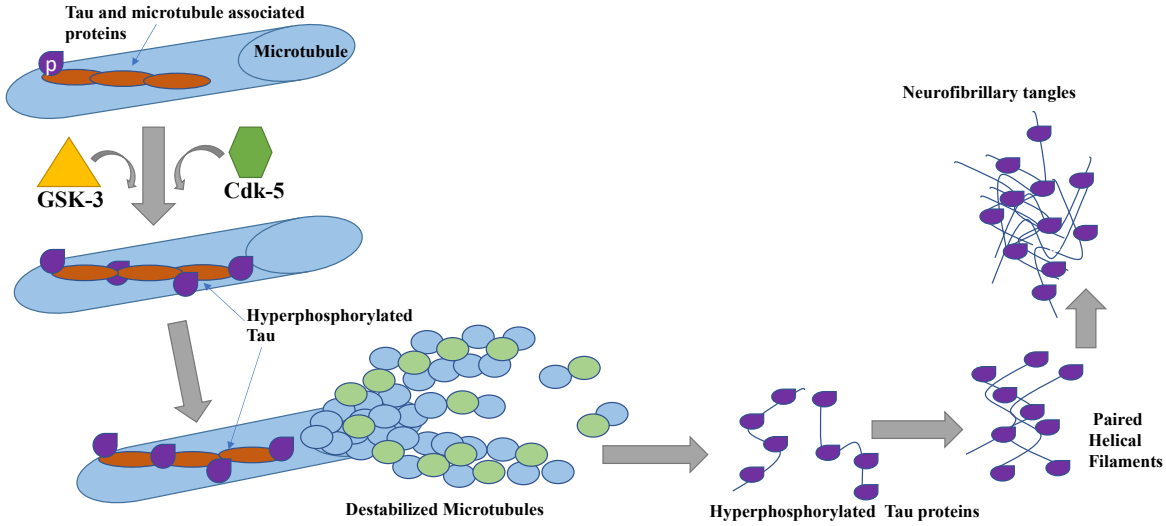

Figure.2.2.2. Neurofibrillary Tangle Formation (31)

2.2.2.3. Synaptic Dysfunction

Synaptic loss is a natural reason for dementia. It can occur with aging but intraneuronal Aβ accumulation can trigger it even earlier. Mild cognitive impairment is shown in patients preceding dementia due to a decline of hippocampal synapses. Memory forms at synapses by the basal transmission of single impulses and long-term potentiation. Signaling molecules are important in synaptic failure due to their aid in memory formation (4).

2.2.2.4. Oxidative Stress and Mitochondrial Failure

Oxidative stress has been defined as a disturbance in the balance between the production of reactive oxygen species (free radicals) and antioxidant defenses, which may lead to tissue injury. Reactive oxygen species (ROS) functions as normal metabolism and respiration, absorption of radiant energy, enzymatic metabolism of chemicals or drugs, and nitric oxide synthesis. On the other hand, it can become pathological due to exposes to chemicals, radiation, or inflammation. But when it becomes pathological, it can cause abnormal protein folding, loss of enzymatic activity, disruption of organelles and plasma membrane, and mutations of DNA (32).

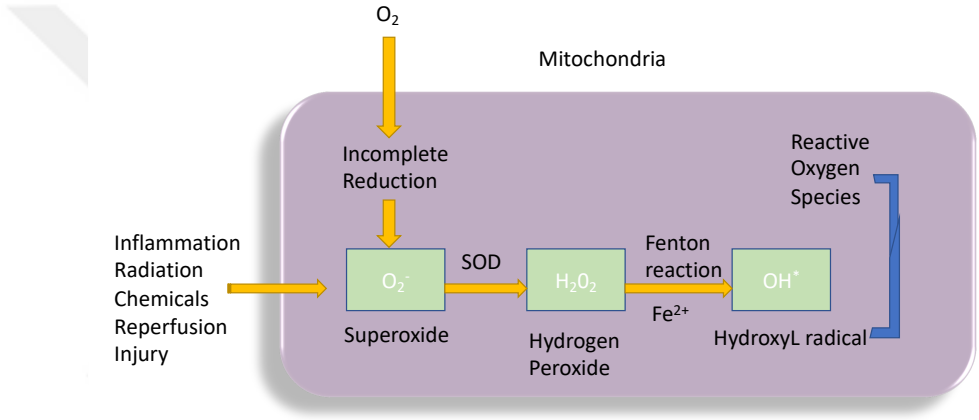

Figure.2.2.3. Reactive oxygen species formation in mitochondria (4)

According to experimental evidence, Aβ peptides inhibit some of the important mitochondrial enzymes in the brain such as cytochrome c oxidase. All metabolic activities that are conducted in mitochondria become impaired for instance ATP production, electron transport, oxygen consumption, and mitochondrial membrane potential. The increase of hydrogen peroxide amount in the mitochondria causes oxidative stress and release of cytochrome c which ends up in apoptosis. Because the apoptotic pathway can be activated when cytochrome c is released from the mitochondria into the cytoplasm. Cytochrome c activates caspases to start apoptosis. Caspases (for cysteine aspartic acid-specific proteases) exist as inactive precursors (procaspases), which are activated to produce directly or indirectly cellular morphologic changes during apoptosis. Proapoptotic Bax and antiapoptotic Bcl-2 proteins are balanced to maintain the release of

cytochrome c in normal physiological conditions. Overexpression of Bcl-2 protein in microglial cells that surrounds amyloid plaques may indicate this protein have a role in the survival features of neurotoxic microglia (33) .

ROS and reactive nitrogen species (RNS) form due to Aβ peptides and their peroxidative attack yield in mitochondrial toxins hydroxynonenal (HNE) and malondialdehyde. These toxins can damage ATPases and calcium (Ca^{2+}) entry mechanisms. Eventually, oxidative stress leads to the deaths of neurons and glial cells (34) .

2.2.2.4. Inflammation and Clearance of Aβ

Aβ can be formed in the cell by the endoplasmic reticulum, Golgi apparatus, and endosomes, or it can come outside of the cell and enter via low-density lipoprotein receptors on the surface of the cell membrane. The ubiquitous apolipoprotein E (APOE) and α2- macroglobulins (α2M) are chaperones in the extracellular production of Aβ. The clearance of Aβ is maintained by receptor-mediated internalization by the participation of astrocytes. Aβ can be engulfed by microglia by phagocytosis. Proinflammatory cytokines and acute phase reactants are released by stimulation of microglia and astrocytes in AD (8) . Aβ peptide aggregation activates microglia by signaling through Toll-like receptors (TLRs) and receptor for advance glycation endproducts (RAGE). Microglia synthesize the transcription factors NF-Kb and AP-1 and these transcription factors induces the expression of inflammatory mediators such as MHC2, COX-2, MCP-1, TNF-ALFA, IL-1BETA, IL-6, and the production of ROS. These inflammatory mediators and ROS act directly on the cholinergic neurons to start inflammation. Cholinergic neurons in the basal forebrain, the neurons that are primarily affected in AD, but other types of neurons, such as glutaminergic and GABAergic neurons may also be affected (35) . Furthermore, these inflammatory mediators and ROS that are released from microglia stimulate astrocytes. Stimulation of astrocytes amplifies proinflammatory mediators and further activation of microglia which induces more neurotoxic effects. (36) In addition to the Aβ peptide activation of microglia, the release of ATP due to apoptosis and necrosis of neurons also results in the activation of microglia through the purinergic P2X7 receptor. Microglia can also play protective roles by mediating clearance of Aβ through ApoE-dependent and ApoE-independent mechanisms. ApoE is a protein that

transporter of lipids. 3 types of isoforms are found in the human brain; ApoE2, ApoE3, ApoE4. ApoE4 is associated with AD pathology (37) .

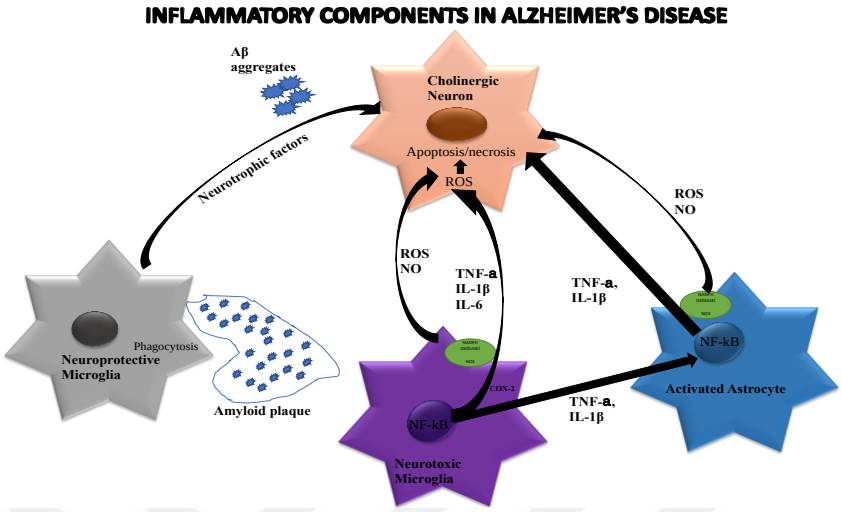

Figure.2.2.4. Inflammation process components in AD (5)

2.2.2.5. Hippocampo-cortical-dissociation Hypothesis

AD brain's hippocampal region is consistently suffered from atrophy. Hippocampus is one of the most important region that is affected by AD. The Hippocampal-cortical-dissociation hypothesis proposed that once the hippocampus is damaged, dissociation occurs between the hippocampus and cerebral cortex which results in failure of gathering information from the hippocampus (23).

2.2.3. Animal Models of AD

Animal models are significant to examine the pathology of diseases and evaluating the potentiality of new therapeutic approaches (18).

Table 2.1. Crucial aspects of animal models to research AD.

Shorter Life Spans.	The aging process can be seen in a shorter period thanks to shorter life spans for some animals. So, AD can be observed in more accurate conditions.
Shorter Gestation Periods and More Progeny.	It is possible to study genetic and early developmental components for adulthood neurodegeneration for several generations each year.
Experimental Potential.	Animal models provide us opportunities to conduct experimental procedures when there is not an option for human study, in vitro, or computational simulations. So, animal models are essential to understand the mechanisms of diseases and improving the therapeutic approaches.

2.2.3.1. Genetic Models

Transgenic techniques are suitable for animal models especially for rodents, due to their shorter lifespan, easy maintenance, and effective costs (30,38) . Besides that, the genetics of rodents is more similar than the nonmammalian vertebrates to humans (39,40). In genetic models of AD, mouse models are the most common type of animal that is used because transgenic techniques for mice are more established than the other rodents (40).

Expression of APP and PSEN1 with a specific FAD mutation is the first transgenic mouse model that is developed (41) . According to the changes of those genes, plaques are developed in the temporal, frontal lobes and cerebellum, and hippocampus. Moreover, synaptic dysfunction, lack of cognition, and gliosis can be observed in these transgenic mouse models. However, the cognitive loss was observed much earlier time than in AD. In addition to that neurodegeneration occurs only a small portion of the brain in these

transgenic mouse models. Also, NFTs are not developed properly in these models.

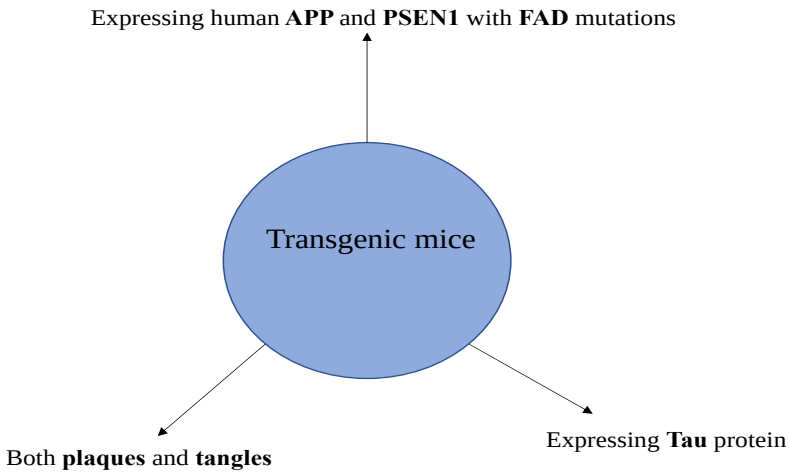

Figure.2.2.5 Types of transgenic mice.(42)

The subsequent type of transgenic mouse model is that expressed human tau containing mutations.(43) NFTs, neurodegeneration, atrophy, and motor deficits can occur in these transgenic mouse models whereas the generated mutations cause irrelevant toxicity or interaction with Aβ with AD in humans. Moreover, mutated tau is overexpressed in these models which leads to a dramatic increase in motor deficits that are not observed in AD patients(44).

The final important type of transgenic mouse model, which has a limited number of studies, indicates that plaques and tangles.

Although both significant features of AD can be observed, the consistent and abundant expression of the results in troubles in the study.

Briefly, rats can be used as transgenic models as well in AD studies. However, the decision of which animal is to be used should be determined by the suitability of the experimental procedures.

2.2.3.2. Neurotoxin Models

There are some chemicals that are used to generate animal models of AD. Basically, these chemicals are decided according to their action mechanism for

cognitive loss. Heavy metals, scopolamine, ethanol, colchicine, streptozotocin, lipopolysaccharide, and okadaic acid are the most common ones (33).

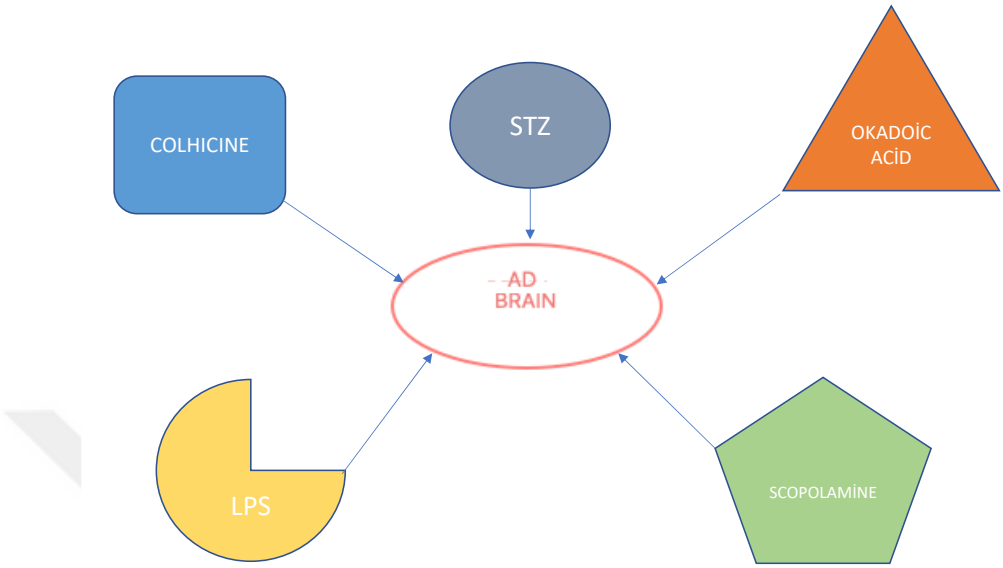

Figure2.2.6. Neurotoxin Models for Alzheimer's Disease (45)

2.2.3.2.A. Colchicine

Colchicine is a drug that is used to model Alzheimer's disease by inhibiting cholinergic neurons and made them dysfunctional (46). Cognitive deficits occur in colchicine-treated animal models due to the hippocampal lesions. Destruction of cholinergic neurons results in neurotoxicity and memory decline. Memory loss in colchicine-treated animal models is related to the decrease in neurotransmitters as serotonin, dopamine, and norepinephrine in the hippocampus region and cerebral cortex (47). In addition to that, colchicine can induce ROS generation in neurons (48). This type of AD model is advantageous to indicate symptoms that are similar to humans like cognitive and pathological changes (23).

2.2.3.2.B. Streptozotocin

Streptozotocin (STZ) is another compound that is used for AD modeling that has an influence on the biochemistry, metabolism, and functions of the brain. This compound is derivative of glucosamine nitrosourea and acquired from *Streptomycesachromogenes*. It is commonly used in cancer treatments as an alkylating agent (44). ROS and RNS are released due to neuronal damage and hyperphosphorylated tau in the existence of STZ.

There are some studies indicate that STZ can also play role in Aβ accumulation in the rain (35,45). Best of this pathological evidence, decreased memory and learning skills are observed with cognitive impairment (39).

2.2.3.2.C. Lipopolysaccharide

Lipopolysaccharide (LPS) is mostly used to investigate amyloidosis and neuroinflammation in both *in vitro* and *in vivo* studies (44). As well as other neurodegenerative diseases, AD can be modeled with induction of LPS in terms of inflammation (49). It is obtained from gram-negative bacteria external membrane. It has been mentioned that LPS has strong resistance to mammalian degradation enzymes which leads to constant proinflammatory cytokine production. Furthermore, the occurrence of inflammation results in oxidative stress enhancement (50).

2.2.3.2.D. Okadaic Acid

Okadaic Acid (OKA) is a kind of polyether toxin that is derived from marine microalgae. Injection of OKA leads to memory loss with inducing tau hyperphosphorylation, inhibiting phosphatases, and neuronal loss. Therefore, it is a good option to model dementia and especially AD. The production of ROS and reduction of mitochondrial activity in the hippocampal neurons are also demonstrated in the studies (51). In addition, the increase of proinflammatory cytokines in the hippocampus and cerebral cortex indicated such as TNF-a and IL-1 (52).

2.2.3.2.E. Scopolamine

Scopolamine is one of the anticholinergic drugs that is used to acquire memory loss in research of AD (33). It is commonly used in the prevention of motion sickness (48).

2.3. Scopolamine

Scopolamine is an anticholinergic drug. It decreases the effectiveness of the activity or concentration of acetylcholine in the synapse without directly altering the concentration itself. Scopolamine regulates some of the receptor sites in the post-synaptic membrane without depolarization, which decreases the potency of acetylcholine. Characterization of the interaction of scopolamine with the CNS muscarinic acetylcholine

receptor demonstrated a two-step process. It starts with the binding of ligand to the receptor followed by isomerization of the receptor-ligand complex to a higher affinity (53) .

Scopolamine distribution in an organism is not well understood, but it is known that it can cross the placenta and BBB. Elimination of scopolamine in the body occurs by renal excretion. Studies show that renal excretion is less than 10%, and less than 5% is unchanged. Scopolamine has been a highly metabolized and conjugated compound (54). Scopolamine is a commonly used model for analyzing dementia-related diseases as it can cause memory and cognitive deficits. This agent was commonly used to antagonize the receptors of muscarinic acetylcholine (ACh) participating in working memory. Deficiency of working memory is a well-known feature of AD. Neurobehavioral studies indicate that scopolamine can impair memory functions in humans and rodents especially short-term memory. (54) Besides that recent studies showed that scopolamine exposure can also make pathological alterations in cellular and molecular level in the brain. These alterations include impaired antioxidative defense system, increased oxidative stress, mitochondrial dysfunction, apoptosis, and neuroinflammation which mimics the AD pathology (10).

Scopolamine can cause atrophy and degeneration of brain neurons in rats. Furthermore, studies show that it also induces Aβ accumulation (9). Scopolamine leads to an increase in phosphorylated tau protein level whereas suppressed the gene expression of tau protein Scopolamine also promotes the activity of a tau kinase, which enhances tau hyper-phosphorylation (56).

Oxidative stress is elevated in AD brain neurons. Studies show that scopolamine is related to increasing Malondialdehyde (MDA) levels in rodents. MDA is a compound and a significant biomarker for oxidative stress that occur from lipid peroxidation which is an oxidative degradation of lipids. (9). Scopolamine also induces ROS accumulation in the cortex and hippocampus which is also an important biomarker for oxidative stress. Eventually, high MDA and ROS levels cause the apoptosis of neurons. (Another pathological cause of AD is neuroinflammation. Interleukin (IL)-1β, IL-4, and tumor necrosis factor (TNF)-α, released from microglia in the brain called pro-inflammatory cytokines which leads to inflammation in AD brain. Scopolamine increases these cytokines in rats (35). Moreover, another pro-inflammatory molecule nitric oxide (NO)

increases in the presence of scopolamine. In addition, VEGF an angiogenic factor that plays role in neuronal differentiation and proliferation is reduced by the presence of scopolamine. So, this reduction causes the impaired neuroprotection in the hippocampus of the brain (55).

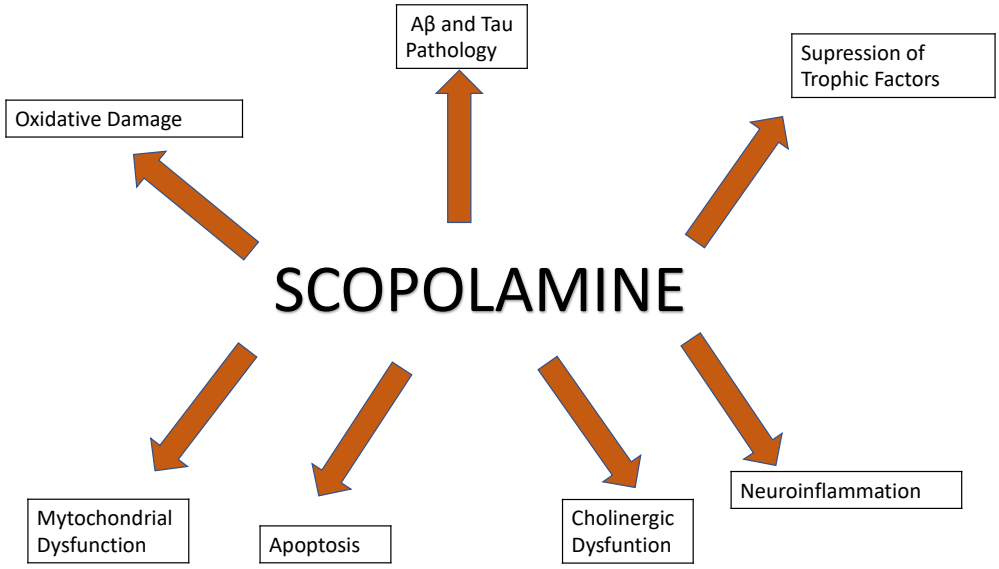

Figure 2.3.1. Effects of Scopolamine (9).

2.4. Selenium

Selenium is an element with atomic number 34 and atomic mass 78.963. There are organic and inorganic forms of selenium which are amino acid-associated organic forms as selenocysteine and selenite (SeO3_2), selenide (Se2_), selenate (SeO4_2), and elemental selenium (Se) as inorganic forms (56).

The body requires selenium in small amounts and the most common functions of it occur from selenoproteins. While there are 25 different kinds of selenoproteins studied in humans, the most well-known types of selenoproteins are selenoprotein P (SELENOP) and glutathione peroxidase (GPx). These proteins function as synthesizing thyroid hormones or DNA and maintaining the immune and reproductive system. On the other hand, it can be said that selenoproteins have a significant role in preventing and controlling oxidative stress. Selenium (Se) is found in the active sites of these enzymes which catalyze reactions to protect tissues against oxidative damage that results in preventing cognitive and behavioral deficits (59). For instance, glutathione peroxidase

enzymes catabolize the hydroperoxides in order to act as an antioxidant agent (59). Also, thioredoxin reductases that contains selenocysteine plays an important role in thioredoxin reduction which leads to a regulation for metabolic activity in the cell. On the other hand, Selenoprotein P act as a transporter for Se between liver and the other organs besides its antioxidant role (61).

The importance of selenium's existence in the body is related to the cognitive functions of humans due to its antioxidant role. Therefore, the brain has the priority of retaining selenium even if there is a depletion. The activity of selenoproteins can be changed by the level of selenium in the body according to their role in homeostasis and transportation. (57) There are several studies that indicate the relation between the Se level and the cognitive functions. For one example of these studies, elderly French people were observed according to their Se levels and their cognitive functions. As a result, a study shows that patients who have higher Se levels have the lowest cognitive deficits. (60). However, these outcomes are significantly related to the dosage of Se due to the small range of tolerating between toxicity and deficiency. It is crucial to managing the optimal amount of dose used in studies in order to prevent cognitive decline.

Besides the antioxidant roles of Se, many other useful functions contribute to the maintenance of the brain. Studies on animal models suggested that (14), selenium treatment can modulate calcium homeostasis in the brain which is essential for synaptic transmission (61).

Moreover, the role of Glutathione peroxidase 4 as a regulator of ferroptosis, which is a type of programmed cell death due to iron that leads to high lipid peroxidation rates (65), have an important impact on neurodegeneration owing to the locations of ferroptosis was occurred in the brain such as hippocampus and forebrain. According to the given information, ferroptosis can be inhibited by rising the amount of Se intake to the brain with increased GPx4 activity which results in the prevention of neuronal death (60) .

In addition, it is known that tau hyperphosphorylation can be reduced by sodium selenate with the aid of phosphatase 2A activation. (63)

Furthermore, the other inorganic compound called selenite is known with the ability to reduce γ-secretase activity through the MAPK pathway that results in the decreased amount of Aβ (67).

In the summary, Se has functions that are considered essential for the maintenance of oxidative stress, neuronal modulations, and calcium channel regulations (68).

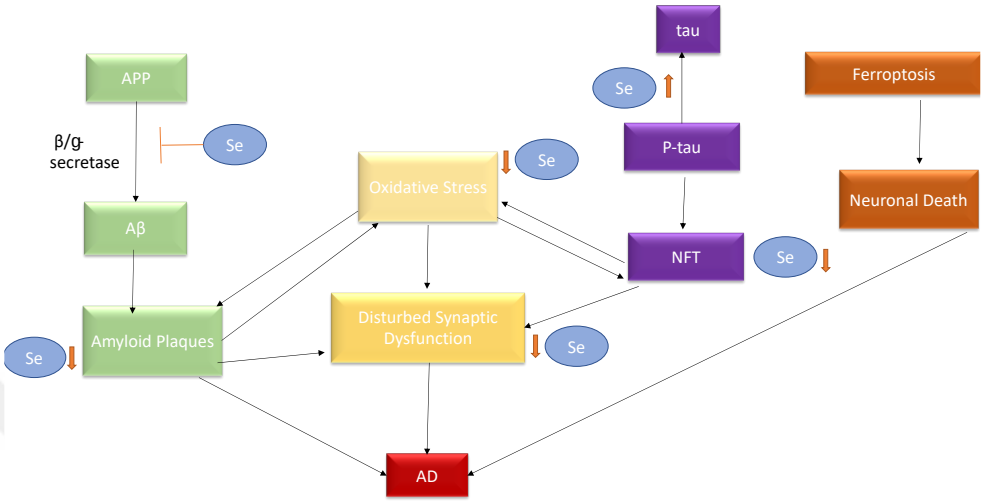

Figure 2.9. Selenium in AD pathogenesis prevention(69).

3. MATERIALS AND METHOD

3.1. Materials

3.1.1. Chemicals and Reagents

- Formaldehyde solution (37 %) (Merck)
- Cresyl violet acetate (Santa Cruz Biotechnology)
- DAB Chromogen (Thermo Fisher Scientific)
- DAB Substrate Buffer (Thermo Fisher Scientific)
- Di-sodium hydrogen phosphate (Merck)
- Entellan mounting medium (BioMount)
- Hydrogen peroxide solution 30 % (Sigma)
- Mayer's Hematoxylin (Thermo Fisher Scientific)
- Phosphate buffered saline tablets (Sigma)
- Saline (Isotonic 9 % NaCl) (Polifarma)
- Sodium chloride (Sigma)
- Sodium dihydrogen phosphate (Sigma)
- Tri-sodium citrate dihydrate (Merck)
- Triton X-100 (Roche)
- Xylene (Sigma)

3.1.2. Antibodies

- Amyloid Beta (Boster, BA1054-0.5)
- iNOS (Abcam iNOS,2977S)
- Vegf (Abcam VEGF, 2479S)

3.1.3. Commercial Kits

- In situ cell death detection kit, POD, Roche (Terminal deoxynucleotidyl transferase enzyme solution, Nucleotide mixture in reaction buffer, Anti-fluorescein antibody conjugated with horse-radish peroxidase)
- Vectastin Universal Quick Kit, Vectastin (Normal Horse Serum, Biotinylated Universal Secondary antibody, Streptavidin/Peroxidase preformed complex)

3.1.4. Laboratory Equipments

- M-polylysin slides (25*75*1,0 mm) (Thermo Scientific)
- Propylen centrifuge tubes; 50 mL, 15 mL, 2 mL,0.5 mL (Isolab)
- Micropipettes

3.1.5. Laboratory Technical Instruments

- Automatic Glass Cover slipper (Leica)
- Stereological workstation and light microscope (Leica)
- Incubator (Memmert)
- Magnetic stirrer (IKAMAG)
- Locomotor activity cage (Commat, MAY)
- Microscope (Leica)
- pH meter (Hanna instruments PH211, Germany)
- Refrigerator
- Staining Automat (Leica)
- Microtome
- Tissue embedding automat
- Tissue Processing automat
- Fume cupboard

3.2. METHODS

3.2.1. Experimental Setup and Groups

Adult male Sprague Dawley rats (250-300 g) were obtained from Yeditepe University Experimental Research Center (YUDETAM). All of the experiments were approved by the Ethical Committee of Yeditepe University Experimental Research Center and the use of animals complied with the US National Institutes of Health Guide for Care and Use of Laboratory Animals (2021-027). Animals were maintained in standard housing conditions with constant temperature, humidity, 12-h light/dark cycles, and free access to food and water. 24 rats were randomly divided into 4 experimental groups as follows: intraperitoneal (IP) saline-injected control group (C) (n=6), IP 1,5 mg/kg/day scopolamine injected group (SC) as control to Alzheimer's disease model (n=6), IP 2 mg/kg/day selenium injected group (SE) as control to treatment (n=6), IP 1,5 mg/kg/day (14) scopolamine and 2 mg/kg/day selenium IP injected group (T) as treatment group (n=6) (56).

Table 3.2.1. The experimental groups and number of animals.

Groups	Numbers
IP saline injected control group (C)	n=6
IP scopolamine injected group (SC)	n=6
IP selenium injected group (SE)	n=6
IP scopolamine and selenium injected group (T)	n=6

All substances were injected for 21 days and on the last day of injections locomotor activity test is conducted for all rats. At the end of 21 days of injections all animals were dissected, and brain tissues were dissected (14).

3.2.2. Drug Treatment

Drug administration of groups are followed as; C group of the rats were intraperitoneally injected with saline, SE group of the rats were intraperitoneally injected with 2 mg/kg/day(56) selenium, SC group of the rats were intraperitoneally injected with 1,5 mg/kg/day(14) scopolamine and T group of the rats were intraperitoneally injected

with scopolamine and 2 mg/kg/day selenium for 21 days. Both selenium and scopolamine were dissolved in saline.

3.2.3. Sacrification of the Animals

After the locomotor activity test, animals were decapitated, and their brains were dissected out and their hippocampus and cerebral cortex regions were reserved and were placed in %10 neutral formaldehyde solution in order to use in histological analysis (55).

3.2.4. Spontaneous Locomotor Activity

Before decapitation of animals, animal activity monitoring system (MAY - Activity Monitoring System - Commat Ltd., TR) was used to record motor activity measurements. (Figure 3.2). Infrared light sources found each side of rectangular frame (45x45x30 cm) in the locomotor activity cage. Electromechanical counter placed on the floor of the cage. Moves of animals disrupt the infrared beams and electromechanical counter counts them as locomotor activity. Each rat was individually placed in the cage and locomotor activity was recorded for 5 minutes. All records were performed between 10 a.m. and 4 p.m. The cage was cleaned with wet towel before each recording. Stereotypic, ambulatory, vertical, horizontal motor activities and distance traveled by the animals were measured (14).

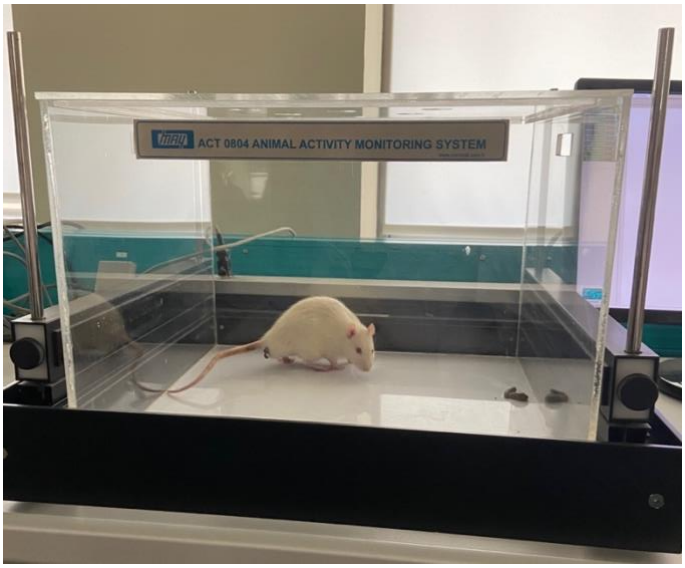

Figure3.2. Spontaneous locomotor activity

3.2.5. Histological Techniques

3.2.5.1. Tissue processing

All brain tissues were put in cassettes and placed into the tissue processor and followed below steps that are indicated in (Table3.2.2.).

Table3.2.2. Steps of Tissue Processing

Fixation	Neutral formaldehyde solution	2 Hours
	Neutral formaldehyde solution	2 Hours
Dehydration	70% Alcohol	2 Hours
	80% Alcohol	2 Hours
	90% Alcohol	2 Hours
	96% Alcohol	2 Hours
	96% Alcohol	2 Hours
	100% Alcohol	2 Hours
Clearing	Xylene I	1.5 Hours
	Xylene II	1.5 Hours
Paraffin Impregnation	Paraffin	3 Hours
	Paraffin	3 Hours

3.2.5.1.A. Fixation

The fixative (10% neutral buffered formalin (pH 7.4)) solution was prepared in advance. 4 g sodium phosphate monobasic (NaH2PO4) and 6.5 g sodium phosphate dibasic (Na2HPO4) were weighed out and dissolved in 900 mL distilled water. 100 mL formaldehyde (37%) was added to the solution to have a final volume of 1000 mL. The tissues were fixed for 4 hours in a neutral formaldehyde solution. (67)

3.2.5.1.B. Dehydration

The tissues were dehydrated in ascending alcohol series (70%, 80%, 90%, 96%, 96%, and 100%) for 2 hours each. (68)

3.2.5.1.C. Clearing

The tissues were cleared in xylene I and II for 1.5 hours each.

3.2.5.1.C. Paraffin Impregnation

All tissues were placed in paraffin for 3 hours. In the end, they are embedded in paraffin blocks with the aid of a tissue embedding device. (68)

3.2.5.2. Sectioning

All paraffin blocks were placed in a microtome and 5 micrometer sections were acquired on the slides.

3.2.5.3. Hematoxylin Eosin Staining

Hematoxylin Eosin staining is a routine staining in histology laboratory and is commonly used to investigate the pathology in tissue sections. Hematoxylin is a positively charged basic dye; therefore, stains negatively charged nucleic acid components in the nucleus blue color. On the contrary eosin dye is a negatively charged acidic dye, so that it stains positively charged structures such as proteins in the cytoplasm pink color. (68)

All the solutions were prepared in advance and put into copulin jars that were found in the staining automat and the protocol explained below was followed:

- The sections were dried in an incubator at 75^{o}C for 20 minutes.
- Then the sections were cleared in xylene I and II for 1 minute each.
- The slides were hydrated in descending alcohol series (100%, 96%, 96% ,90%) for 2 minutes each.
- All sections were washed with distilled water.
- The sections were stained with Mayer’s hematoxylin solution for 5 minutes and rinsed in water for 2 minutes.
- The slides were decolorized in acid alcohol (396 mL 70% ethanol was mixed with 4 mL glacial acetic acid) for 1 minute.
- The slides were washed in tap water for 1 minute.
- The sections were subjected to 80% ethanol for 2 minutes.

- Then the sections were counterstained with Eosin for 3 minutes.
- The sections were dehydrated in ascending alcohol series (90%, 96%, 96%, 96%, and 100%) for 1 minute each.
- Finally, the slides were cleared in xylene I and II for 2 minutes each.
- The slides were coverslipped in entellan mounting medium using an automatic glass coverslipper.

3.2.5.4. Cresyl Violet Staining

Cresyl violet is a basic dye and stains Nissl substance in the cytoplasm of neurons dark blue. Cresyl violet staining is generally used to demonstrate the structural features of the neurons. (72)Two solutions were prepared in advance. To prepare solution A, sodium acetate was dissolved in distilled water. For solution B, glacial acetic acid was diluted with distilled water. Then the two solutions were mixed, and the pH was adjusted to 3.8-4.0 with acetic acid. Cresyl violet acetate was dissolved in this solution and left on the magnetic stirrer overnight in dark. The staining solution was filtered with a filter paper before staining the sections. (73) All of the solutions were put into copulin jars, and the protocol explained below was followed:

1) The sections were dried in an incubator at 75°C for 20 minutes.
2) The sections were placed in xylene solution for 20 minutes at room temperature.
3) Then the slides were washed with distilled water for 1 minute.
4) The sections were stained with Cresyl Violet for 20 minutes.
5) The slides were washed with distilled water.
6) The sections were then dehydrated in ascending alcohol series (70%, 80%, 90%, 96%, 96%, and 100%) for 1 minute each.
7) Finally, the slides were cleared in xylene I and II for 2 minutes each.
8) The slides were coverslipped in entellan mounting medium using an automatic glass coverslipper.

3.2.5.5. Silver Staining

Neuritic plaques and neurofibrillary tangles can be observed with The Bielschowsky silver method. (74) Four solutions were prepared in advance. At first, 20 g silver nitrate was dissolved in distilled water to produce a silver nitrate solution. Then, 0,5 g citric acid was dissolved in 100 ml distilled water, 20 ml formalin, and 1 drop of

concentrated nitric acid was added in order to have a developer solution. Moreover, 200 ml 28% ammonium hydroxides were evaporated in an open beaker under the hood for 20 mins to obtain evaporated ammonia. Finally, 5g 1% sodium thiosulphate was dissolved in 100 ml distilled water, and Hypo was acquired. All of the solutions were put into copulin jars and the protocol explained below was followed:

1. The sections were dried in an incubator at 75°C for 20 minutes.
2. The sections were placed in xylene solution for 20 minutes at room temperature.
3. Then the slides were washed with distilled water for 3 minutes.
4. The sections were stained with Silver Nitrate solution for 20 minutes.
5. Then the slides were washed with distilled water for 3 minutes.
6. Evaporated ammonia was put in silver nitrate solution drop by drop and stirred until the solution became clear.
7. The slides were incubated in evaporated ammonia added silver nitrate solution for 15 mins in a dark place.
8. 3 drops of evaporated ammonia were put in distilled water and slides were washed in this solution.
9. 3 drops of developer solutions were placed in ammonia/silver solution and stirred. Then sections were incubated in this solution for 5 min.
10. Then the slides were washed with distilled water for 3 minutes.
11. The slides were incubated in HYPO for 5 mins.
12. Then the slides were washed with distilled water for 1 minute.
13. Sections were dehydrated in 100% for 2 min and cleared in xylene for 2 min.
14. The slides were coverslipped in entellan mounting medium with the aid of an automatic glass cover slipper

3.2.5.6. Immunohistochemistry for iNOS

Nitric oxide is an inorganic compound that plays important role in neurotransmission and cytotoxicity. NO production is maintained by the nitric oxide synthase (NOS) family. (75)Inducible nitric oxide synthase (iNOS) is one of these synthases however the aberrant amount of its induction can cause damages in cells and progress the pathology of diseases such as Alzheimer's Disease. (76) Five solutions were prepared in advance. At first, 3% hydrogen peroxide solution was prepared with 1ml 30% Hydrogen peroxide stock solution and 99 ml PBS. After that, 0,1 g tri–Na Citrate x

2H2O and 0,1 ml Triton X-100 were dissolved in 100 ml distilled water in order to prepare 100 ml 0.5 M permeabilization solution. Next, 5.88 g tri–Na Citrate x $2H_2O$ was dissolved in 200 ml distilled water, and pH was adjusted to 6 with HCL titration resulting in 200 ml 0,1 M citrate buffer (retrieval solution). Furthermore, to have a washing solution, one phosphate-buffered saline (PBS) tablet (Sigma) was dissolved in 100 mL distilled water. Finally, 10 µl DAB was added to the 200 µl substrate and kept on ice.

All the solutions were put into copulin jars, and the protocol explained below was followed:

1. The sections were dried in an incubator at 75°C for 20 minutes.
2. The sections were placed in xylene solution for 20 minutes at room temperature.
3. The slides were then rehydrated in descending alcohol series (100%, 96%, 90%, 80%, and 70%) for 3 minutes each.
4. Then the slides were washed with PBS for 3 minutes at room temperature.
5. The slides were incubated in permeabilization solution for 8 mins in ice.
6. Then the slides were washed with PBS for 3 minutes at room temperature.
7. The slides were placed in citrate buffer solution (pH 6.0) in a 750-watt microwave for 1 min for antigen unmasking.
8. Then the slides were washed with cold PBS for 5 minutes.
9. Then the slides were washed with PBS for 5 minutes at room temperature.
10. The slides were placed in 3% hydrogen peroxide solution for 30 minutes in order to quench endogenous peroxidase activity.
11. Then the slides were washed with PBS for 5 minutes.
12. All specimens were incubated in blocking solution (2.5% RTU Normal Horse Serum VECTASTAIN KIT) for 30 min in a humidified chamber.
13. Blocking solution was removed from slides and slides washed with PBS for 5 min.
14. Primary diluted (1:200) antibody (iNOS) was dropped on all sections and incubated at 4 °C overnight in a humidified chamber
15. Then the slides were washed with PBS for 5 minutes.
16. Secondary antibody (RTU Biotynlated Universal Antibody Anti-Rabbit/mouse IgG) was dropped on all sections and incubated at room temperature for 30 min in a humidified chamber.
17. Then the slides were washed with PBS for 5 minutes.

18. Vectastain RTU ABC Reagent was dropped on all sections and incubated at room temperature for 30 min in a humidified chamber.
19. Then the slides were washed with PBS for 5 minutes.
20. All slides were incubated in DAB chromogen & peroxidase substrate mixture for 3 min.
21. Then the slides were washed with PBS for 5 minutes.
22. Each specimen was counterstained with Gill's hematoxylin for 4 min, then rinsed in tap water.
23. Sections were dehydrated at in 100 % for 2 min and cleared in xylene for 2 min.
24. The slides were coverslipped in entellan mounting medium with the aid of an automatic glass cover slipper.

3.2.5.7. Immunohistochemistry for VEGF

Endothelial cell proliferation, promoting cell migration, and inhibition of apoptosis are promoted by Vascular endothelial growth factor (VEGF). (74) VEGF has an important role in the nervous system besides angiogenesis, affecting neural cells directly such as neural stem cells. (75) Five solutions were prepared in advance. At first, 3% hydrogen peroxide solution was prepared with 1ml 30% Hydrogen peroxide stock solution and 99 ml PBS. Next, 5.88 g tri–Na Citrate x $2H_2O$ was dissolved in 200 ml distilled water, and pH was adjusted to 6 with HCl titration resulting in 200 ml 0,1 M citrate buffer (retrieval solution). Furthermore, to have a washing solution, one phosphate-buffered saline (PBS) tablet (Sigma) was dissolved in 100 mL distilled water. Finally, 10 µl DAB was added to the 200 µl substrate and kept on ice.

All the solutions were put into copulin jars, and the protocol explained below was followed:

1. The sections were dried in an incubator at 75°C for 20 minutes.
2. The sections were placed in xylene solution for 20 minutes at room temperature.
3. The slides were then rehydrated in descending alcohol series (100%, 96%, 90%, 80%, and 70%) for 3 minutes each.
4. Then the slides were washed with PBS for 3 minutes at room temperature.
5. The slides were placed in citrate buffer solution (pH 6.0) in a 750-watt microwave for 1 min for antigen unmasking.
6. Then the slides were washed with cold PBS for 5 minutes.

7. Then the slides were washed with PBS for 5 minutes at room temperature.
8. The slides were placed in 3% hydrogen peroxide solution for 30 minutes in order to quench endogenous peroxidase activity.
9. Then the slides were washed with PBS for 5 minutes.
10. All specimens were incubated in blocking solution (2.5% RTU Normal Horse Serum VECTASTAIN KIT) for 30 min in a humidified chamber.
11. Then the slides were washed with PBS for 5 minutes.
12. Blocking solution was removed from slides and slides washed with PBS for 5 min.
13. Primary diluted (1:100) antibody (VEGF) was dropped on all sections and incubated at 4 ° C overnight in a humidified chamber
14. Then the slides were washed with PBS for 5 minutes.
15. Secondary antibody (RTU Biotynlated Universal Antibody Anti-Rabbit/mouse IgG) was dropped on all sections and incubated at room temperature for 30 min in a humidified chamber.
16. Then the slides were washed with PBS for 5 minutes.
17. Vectastain RTU ABC Reagent was dropped on all sections and incubated at room temperature for 30 min in a humidified chamber.
18. Then the slides were washed with PBS for 5 minutes.
19. All slides were incubated in DAB chromogen & peroxidase substrate mixture for 3 min.
20. Then the slides were washed with PBS for 5 minutes.
21. Each specimen was counterstained with Gill's hematoxylin for 4 min, then rinsed in tap water.
22. Sections were dehydrated in 100 percent for 2 min and cleared in xylene for 2 min.
23. The slides were coverslipped in Entellan mounting medium with the aid of an automatic glass cover slipper.

3.2.5.8. Immunohistochemistry for Amyloid Beta

Amyloid-Beta protein is one of the most important pathological hallmarks in AD. Immunochemistry is a common way to demonstrate intracellular Aβ existence in cells. Four solutions were prepared in advance. At first, 3% hydrogen peroxide solution was prepared with 1ml 30% Hydrogen peroxide stock solution and 99 ml PBS. Next, 5.88 g tri–Na Citrate x 2H2O was dissolved in 200 ml distilled water, and pH was adjusted to 6

with HCl titration resulting in 200 ml 0,1 M citrate buffer (retrieval solution). Furthermore, to have a washing solution, one phosphate-buffered saline (PBS) tablet (Sigma) was dissolved in 100 mL distilled water. Finally, 10 µl DAB was added to the 200 µl substrate and kept on ice.

All the solutions were put into copulin jars, and the protocol explained below was followed:

1. The sections were dried in an incubator at 75°C for 20 minutes.
2. The sections were placed in xylene solution for 20 minutes at room temperature.
3. The slides were then rehydrated in descending alcohol series (100%, 96%, 90%, 80%, and 70%) for 3 minutes each.
4. Then the slides were washed with PBS for 1 minute at room temperature.
5. The slides were placed in citrate buffer solution (pH 6.0) in a 750-watt microwave for 1 min for antigen unmasking.
6. Then the slides were washed with cold PBS for 5 minutes.
7. Then the slides were washed with PBS for 5 minutes at room temperature.
8. The slides were placed in 3% hydrogen peroxide solution for 30 minutes in order to quench endogenous peroxidase activity.
9. Then the slides were washed with PBS for 5 minutes.
10. All specimens were incubated in blocking solutions (2.5% RTU Normal Horse Serum VECTASTAIN KIT) for 30 min in a humidified chamber.
11. Then the slides were washed with PBS for 5 minutes.
12. Blocking solution was removed from slides and slides washed with PBS for 5 min.
13. Primary antibody (Aβ) was dropped on all sections and incubated at 4 °C overnight in a humidified chamber
14. Then the slides were washed with PBS for 5 minutes.
15. Secondary antibody (RTU Biotynlated Universal Antibody Anti-Rabbit/mouse IgG) was dropped on all sections and incubated at room temperature for 30 min in a humidified chamber.
16. Then the slides were washed with PBS for 5 minutes.
17. Vectastain RTU ABC Reagent was dropped on all sections and incubated at room temperature for 30 min in a humidified chamber.
18. Then the slides were washed with PBS for 5 minutes.

19. All slides were incubated in DAB chromogen & peroxidase substrate mixture for 3 min.

20. Then the slides were washed with PBS for 5 minutes.

21. Each specimen was counterstained with Gill's hematoxylin for 4 min, then rinsed in tap water.

22. Sections were dehydrated in 100% for 2 min and cleared in xylene for 2 min.

23. The slides were coverslipped in entellan mounting medium with the aid of an automatic glass cover slipper.

3.2.5.9. TUNEL Assay: (In situ Cell Detection Kit, Pod) Roche*

TUNEL assay is a reliable method to detect apoptotic neuron death. DNA double-strand breaks which occur during apoptosis are precisely labeled and visualized with TUNEL assay. In this technique, the terminal deoxynucleotidyl transferase (TdT) enzyme adds fluorescein-labeled nucleotides to the free 3'-OH DNA ends which are then visualized with an anti-fluorescein antibody labeled with POD and substrate reaction (79). The protocol explained below was followed:

1) The sections were dried in an incubator at 75°C for 20 minutes.

2) The sections were placed in xylene solution for 20 minutes at room temperature.

3) The slides were then rehydrated in descending alcohol series (100%, 96%, 90%, 80%, and 70%) for 3 minutes each.

4) Then the slides were washed with PBS for 1 minute at room temperature.

5) The slides were placed in a citrate buffer solution in a 750-watt microwave for 1 min.

6) Then the slides were washed with cold PBS for 1 minute.

7) Then the slides were washed with PBS for 1 minute at room temperature.

8) A hydrophobic barrier was made around the tissue with a barrier pen. The slides were incubated in a blocking solution (normal horse serum) in a humidified chamber at room temperature for 30 minutes.

9) Then the slides were washed with PBS for 1 minute at room temperature.

10) TUNEL reaction mixture (45 µl label solution was mixed with 5 µl enzyme solution for one section) was prepared. The sections were incubated in a TUNEL reaction mixture in dark, 37°C humidified chambers for 60 minutes.

11) Then the slides were washed with 1X PBS three times for 5 minutes each.

12) Converter-POD was added to the sections and incubated in dark, 37°C humidified chambers for 30 minutes.

13) Then the slides were washed with 1X PBS three times for 5 minutes each.

14) The reaction was visualized by using DAB (1000 µl DAB substrate buffer was mixed with 50 µl DAB chromogen) solution as a chromogen.

15) Then the slides were washed with 1X PBS three times for 5 minutes each.

16) The sections were counterstained with Mayer's hematoxylin and rinsed in tap water.

17) Sections were dehydrated in ascending alcohol concentrations, cleared in xylene.

18) The slides were coverslipped in entellan mounting medium

3.2.6. Analysis by Light Microscopy

Each section was examined under light microscope (Leica DM 4000B, Wetzlar, Germany) and photographed by CCD digital camera (Optronics Microfire 1600x1200P, Goleta, CA, USA) with the aid of LAS Version 4.1.0 program. Hematoxylin and eosin, Silver and Cresyl violet stained sections were evaluated histopathologically. H-score analysis were performed on iNOS, VEGF and Amyloid-Beta immunohistochemical stained sections. Finally, apoptotic index was calculated according to analysis of Tunel assay performed sections.

3.2.7. H-score Analysis for iNOS, VEGF and Amyloid-Beta Immunohistochemistry

The H-score ("histo" score) is calculated by multiplying the proportion of staining by an ordinal value corresponding to the intensity level. The final score varied from 0 (no staining in the tumor) to 300 (no staining in the tumor) (diffuse intense staining of the tumor). To calculate H-score, three sections of each animal were scored with their percentages as their staining intensity from 0 to 3 degrees (0=none, 1=mild, 2=moderate, 3=severe). The percentage of cells at each staining intensity level is calculated. Percentages and degrees were multiplied with the following formula:

$$[1 \times (\%\ \text{cells}\ 1+) + 2 \times (\%\ \text{cells}\ 2+) + 3 \times (\%\ \text{cells}\ 3+)]$$

The final score, ranging from 0 to 300, gives more relative number to indicate staining-intensity in a sample tissue. Then the average of all sections were calculated (78).

3.2.8. Apoptotic Index Calculation for TUNEL Assay

To calculate Apoptotic index, each section of every animal divided in to five area and both apoptotic cells and normal cells were counted in every area. Apoptotic cells were summed in five area for each animal and normal cells were summed in each animal. Then apoptotic cells divided to apoptotic + normal cells to obtain apoptotic index (80).

3.2.9. Statistics

GraphPad Prism®6 was used as the statistical analyses program. All data were analyzed as mean ± SEM. Shapiro-Wilk normality test was used in order to determine normal distribution of data. Data were considered as significant if P values lower than 0.05. Tukey's multiple comparison test was used to compare all groups data.

4.RESULTS

4.1. SPONTANEOUS LOCOMOTOR ACTIVITY

To examine the effects of selenium on the motor activity of the animals, the locomotor activities of the animals were measured with a motor activity monitoring system. Stereotypic, ambulatory, vertical, horizontal motor activities and distance traveled by the animal were measured.

4.1.1. Distance Travelled

According to the examination prior to the decapitation of the animals, as expected, the distance travelled by animals in Sc group have considerably decreased compared to C group ($p<0.01$). Similarly, animals in Se and T groups have also experienced a decrease in their locomotor activity i.e., when compared to C group, though no statistical significance was calculated for both groups. Distance covered by animals in Se, and T groups are significantly close, with Se being slightly higher, nevertheless there has been no statistical significance observed between Se and T groups. When looked at the last measurements before the decapitation of animals, it can be seen that distance travelled by animals is the lowest in Sc group compared to Se, T and C groups. In other words, animals in T group experienced an increase in locomotor activity compared to Sc group when treated with Se despite being statistically insignificant.

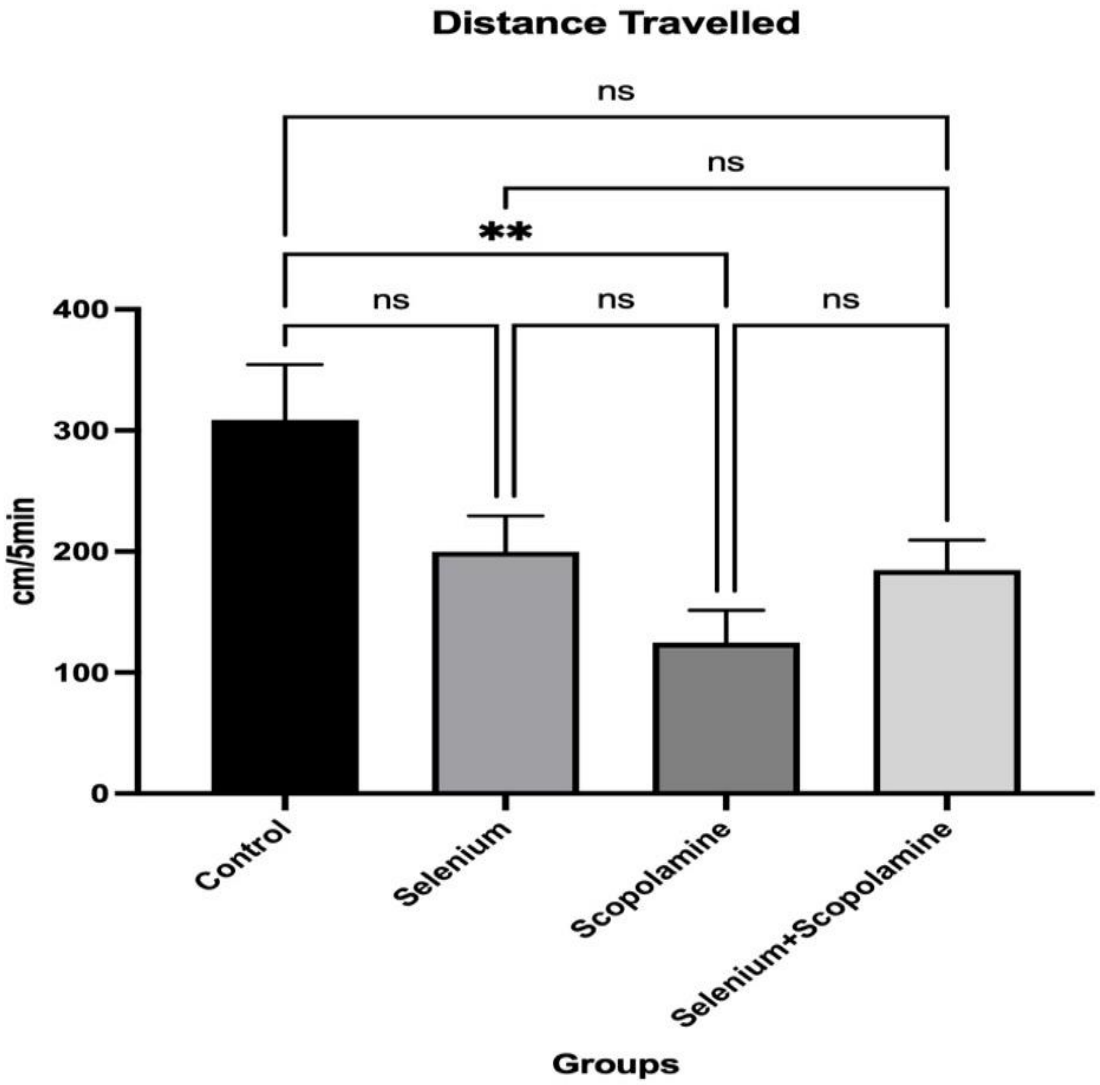

Figure 4.1.1. Graphs comparing distance traveled by the animals.
Saline treated control group (C), selenium injected (SE), scopolamine injected (SC), scopolamine and selenium injected (T) groups (*$p<0.05$, ***$p<0.01$, ns $p>0.05$.)

Table 4.1.1. Table of Distance Traveled Statistics

Distance Travelled				
Tukey's multiple comparisons test	Mean 1	Mean 2	Mean Diff.	P Value
Control vs. Selenium	300,4	199,8	100,6	0,1682
Control vs. Scopolamine	300,4	124,8	175,6	0,0073
Control vs. Selenium+Scopolamine	300,4	184,6	115,8	0,0944
Selenium vs. Scopolamine	199,8	124,8	75	0,3893
Selenium vs. Selenium+Scopolamine	199,8	184,6	15,2	0,987
Scopolamine vs. Selenium+Scopolamine	124,8	184,6	-59,8	0,5749

4.1.2. Stereotypic Activity

As anticipated, animals in Sc Group have the lowest stereotypic activity compared to C, Se and T Groups ($p<0.001$, $p<0.0001$ and $p<0.05$ respectively). However, after selenium treatment, it had been observed that animals in T group have experienced an increase in their stereotypic activity compared to Sc Group($p<0.05$). Even though there is no statistical significance, stereotypic activity of the animals in T group is lower than C group. Moreover, an increase of stereotypic activity was seen in animals treated only with selenium when compared to C Group without any statistical significance.

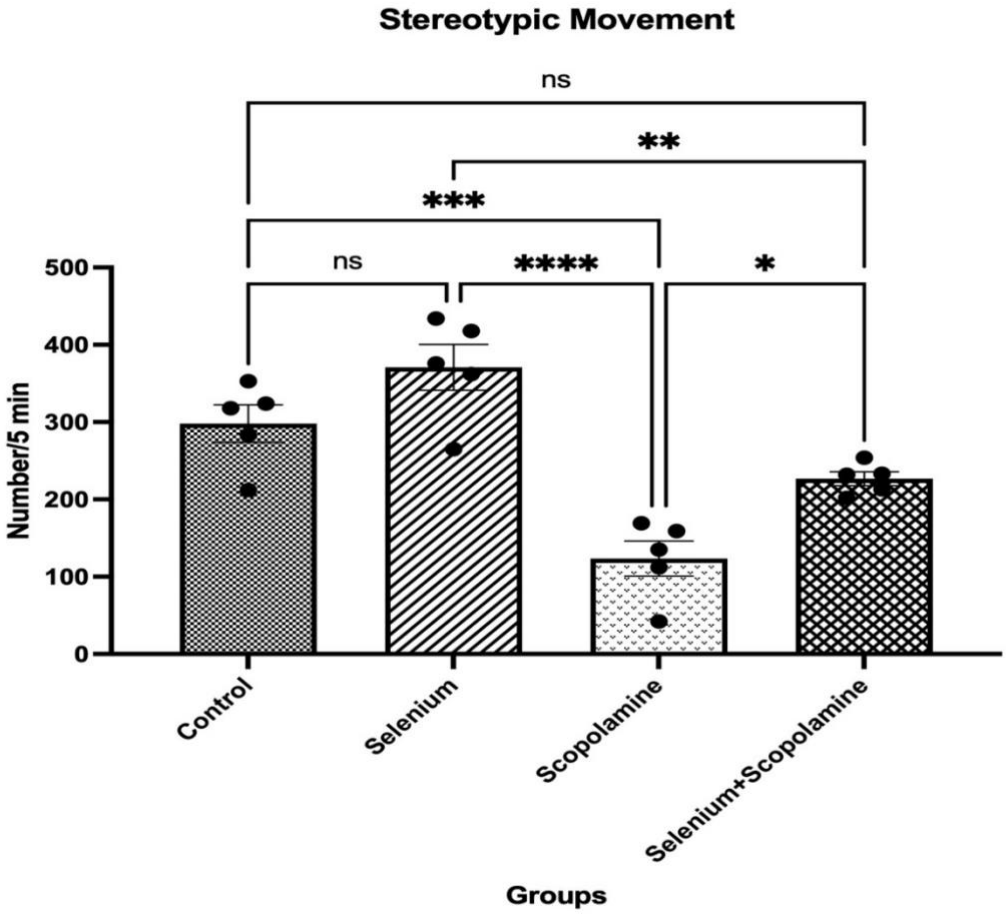

Figure 4.1.2. Graphs comparing stereotypic movement of animals.
Saline treated control group (C), selenium injected (SE), scopolamine injected (SC), scopolamine, and selenium injected (T) groups. Data are presented as the number of stereotypic movements in 5 minutes. (*$p<0.05$, ***$p<0.01$, ns $p>0.05$.)

Table 4.1.2. Table of Stereotypic Activity Statistics

Stereotypic Activity				
Tukey's multiple comparisons test	Mean 1	Mean 2	Mean Diff,	P Value
Control vs. Selenium	291,4	295,6	-4,2	0,9991
Control vs. Scopolamine	291,4	141,4	150	0,0011
Control vs. Selenium+Scopolamine	291,4	226,8	64,6	0,2112
Selenium vs. Scopolamine	295,6	141,4	154,2	0,0008
Selenium vs. Selenium+Scopolamine	295,6	226,8	68,8	0,1699
Scopolamine vs. Selenium+Scopolamine	141,4	226,8	-85,4	0,0664

4.1.3. Ambulatory Activity

Ambulatory activity of Sc group has significantly decreased ($p<0.01$) compared to C Group. Ambulatory activities of the animals in Se group and T group have also slightly dropped compared to C group, though there was no statistical significance calculated for both groups. Animals in Sc group had lower ambulatory activity rates compared to Se and T groups ($p<0.01$, $p<0.05$ respectively). Nonetheless, subsequent to the selenium treatment, ambulatory activity of T Group has significantly increased compared to Sc group ($p<0.05$).

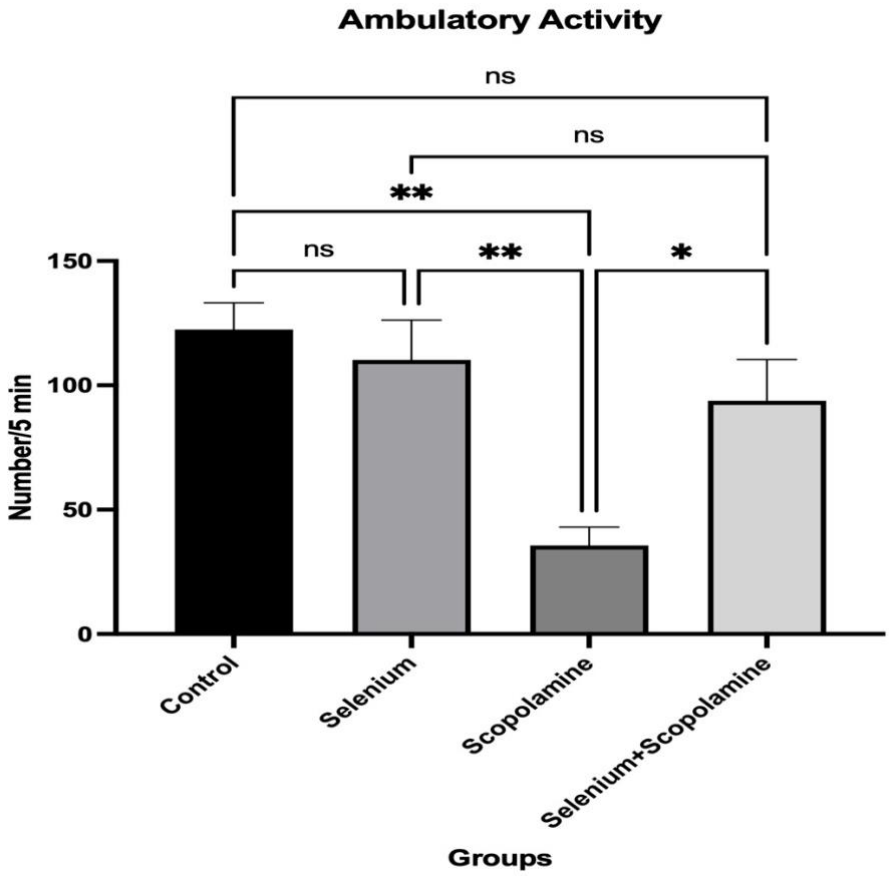

Figure 4.1.3. Graphs comparing ambulatory movement of animals
Saline treated control group (C), selenium injected (SE), scopolamine injected (SC), scopolamine and selenium injected (T) groups. (*p<0.05, ***p<0.01, ns p>0.05.)

Table 4.1.3. Table of Ambulatory Activity Statistics

Ambulatory Activity				
Tukey's multiple comparisons test	Mean 1	Mean 2	Mean Diff,	P Value
Control vs. Selenium	122,4	110,2	12,2	0,9139
Control vs. Scopolamine	122,4	93,8	28,6	0,4466
Control vs. Selenium+Scopolamine	122,4	35,6	86,8	0,0014
Selenium vs. Scopolamine	110,2	93,8	16,4	0,818
Selenium vs. Selenium+Scopolamine	110,2	35,6	74,6	0,0054
Scopolamine vs. Selenium+Scopolamine	93,8	35,6	58,2	0,0313

4.1.4. Horizontal Activity

In line with the measurements before the decapitation of the animals, horizontal activity of Sc group duly decreased compared to C group ($p<0.0001$). Similarly, a slight decrease was observed in the horizontal activities of the animals in Se group and T group compared to C group (ns, $p<0.01$ respectively). T group has a lower horizontal activity compared to Se group ($p<0.05$). On the other hand, selenium treatment increased horizontal activity in T group resulting in a higher horizontal activity rate compared to Sc group, yet there was no statistical significance calculated.

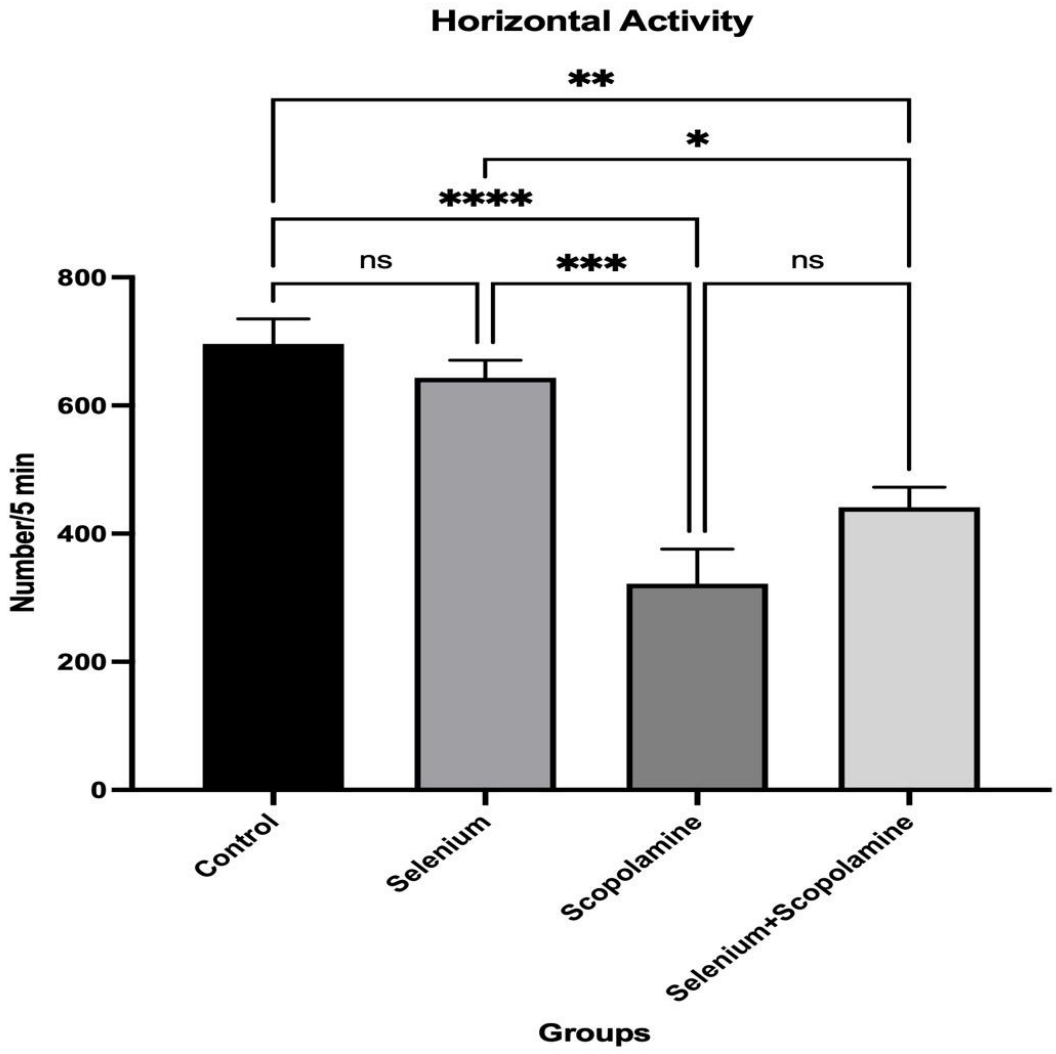

Figure 4.1.4. Graphs comparing horizontal movement of animals.
Saline treated control group (C), selenium injected (SE), scopolamine injected (SC), scopolamine and selenium injected (T) groups. (*$p<0.05$, ***$p<0.01$, ns $p>0.05$.)

Table 4.1.4. Table of Horizontal Activity Statistics

Horizontal Activity				
Tukey's multiple comparisons test	Mean 1	Mean 2	Mean Diff,	P Value
Control vs. Selenium	696,2	643,4	52,8	0,7803
Control vs. Scopolamine	696,2	321,8	374,4	<0,0001
Control vs. Selenium+Scopolamine	696,2	441,2	255	0,0016
Selenium vs. Scopolamine	643,4	321,8	321,6	0,0002
Selenium vs. Selenium+Scopolamine	643,4	441,2	202,2	0,0109
Scopolamine vs. Selenium+Scopolamine	321,8	441,2	-119,4	0,1822

4.1.5. Vertical Activity

Expectedly, Sc group has the lowest rate of vertical activity compared to group C, group Se and group T ($p<0.001$, $p<0.001$ and ns respectively). No important differences were observed between group C and group Se, also no statistical significance was calculated. However, when group Se is compared to group T, it can be seen that animals in group T have lower vertical activity than the animals in group Se ($p<0.05$). Although selenium treatment slightly increased the vertical activity rate of group T compared to group Sc, there was no statistical significance calculated.

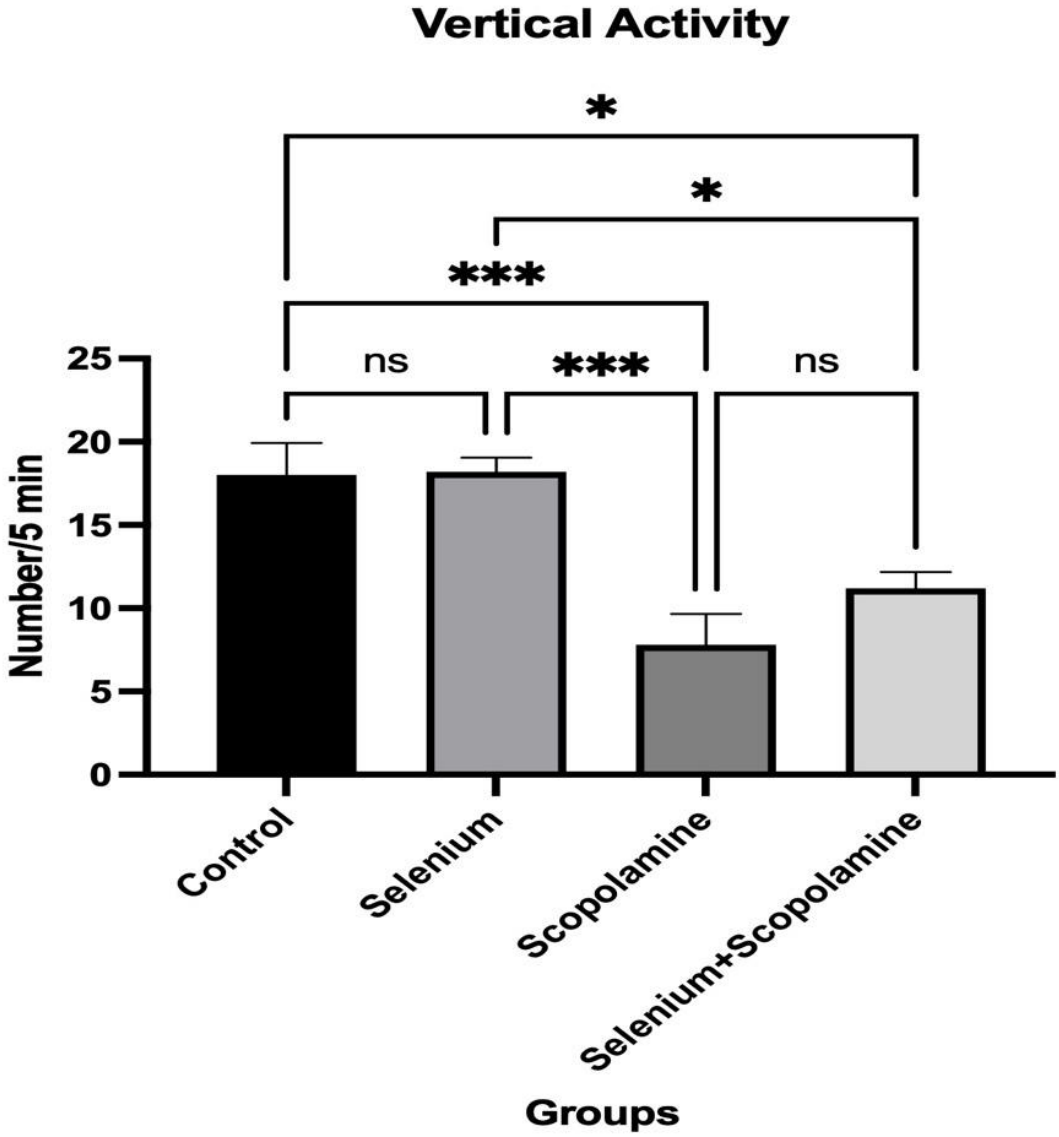

Figure 4.1.4. Graphs comparing vertical movement of animals
Saline treated control group (C), selenium injected (SE), scopolamine injected (SC), scopolamine and selenium injected (T) groups. (*p<0.05, ***p<0.01, ns p>0.05.)

Table 4.1.5. Table of Vertical Activity Statistics

Vertical Activity				
Tukey's multiple comparisons test	Mean 1	Mean 2	Mean Diff,	P Value
Control vs. Selenium	18	18,2	-0,2	0,9997
Control vs. Scopolamine	18	7,8	10,2	0,0009
Control vs. Selenium+Scopolamine	18	11,2	6,8	0,0239
Selenium vs. Scopolamine	18,2	7,8	10,4	0,0007
Selenium vs. Selenium+Scopolamine	18,2	11,2	7	0,0198
Scopolamine vs. Selenium+Scopolamine	7,8	11,2	-3,4	0,3963

4.2. HISTOLOGY

Amyloid beta and TUNEL positive neurons were counted in cerebral cortex and hippocampus. Moreover, VEGF and iNOS positive neurons were demonstrated in 10x, 20x, 40x objective. Finally, hematoxylin and eosin, silver and cresyl violet stainings were conducted in order to observe general histopathological changes.

4.2.1. Hematoxylin Eosin Staining

Hematoxylin&Eosin staining were performed in order to histopathologically examine the tissues According to evaluation of H&E stained sections; amyloid plaques and neurofibrillary tangles were determined in SC and T group sections in compared to C and SE groups. These abnormalities were observed most densely in SC group whereas they are less densely seen in T group. On the other hand, no abnormalities were observed in C and SE groups.

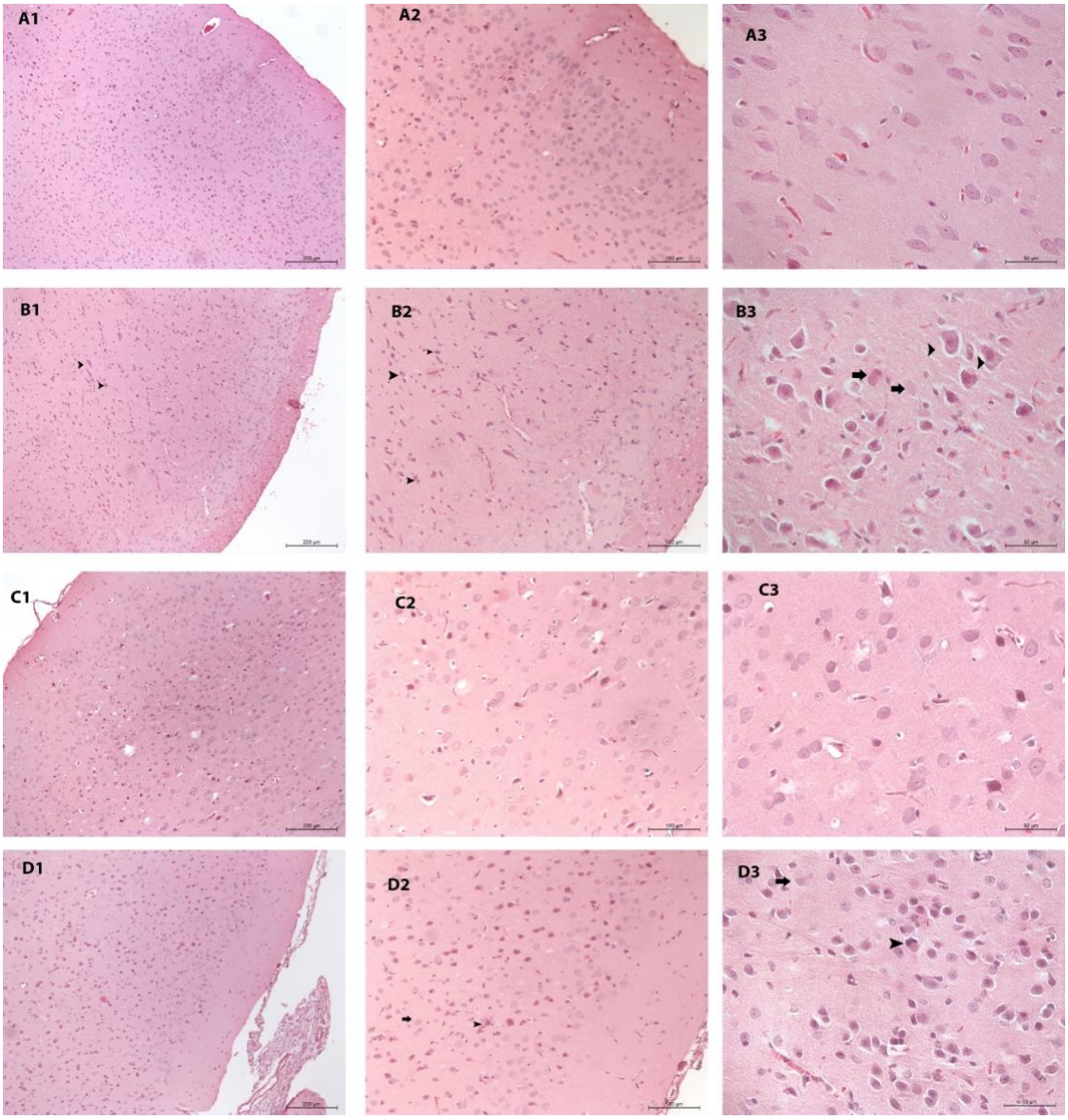

Figure 4.2.1.1. Photomicrographs demonstrate Hematoxylin&Eosin staining in the cerebral cortex.
A1, A2, A3 represents saline treated control group (C), B1, B2, B3 scopolamine injected (SC), C1, C2, C3 represents selenium injected (SE), D1, D2, D3 represents scopolamine, and selenium injected (T) groups. The magnification is x10, x20, x40 left to right, respectively. Scale bar represents 200 μm in x10, 100 μm in x20, 50 μm in x40. Arrowheads indicates neurofibrillary tangles while arrows indicate amyloid plaques.

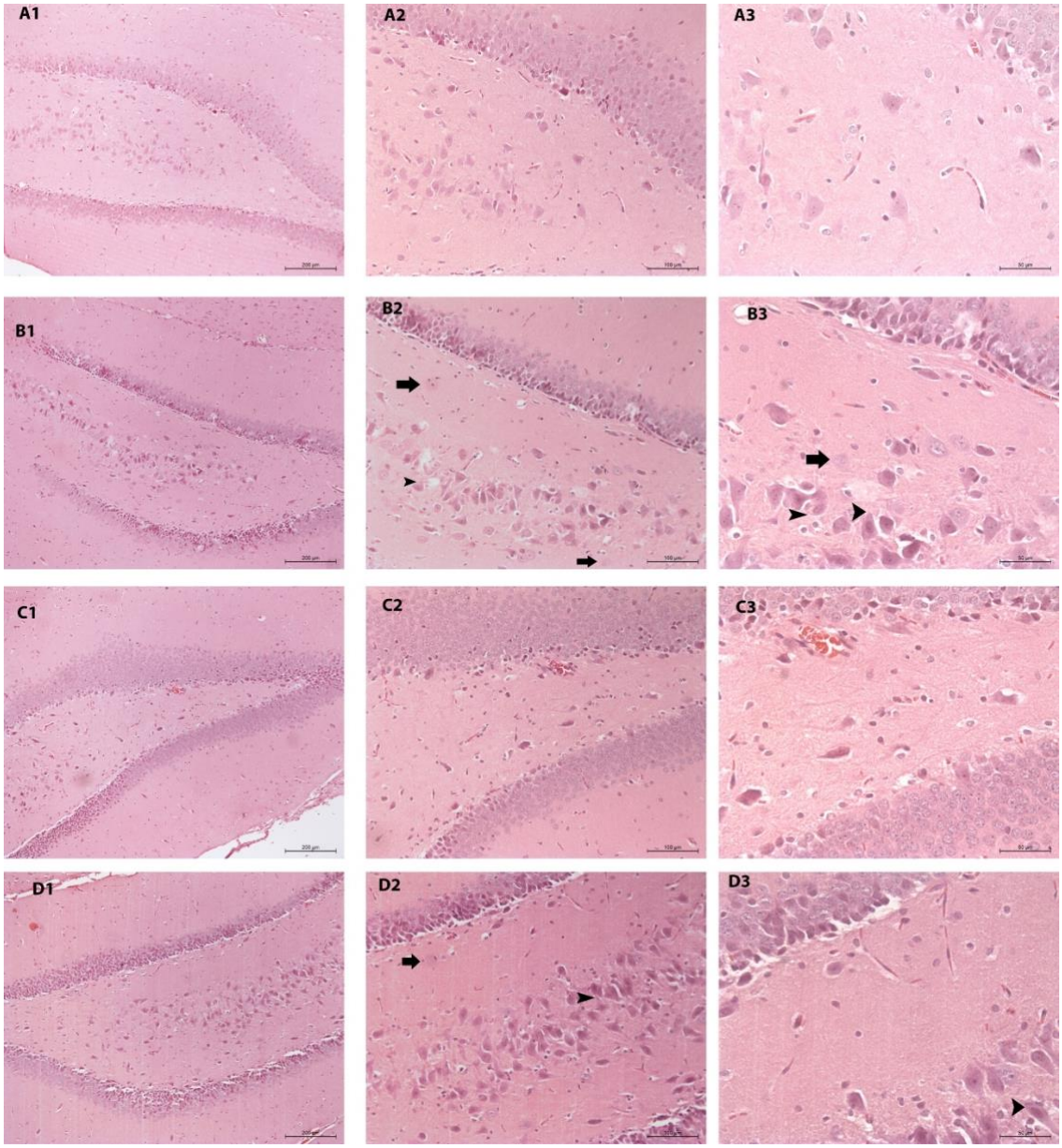

Figure 4.2.1.2 Photomicrographs demonstrate Hematoxylin&Eosin staining in the hippocampus.
A1, A2, A3 represents saline treated control group (C), B1, B2, B3 scopolamine injected (SC), C1, C2, C3 represents selenium injected (SE), D1, D2, D3 represents scopolamine, and selenium injected (T) groups. The magnification is x10, x20, x40 left to right, respectively. Scale bar represents 200 μm in x10, 100 μm in x20, 50 μm in x40. Arrowheads indicates neurofibrillary tangles while arrows indicate amyloid plaques.

4.2.2. Cresyl Violet Staining

Cresyl Violet were performed in order to histopathologically examine the tissues. According to evaluation of Cresyl Violet stained sections, amyloid plaques and neurofibrillary tangles were determined in SC and T group sections in compared to C and SE groups. These abnormalities were observed most densely in SC group whereas they are less densely seen in T group. On the other hand, no abnormalities were observed in C and SE groups.

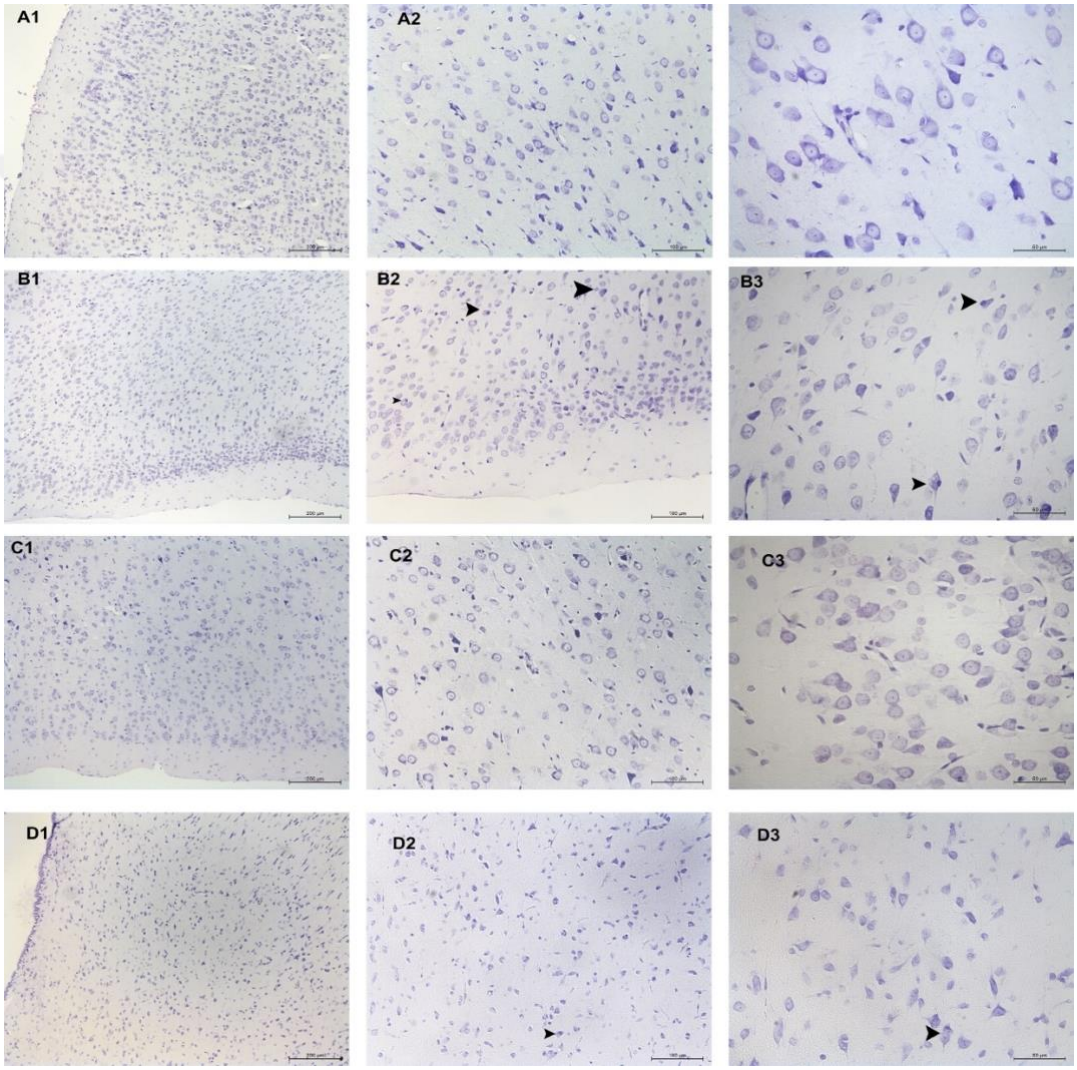

Figure 4.2.1.3. Photomicrographs demonstrate Cresyl Violet staining in the cerebral cortex.
A1, A2, A3 represents saline treated control group (C), B1, B2, B3 scopolamine injected (SC), C1, C2, C3 represents selenium injected (SE), D1, D2, D3 represents scopolamine, and selenium injected (T) groups. The magnification is x10, x20, x40 left to right, respectively. Scale bar represents 200 μm in x10, 100 μm in x20, 50 μm in x40. Arrowheads indicates neurofibrillary tangles.

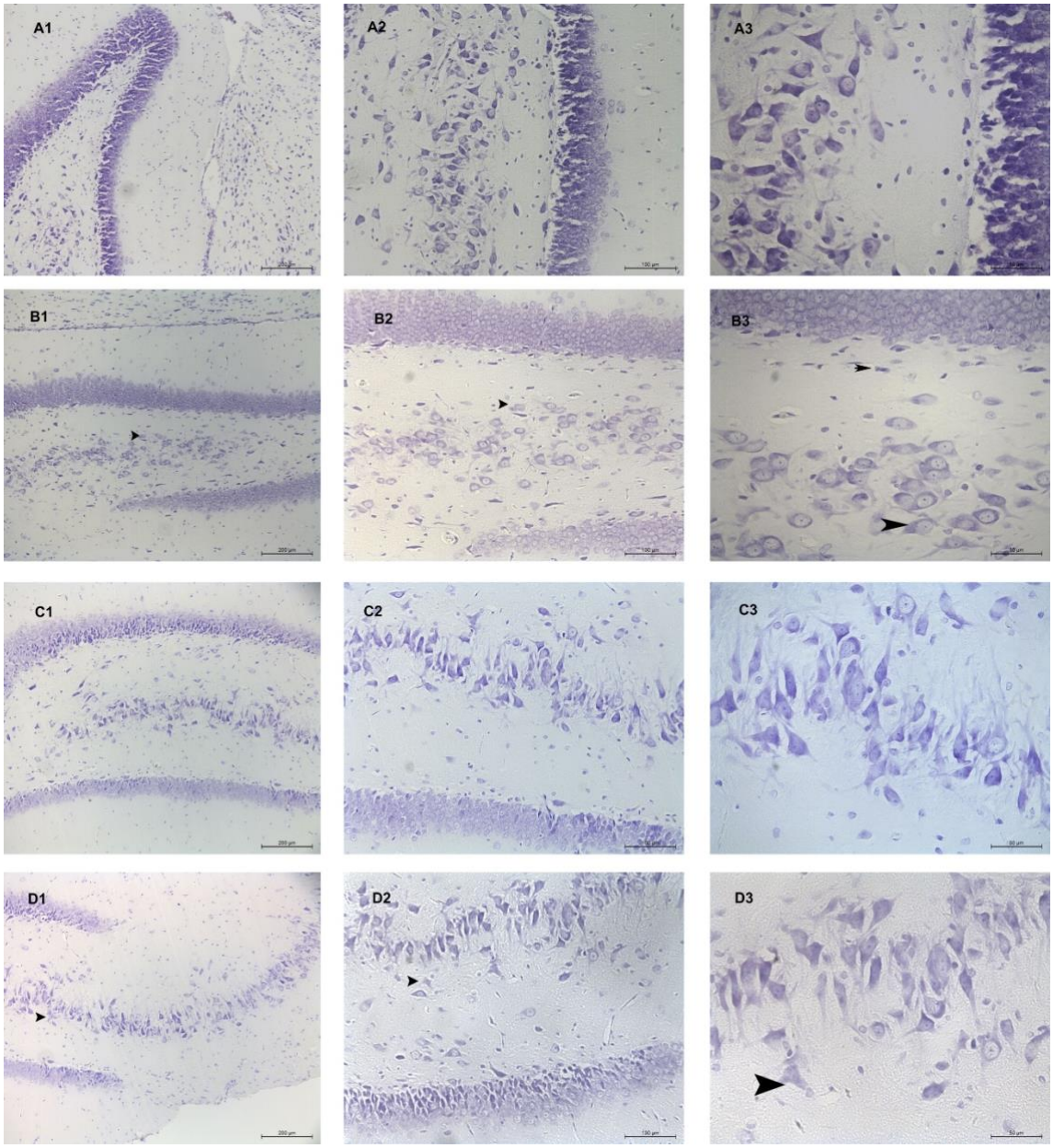

Figure 4.2.1.4. Photomicrographs demonstrate Cresyl Violet staining in hippocampus. A1, A2, A3 represents saline treated control group (C), B1, B2, B3 scopolamine injected (SC), C1, C2, C3 represents selenium injected (SE), D1, D2, D3 represents scopolamine, and selenium injected (T) groups. The magnification is x10, x20, x40 left to right, respectively. Scale bar represents 200 μm in x10, 100 μm in x20, 50 μm in x40. Arrowheads indicates neurofibrillary tangles.

4.2.3. Silver Staining

Silver staining were performed in order to histopathologically examine the tissues. According to evaluation of Silver stained sections, amyloid plaques and neurofibrillary tangles were determined in SC and T group sections in compare to C and SE groups. These abnormalities were observed most densely in SC group whereas they are less densely seen in T group. On the other hand, no abnormalities were observed in C and SE groups.

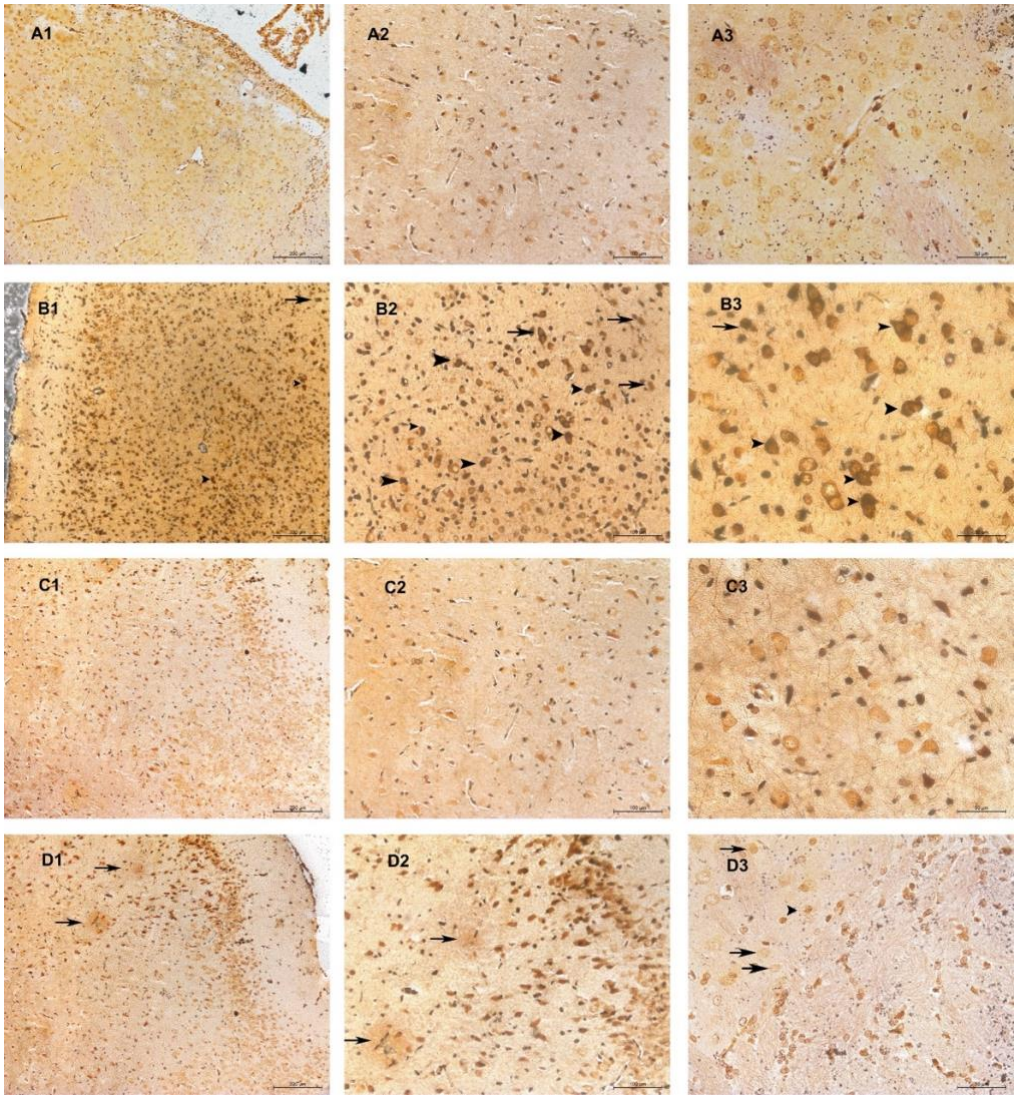

Figure 4.2.1.5. Photomicrographs demonstrate silver staining in Cerebral Cortex. A1, A2, A3 represents Saline treated control group (C), B1, B2, B3 scopolamine injected (SC), C1, C2, C3 represents selenium injected (SE), D1, D2, D3 represents scopolamine, and selenium injected (T) groups. The magnification is x10, x20, x40 left to right, respectively. Scale bar represents 200 μm in x10, 100 μm in x20, 50 μm in x40. Arrowheads indicates neurofibrillary tangles while arrows indicate amyloid plaques.

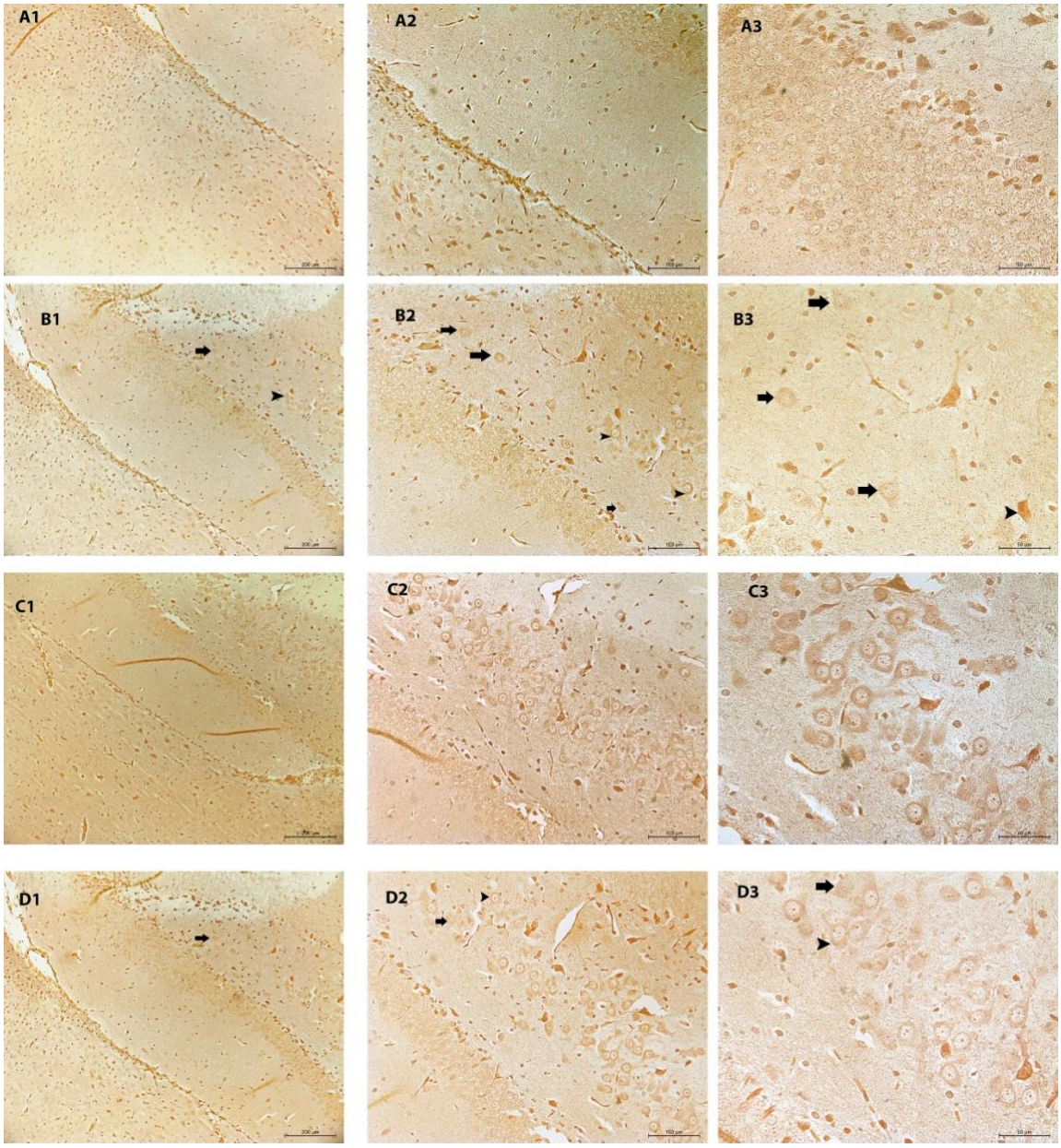

Figure 4.2.1.6. Photomicrographs demonstrate silver staining in hippocampus. A1, A2, A3 represents Saline treated control group (C), B1, B2, B3 scopolamine injected (SC), C1, C2, C3 represents selenium injected (SE), D1, D2, D3 represents scopolamine, and selenium injected (T) groups. The magnification is x10, x20, x40 left to right, respectively. Scale bar represents 200 µm in x10, 100 µm in x20, 50 µm in x40. Arrowheads indicates neurofibrillary tangles while arrows indicate amyloid plaques.

4.2.2. TUNEL Assay

Coronal sections from all the groups were examined for TUNEL positive neurons. TUNEL assay gives reliable data on the number of apoptotic neurons. Photomicrographs demonstrate sections taken from the cerebral cortex and hippocampus. Apoptotic Index ($P<0.05$) were calculated for all groups.

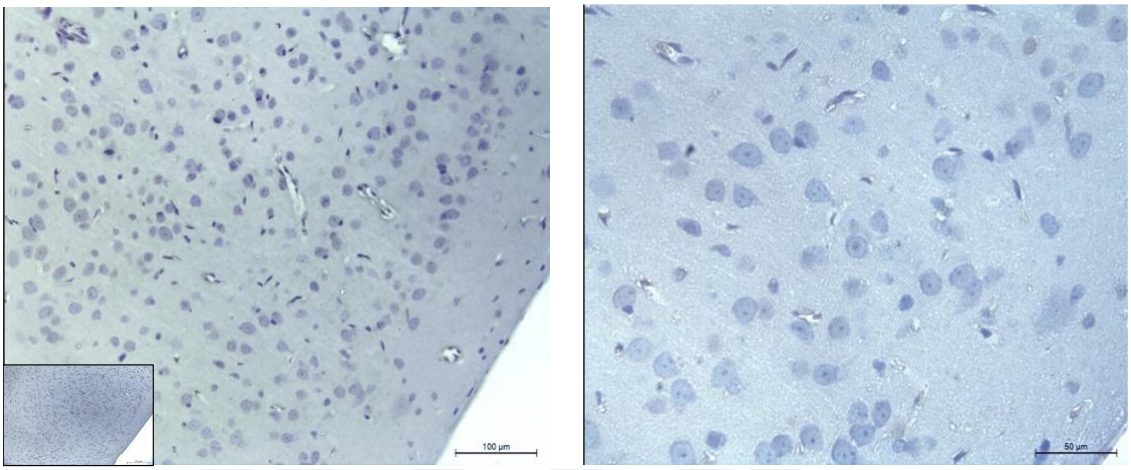

Figure 4.2.2.1. Photomicrographs demonstrate TUNEL negative control

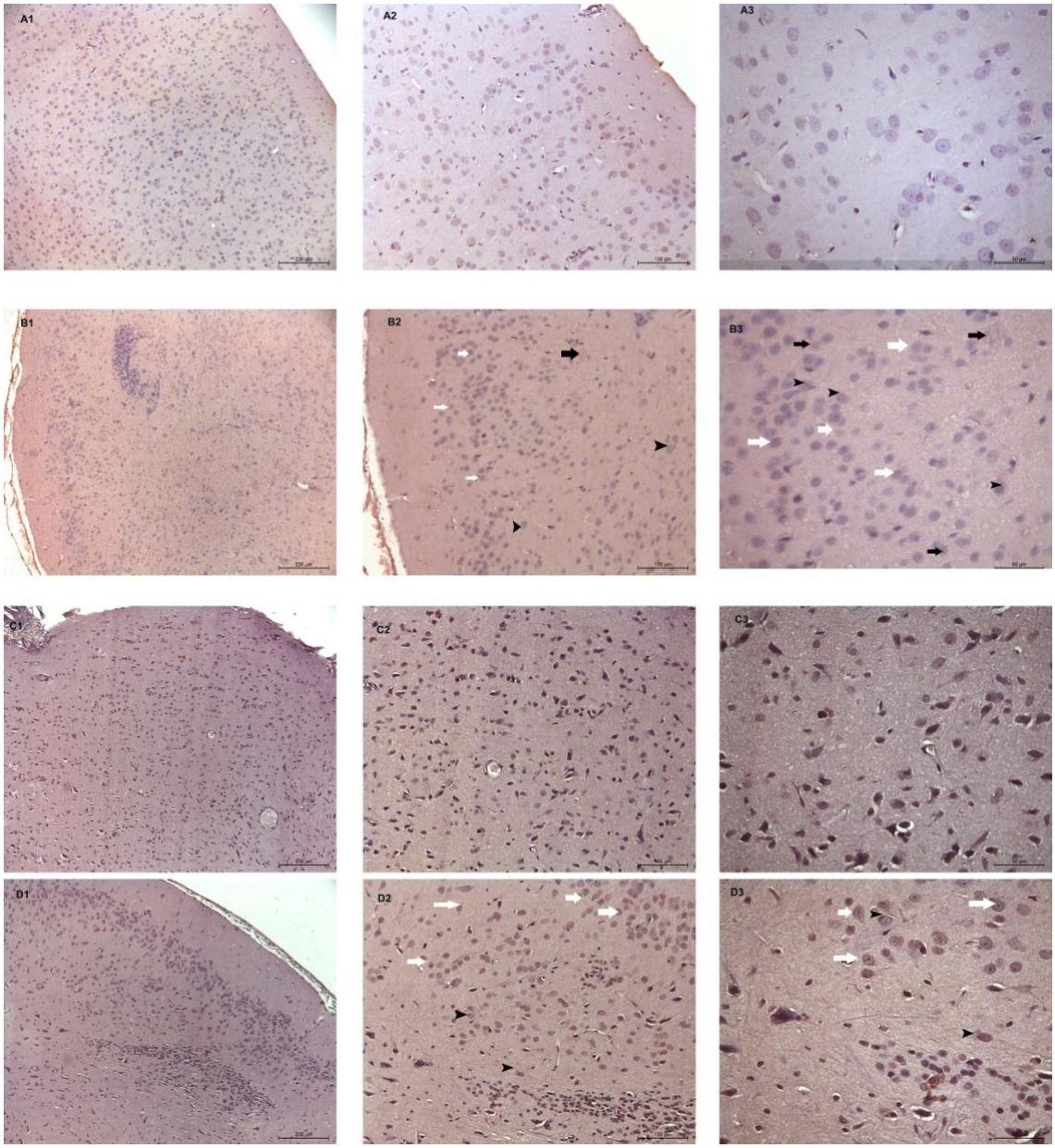

Figure 4.2.2.2. Photomicrographs demonstrate TUNEL positive cells in the cerebral cortex.
A1, A2, A3 represents saline treated control group (C),B1, B2, B3 scopolamine injected (SC), C1, C2, C3 represents selenium injected (SE), D1,D2, D3 represents scopolamine, and selenium injected (T) groups. The magnification is x10, x20, x40 left to right, respectively. Scale bar represents 200 μm in x100 ,100 μm in x20, 50 μm in x40. Arrowheads indicates neurofibrillary tangles while black arrows indicate amyloid plaques, white arrows indicate apoptotic cells.

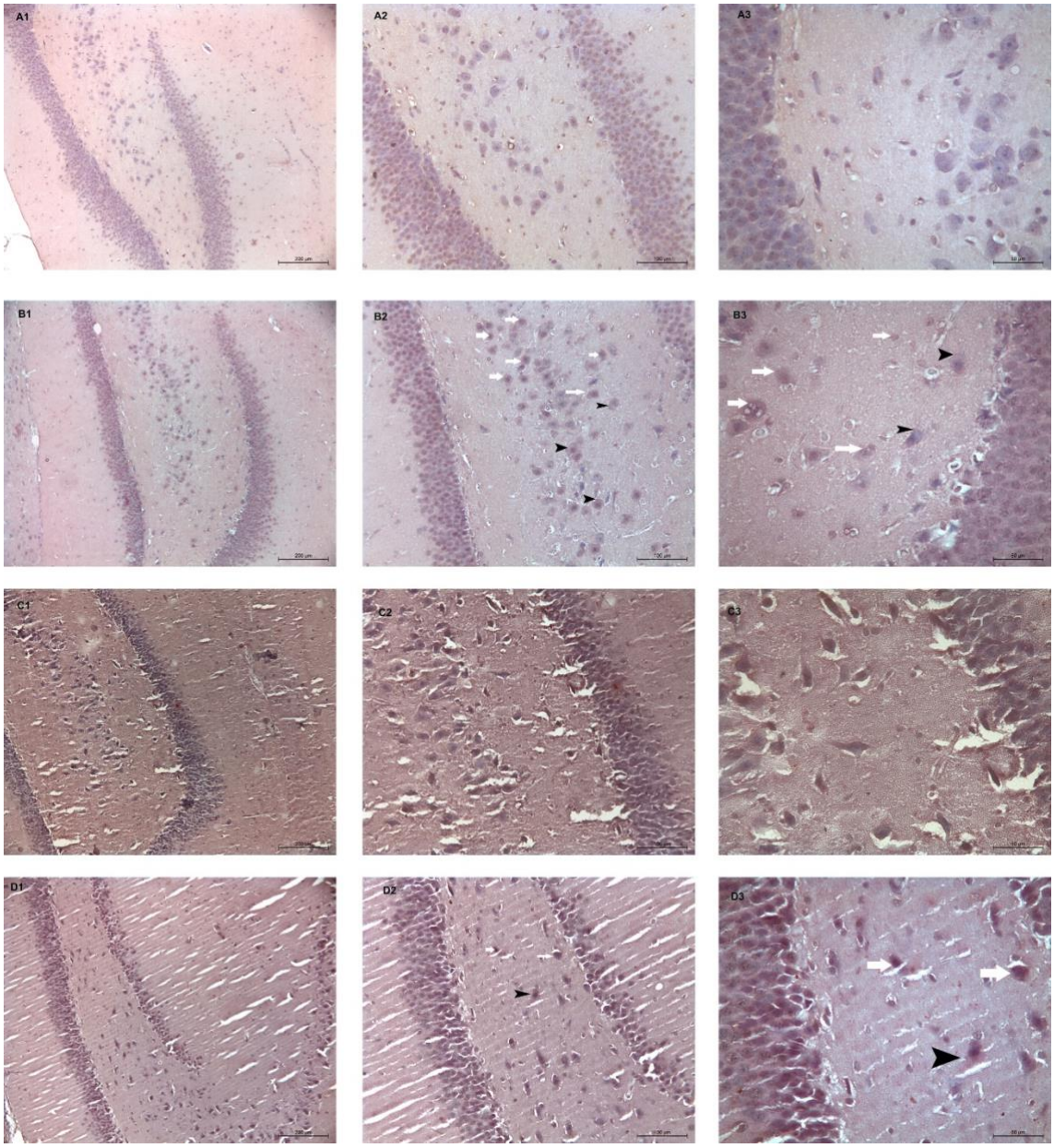

Figure 4.2.2.3. Photomicrographs demonstrate TUNEL positive cells in the hippocampus.
A1, A2, A3 represents Saline treated control group (C), B1, B2, B3 scopolamine injected (SC), C1, C2, C3 represents selenium injected (SE), D1, D2, D3 represents scopolamine, and selenium injected (T) groups. The magnification is x10, x20, x40 left to right, respectively. Scale bar represents 200 μm in x10, 100 μm in x20, 50 μm in x40. Arrowheads indicates neurofibrillary tangles while black arrows indicate amyloid plaques, white arrows indicate apoptotic cells.

.

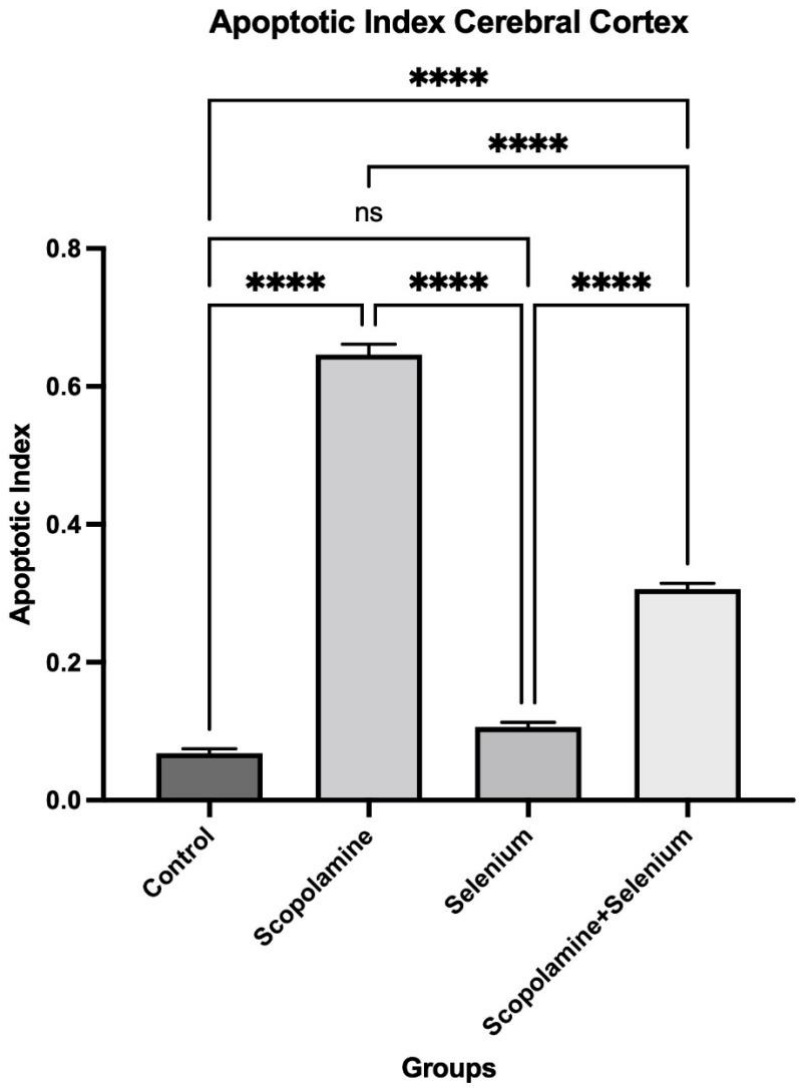

Figure 4.2.2.4. Graph of Apoptotic Index for Cerebral Cortex (P<0.05)

When comparing the apoptotic index of cerebral cortex, it can be said that Sc Group and T Group have a higher apoptotic index for than Group C (p<0,0001, p<0,0001 respectively). T Group has a lower the apoptotic index than Sc Group(p<0,0001) for cerebral cortex. The apoptotic index of Group Sc in cerebral cortex region is relatively higher than the Group Se (p<0,0001) according to Tukey's Multiple Comparison Test.

Table 4.2.2.1. Table of Apoptotic Index for Cerebral Cortex

Apoptotic Index Cerebral Cortex				
Tukey's multiple comparisons test	Mean 1	Mean 2	Mean Diff	P Value
Control vs. Scopolamine	0,068	0,646	-0,578	<0,0001
Control vs. Selenium	0,068	0,106	-0,038	0,0704
Control vs. Scopolamine+Selenium	0,068	0,306	-0,238	<0,0001
Scopolamine vs. Selenium	0,646	0,106	0,54	<0,0001
Scopolamine vs. Scopolamine+Selenium	0,646	0,306	0,34	<0,0001
Selenium vs. Scopolamine+Selenium	0,106	0,306	-0,2	<0,0001

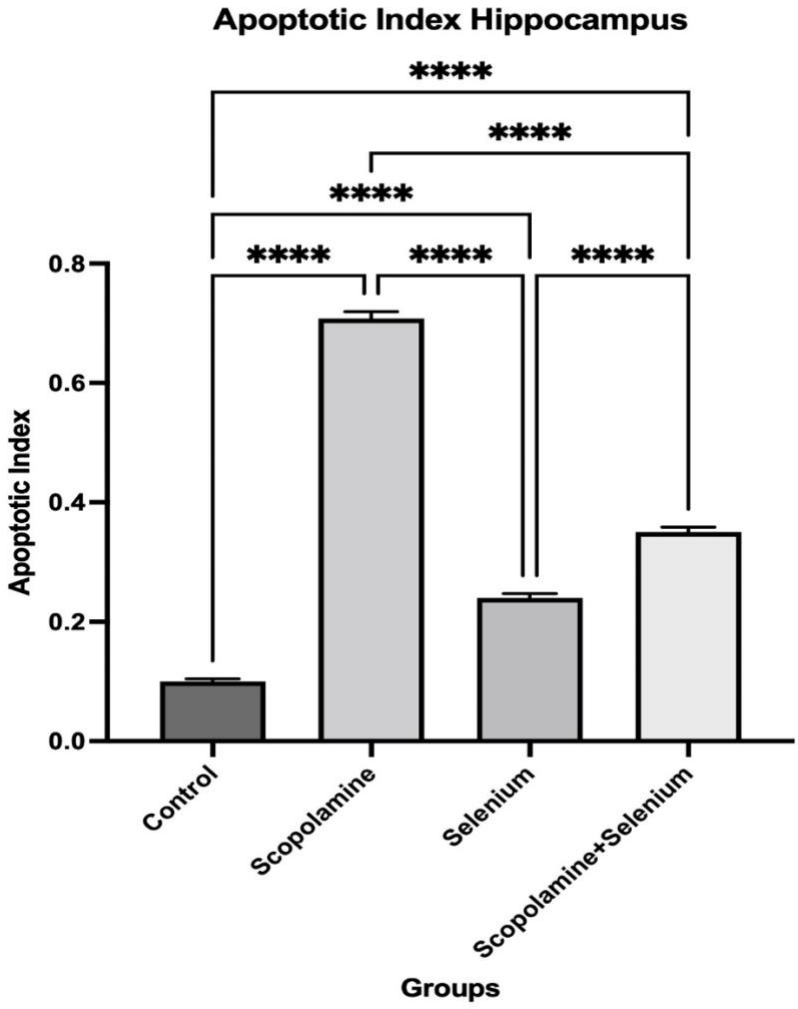

Figure 4.2.2.5. Graph of Apoptotic Index for Hippocampus(P<0.05)

Having looked at the the apoptotic index of hippocampus, it can be said that Sc Group and T Group have a higher apoptotic index for than Group C ($p<0,0001$, $p<0,0001$ respectively). T Group has a lower the apoptotic index than Sc Group ($p<0,0001$) for hippocampus. Sc Group in hippocampus region has a higher the apoptotic index than the Se Group of hippocampus ($p<0,0001$) according to Tukey's Multiple Comparison Test.

Table 4.2.2.4. Table of Apoptotic Index for Hippocampus

Apoptotic Index Hippocampus				
Tukey's multiple comparisons test	Mean 1	Mean 2	Mean Diff	P Value
Control vs. Scopolamine	0,1	0,708	-0,608	<0,0001
Control vs. Selenium	0,1	0,24	-0,14	<0,0001
Control vs. Scopolamine+Selenium	0,1	0,35	-0,25	<0,0001
Scopolamine vs. Selenium	0,708	0,24	0,468	<0,0001
Scopolamine vs. Scopolamine+Selenium	0,708	0,35	0,358	<0,0001
Selenium vs. Scopolamine+Selenium	0,24	0,35	-0,11	<0,0001

4.2.3. Immunohistochemistry for iNOS

Coronal sections from all of the groups were examined for iNOS immunoreactive neurons. Photomicrographs demonstrate sections taken from the cerebral cortex and hippocampus stained with iNOS Immunohistochemistry. H-scores were calculated for all groups.

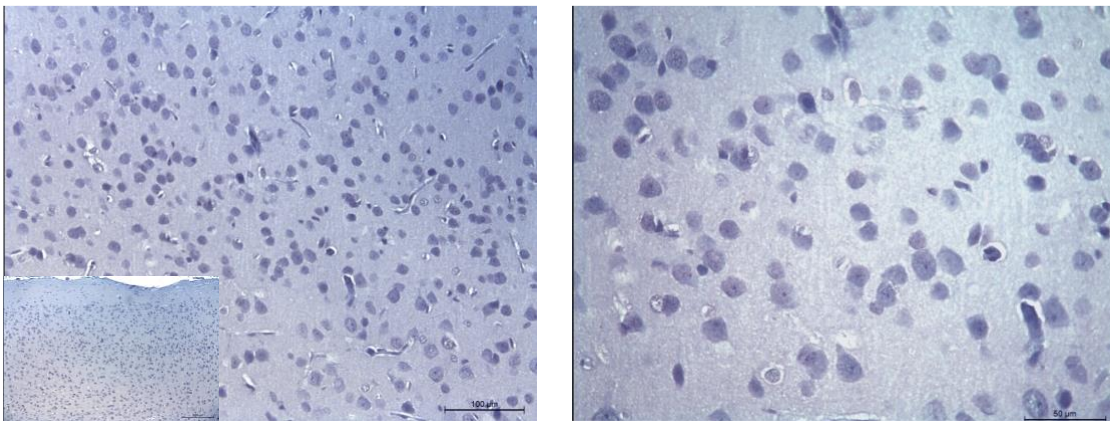

Figure 4.2.3.1. Photomicrographs demonstrate iNOS negative control

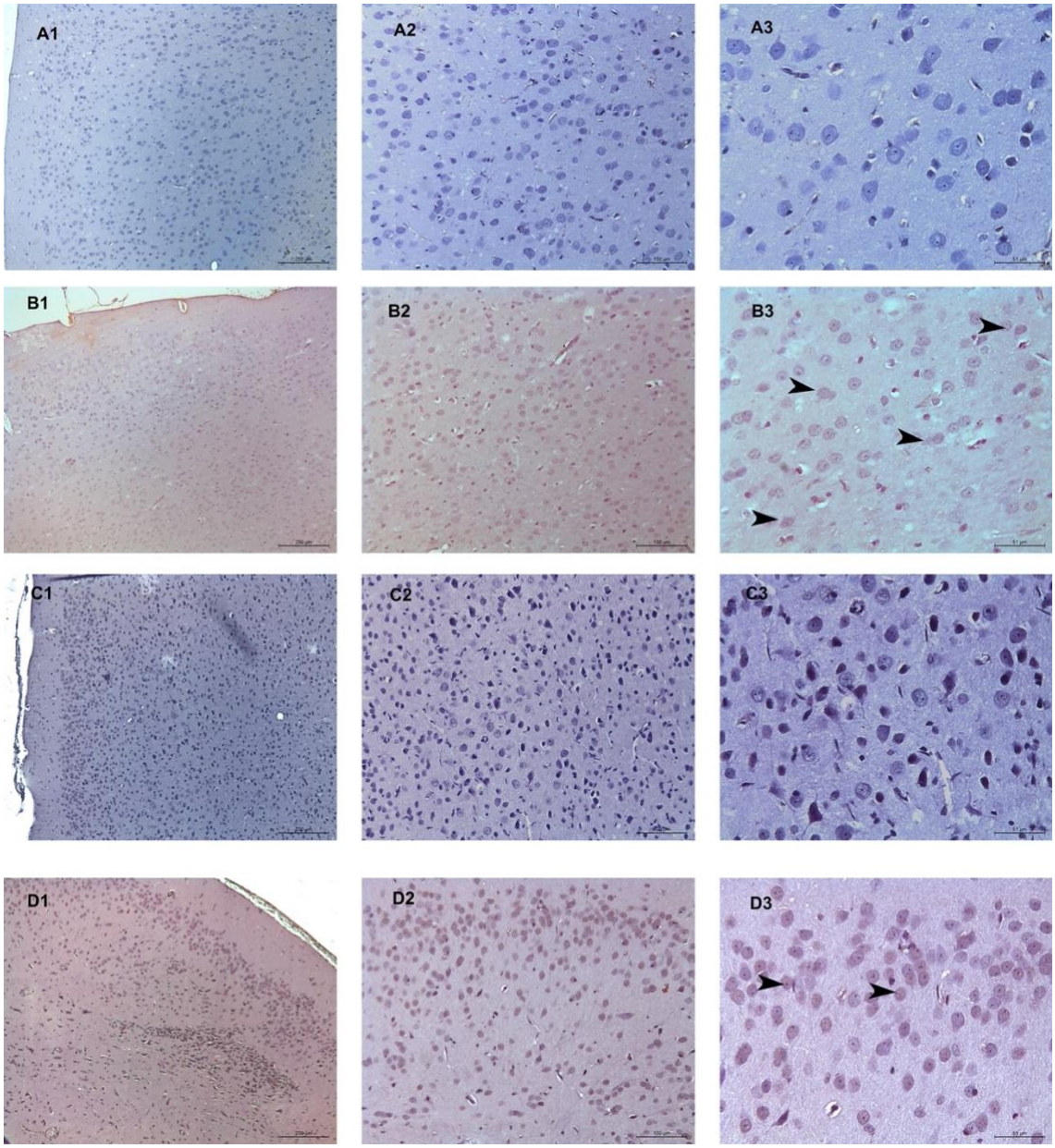

Figure 4.2.3.2. Photomicrographs demonstrate iNOS immunoreactivity in the cerebral cortex.
A1, A2, A3 represents Saline treated control group (C), B1, B2, B3 scopolamine injected (SC), C1, C2, C3 represents selenium injected (SE), D1, D2, D3 represents scopolamine, and selenium injected (T) groups. The magnification is x10, x20, x40 left to right, respectively. Scale bar represents 200 μm in x10, 100 μm in x20, 50 μm in x40. Arrowheads indicates neurofibrillary tangles while arrows indicate amyloid plaques.

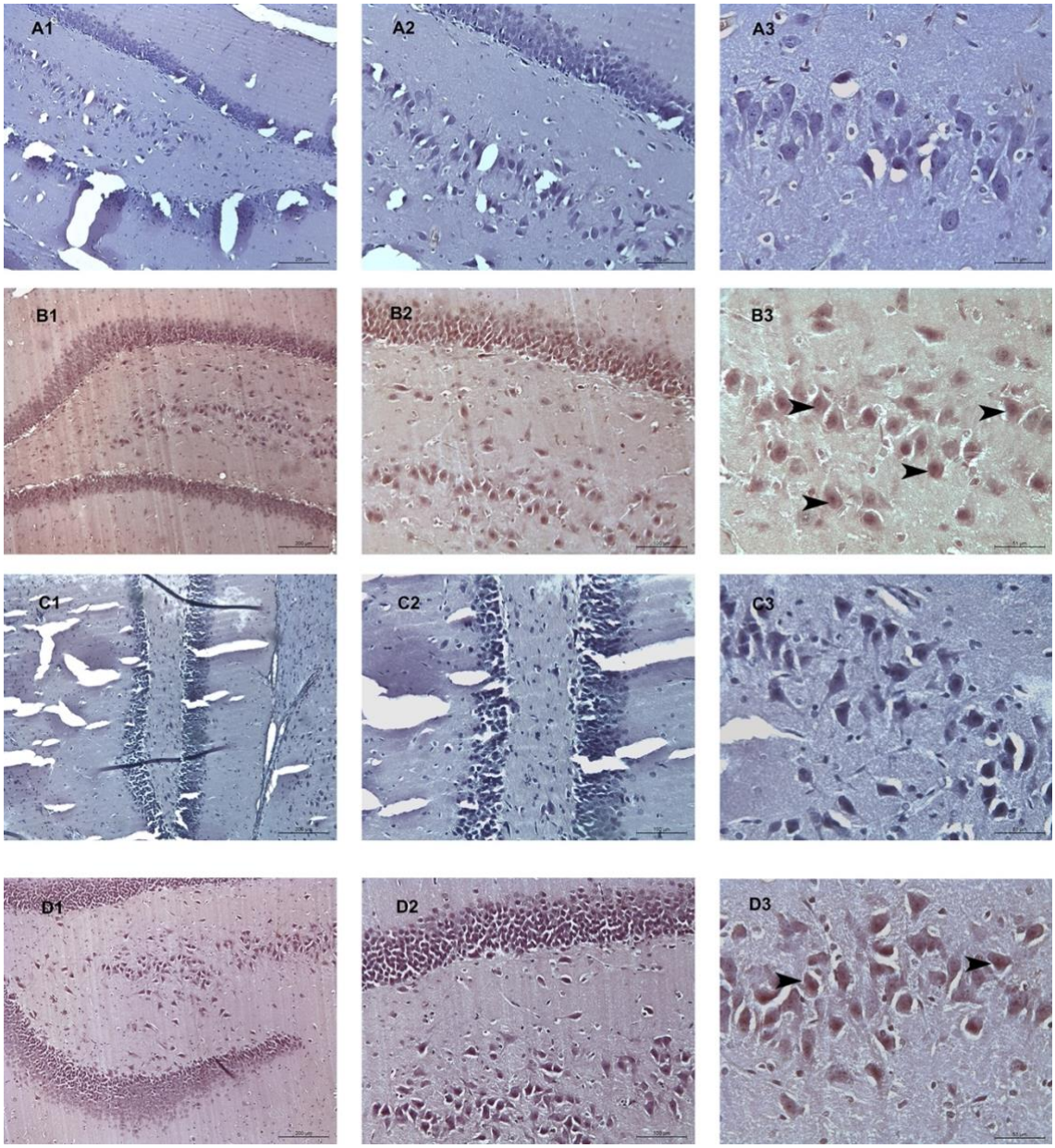

Figure 4.2.3.3 Photomicrographs demonstrate iNOS immunoreactivity in the hippocampus.
A1, A2, A3 represents Saline treated control group (C), B1, B2, B3 scopolamine injected (SC), C1, C2, C3 represents selenium injected (SE), D1, D2, D3 represents scopolamine, and selenium injected (T) groups. The magnification is x10, x20, x40 left to right, respectively. Scale bar represents 200 μm in x10, 100 μm in x20, 50 μm in x40. Arrowheads indicates neurofibrillary tangles while arrows indicate amyloid plaques.

Table 4.2.3.1. Cerebral Cortex iNOS immunostaining H-score

Cerebral Cortex iNOS H-Score				
Tukey's multiple comparisons test	Mean 1	Mean 2	Mean Diff	P Value
Control vs. Scopolamine	31,6	46,10	-14,5	<0,0001
Control vs. Selenium	31,6	30,60	1,00	0,9376
Control vs. Scopolamine+Selenium	31,6	40,52	-8,92	0,0005
Scopolamine vs. Selenium	46,1	30,60	15,5	<0,0001
Scopolamine vs. Scopolamine+Selenium	46,1	40,52	5,58	0,0248
Selenium vs. Scopolamine+Selenium	30,6	40,52	-9,92	0,0002

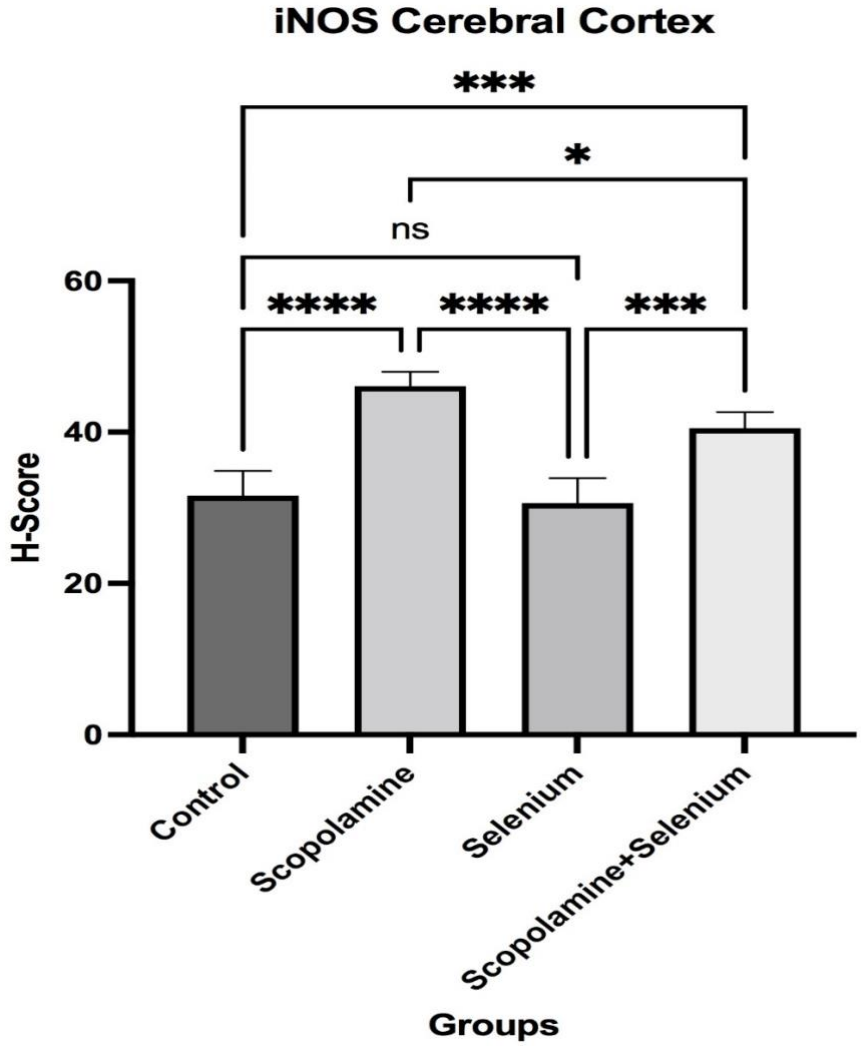

Figure 4.2.3.4. Graph of iNOS H-score Cerebral Cortex (P<0.05)

When comparing the H-Scores of cerebral cortex iNOS, it can be seen that Sc Group and T Group have a higher H-Score for iNOS than Group C, whereas Se Group has a slightly lower H-Score for iNOS ($p<0,0001$, $p=0,0005$, ns respectively). Sc Group has a higher H-Score for iNOS than Se Group ($p<0,0001$) T Group has a lower H-Score for iNOS immunochemistry than Sc Group for cerebral cortex($p=0,0248$).

Table 4.2.3.2 Hippocampus iNOS immunostaining H-score

Hippocampus iNOS H-Score				
Tukey's multiple comparisons test	Mean 1	Mean 2	Mean Diff	P Value
Control vs. Scopolamine	30,40	42,18	-11,78	<0,0001
Control vs. Selenium	30,40	30,84	-0,44	0,9906
Control vs. Scopolamine+Selenium	30,40	36,72	-6,32	0,0031
Scopolamine vs. Selenium	42,18	30,84	11,34	<0,0001
Scopolamine vs. Scopolamine+Selenium	42,18	36,72	5,46	0,0099
Selenium vs. Scopolamine+Selenium	30,84	36,72	-5,88	0,0056

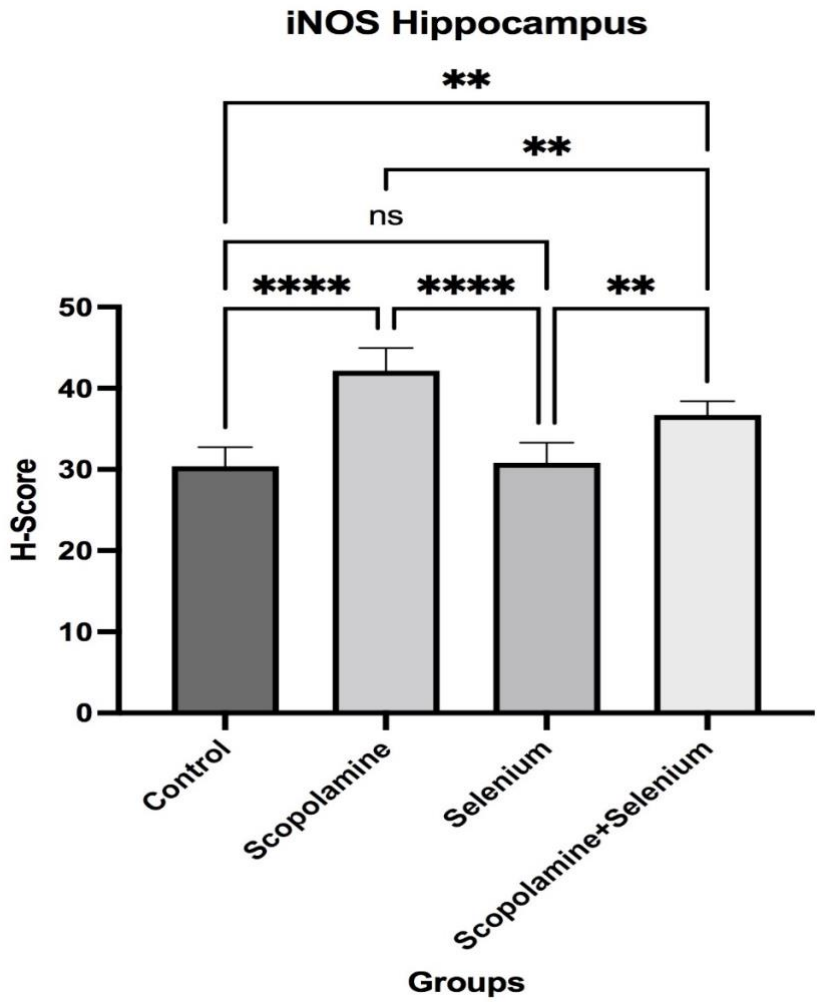

Figure 4.2.3.5. Graph of iNOS H-score Hippocampus(P<0.05)

Having looked at the the H-Scores of hippocampus iNOS, it can be seen that Sc Group and T Group have a higher H-Score for iNOS than Group C (p<0,0001, p=0,0031 respectively). Sc Group has a higher H-Score for iNOS than Se Group (p<0,0001) T Group has a lower H-Score for iNOS immunochemistry than Sc Group for hippocampus (p=0,0099). Sc Group in hippocampus region has a higher H-Score for iNOS immunochemistry than the Se Group of hippocampus (p<0,0001).

4.2.4. Immunohistochemistry for VEGF

Coronal sections from all of the groups were examined for VEGF immunoreactive neurons. Photomicrographs demonstrate sections taken from the cerebral cortex and hippocampus stained with VEGF Immunohistochemistry. H-scores were calculated for all groups.

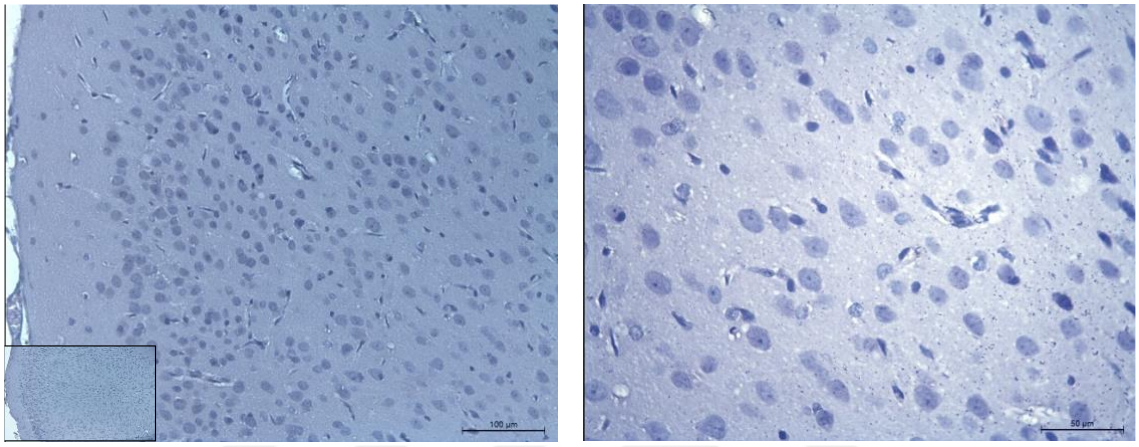

Figure 4.2.4.1. Photomicrographs demonstrate VEGF negative control

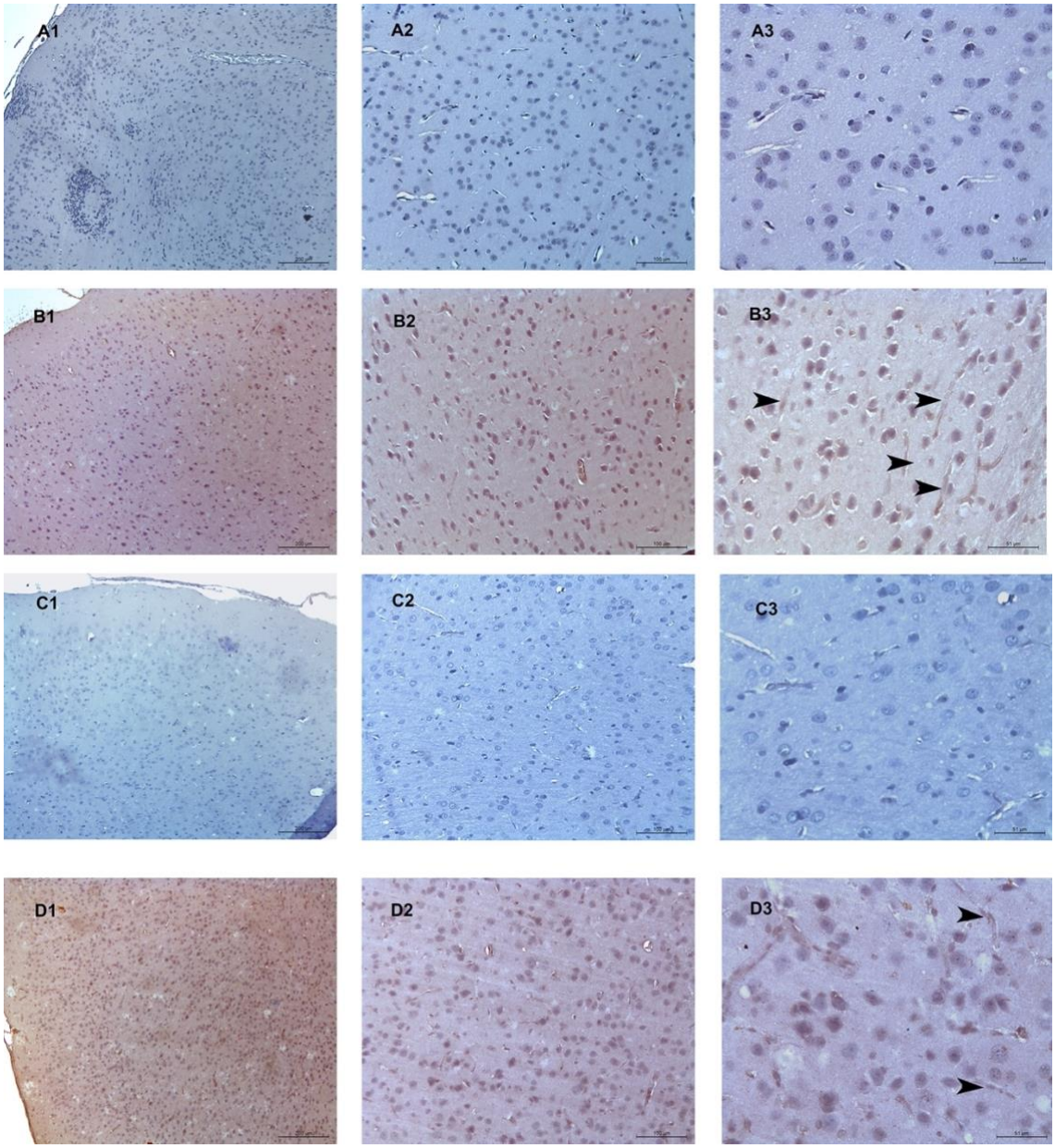

Figure 4.2.4.2. Photomicrographs demonstrate VEGF immunoreactivity in cerebral cortex
A1, A2, A3 represents Saline treated control group (C), B1, B2, B3 scopolamine injected (SC), C1, C2, C3 represents selenium injected (SE), D1, D2, D3 represents scopolamine, and selenium injected (T) groups. The magnification is x10, x20, x40 left to right, respectively. Scale bar represents 200 μm in x10, 100 μm in x20, 50 μm in x40. Arrowheads indicates neurofibrillary tangles while arrows indicate amyloid plaques.

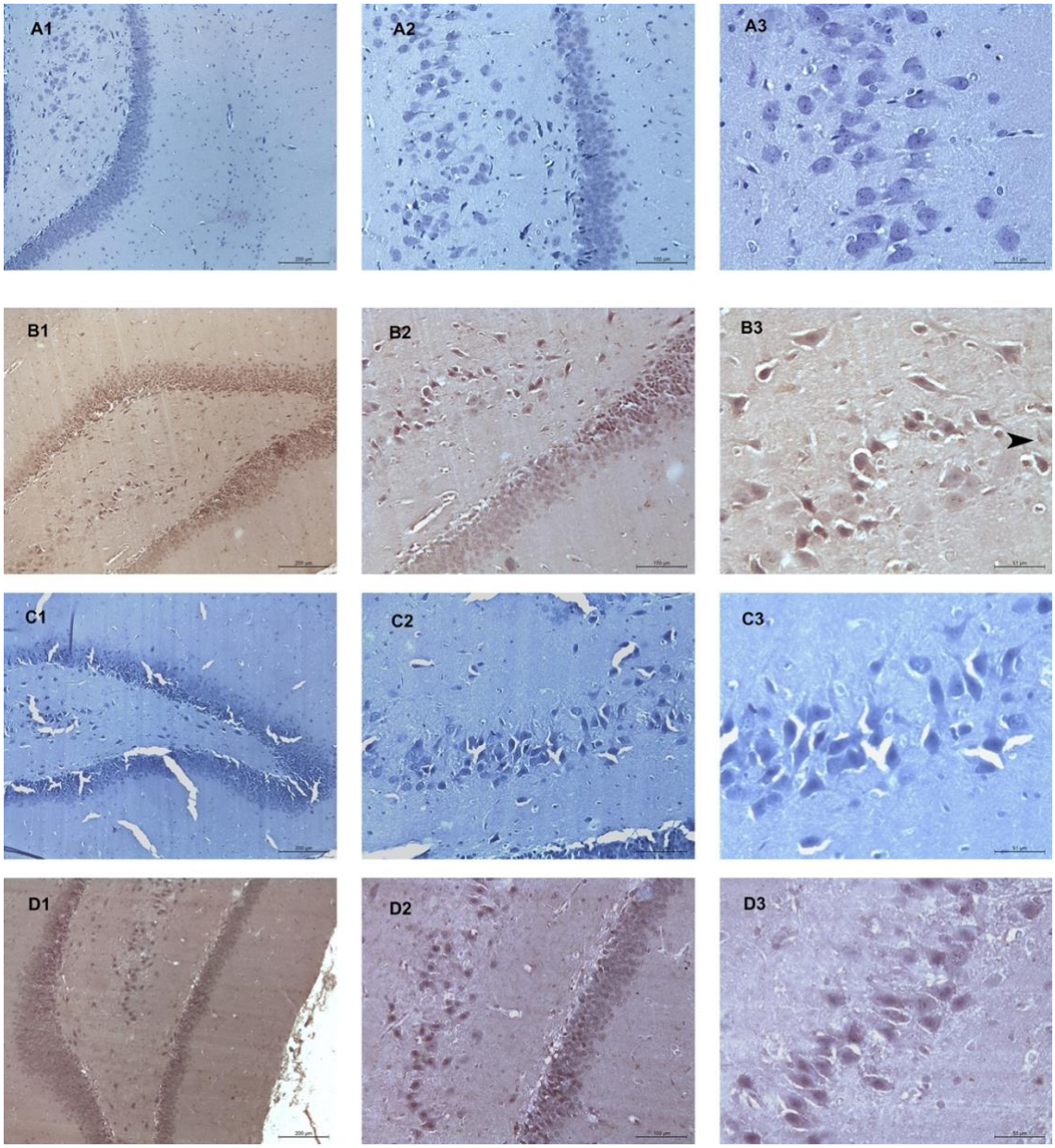

Figure 4.2.4.3. Photomicrographs demonstrate VEGF immunoreactivity in hippocampus.
A1, A2, A3 represents Saline treated control group (C), B1, B2, B3 scopolamine injected (SC), C1, C2, C3 represents selenium injected (SE), D1, D2, D3 represents scopolamine, and selenium injected (T) groups. The magnification is x10, x20, x40 left to right, respectively. Scale bar represents 200 μm in x10, 100 μm in x20, 50 μm in x40. Arrowheads indicates neurofibrillary tangles while arrows indicate amyloid plaques.

Table 4.2.4.1. Cerebral Cortex VEGF immunostaining H-score

Cerebral Cortex Vegf H-Score				
Tukey's multiple comparisons test	Mean 1	Mean 2	Mean Diff	P Value
Control vs. Scopolamine	26,16	35,30	-9,14	<0,0001
Control vs. Selenium	26,16	28,58	-2,42	0,1211
Control vs. Scopolamine+Selenium	26,16	31,12	-4,96	0,0009
Scopolamine vs. Selenium	35,30	28,58	6,72	<0,0001
Scopolamine vs. Scopolamine+Selenium	35,30	31,12	4,18	0,0041
Selenium vs. Scopolamine+Selenium	28,58	31,12	-2,54	0,0981

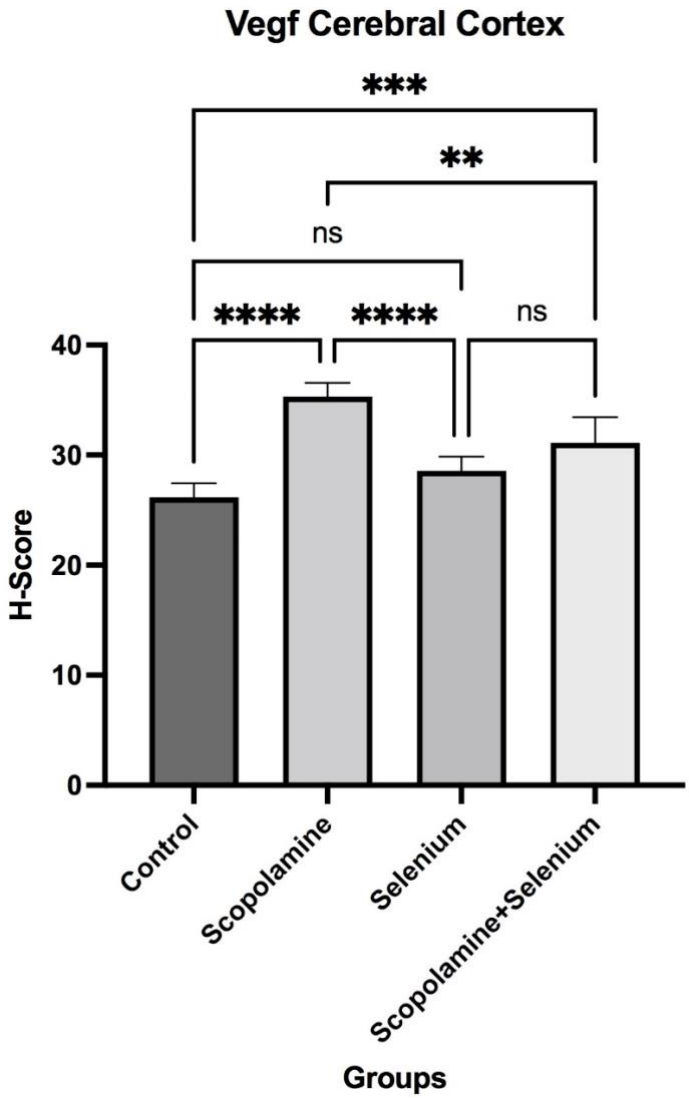

Figure 4.2.4.4. Graph of VEGF H-score Cerebral Cortex(P<0.05)

H-Score graphs of VEGF cerebral cortex C Group has a lower H-Score for VEGF than Group Sc, Group Se and Group T (p<0,0001, ns, 0,0009 respectively). H-Score for VEGF of Group T is slightly lower than H-Score for VEGF of Group Sc(p=0,0041). H-Score for VEGF of Group Sc in cerebral cortex region is considerably higher than the H-Score for VEGF of Group Se with a p value smaller than 0,0001 according to Tukey's multiple comparisons test.

Table 4.2.4.2. Hippocampus VEGF immunostaining H-score

Hippocampus Vegf H-Score				
Tukey's multiple comparisons test	Mean 1	Mean 2	Mean Diff	P Value
Control vs. Scopolamine	28,52	38,98	-10,46	<0,0001
Control vs. Selenium	28,52	31,58	-3,06	0,1615
Control vs. Scopolamine+Selenium	28,52	37,54	-9,02	<0,0001
Scopolamine vs. Selenium	38,98	31,58	7,40	0,0003
Scopolamine vs. Scopolamine+Selenium	38,98	37,54	1,44	0,7279
Selenium vs. Scopolamine+Selenium	31,58	37,54	-5,96	0,0027

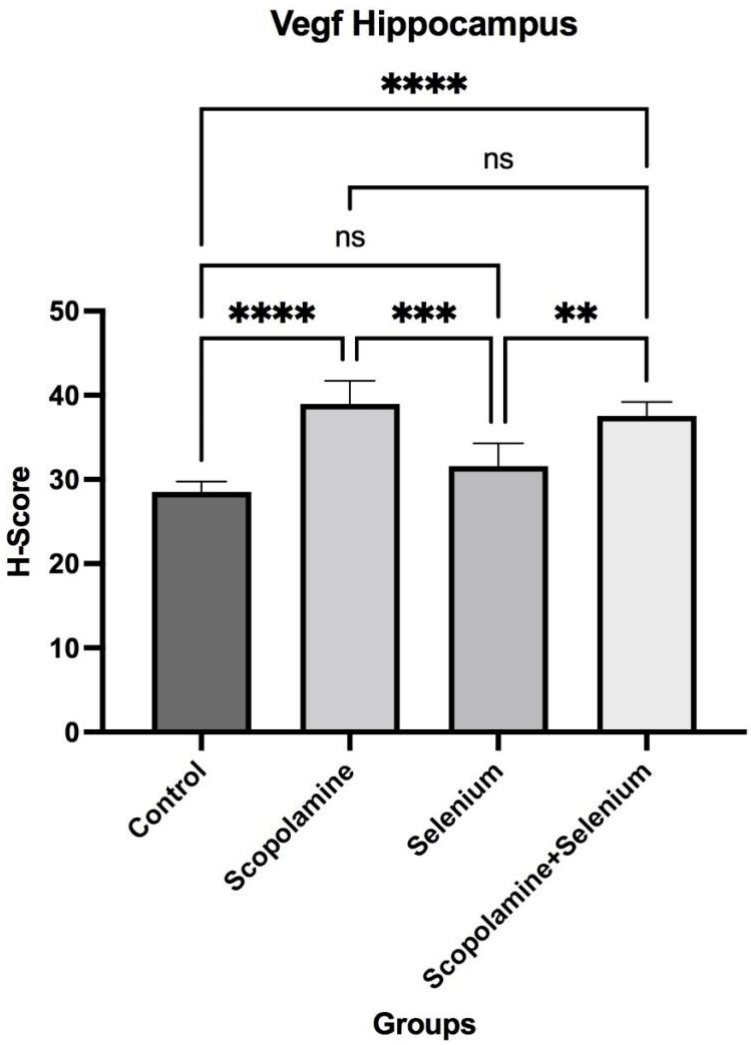

Figure 4.2.4.5. Graph of VEGF H-score Hippocampus(P<0.05)

H-Score for VEGF of C Group is also lower than Group Sc, Group Se and Group T in hippocampus region as well (p<0,0001, ns, p<0,0001 respectively). H-Score for VEGF of Group T is slightly lower than H-Score for VEGF of Group S in hippocampus region (p>0.05). H-Score for VEGF of Group Se is also significantly smaller than the H-Score for VEGF of Group Sc in hippocampus region with a p value of 0,0003 according to Tukey's multiple comparisons test.

4.2.5. Immunohistochemistry for Amyloid Beta

Coronal sections from all of the groups were examined for amyloid-beta immunoreactive neurons. Photomicrographs demonstrate sections taken from the cerebral cortex and hippocampus stained with Amyloid-beta Immunohistochemistry. H-scores were calculated for all groups. (Figure 4.2 and Figure 4.2.).

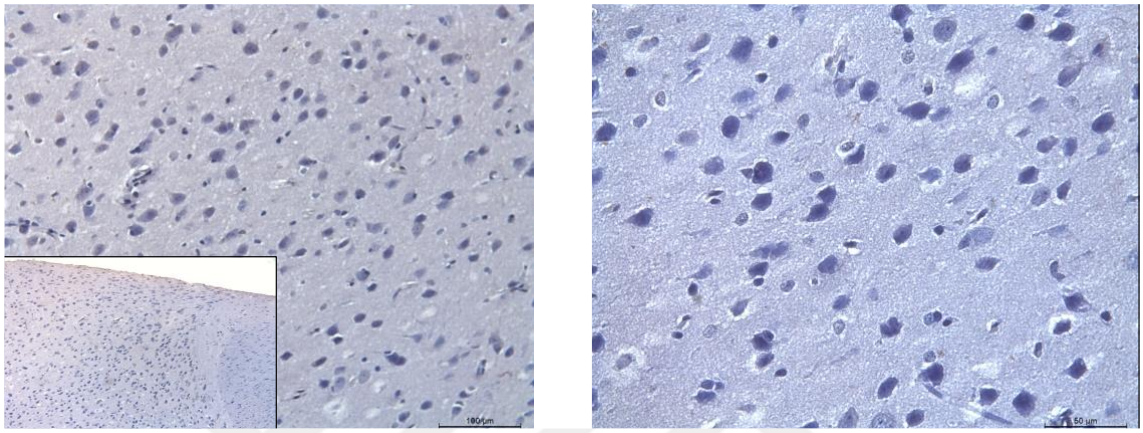

Figure 4.2.5.1. Photomicrographs demonstrate Amyloid beta negative control

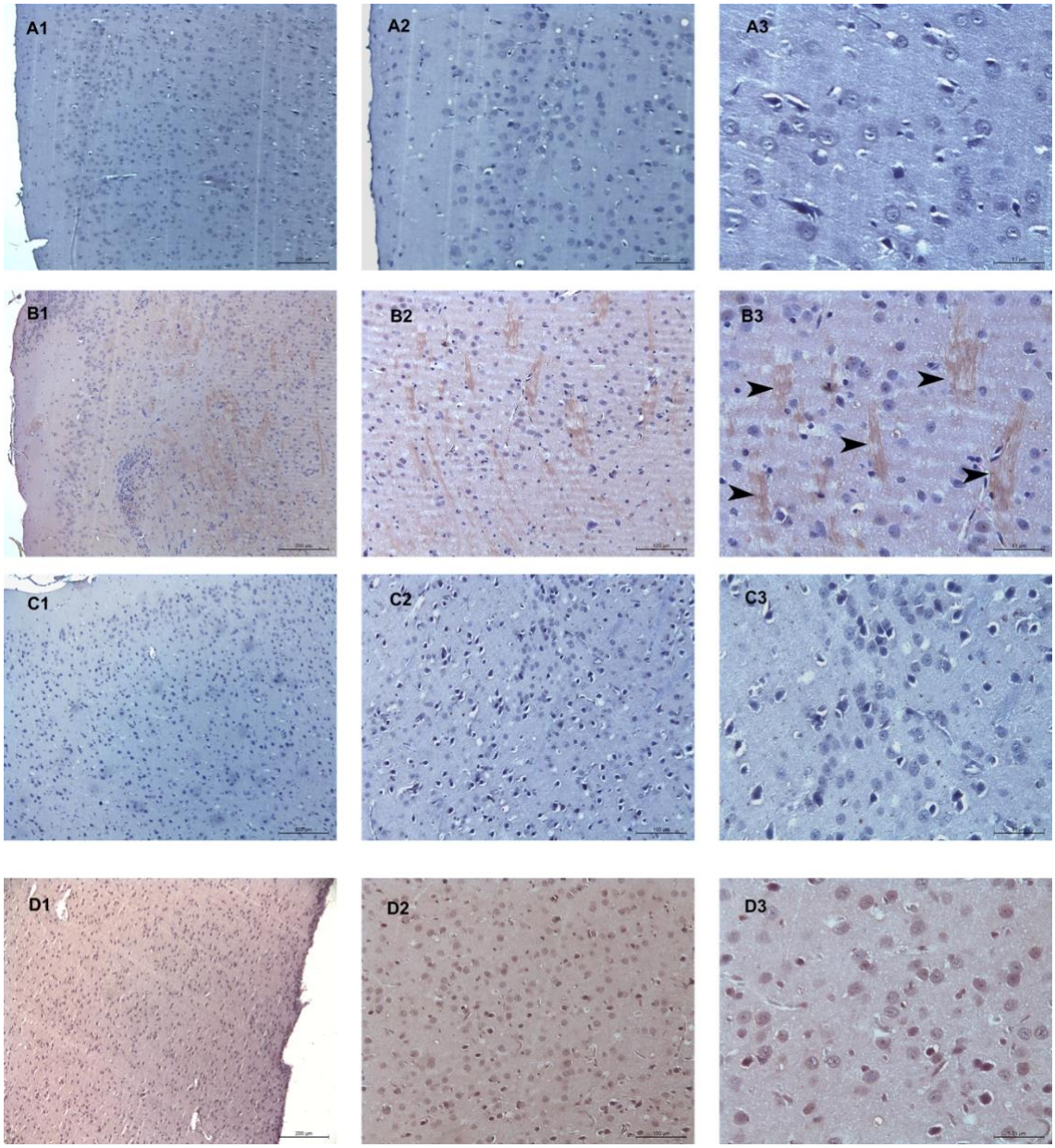

Figure 4.2.5.2. Photomicrographs demonstrate Amyloid beta immunoreactivity in cerebral cortex.
A1, A2, A3 represents Saline treated control group (C), B1, B2, B3 scopolamine injected (SC), C1, C2, C3 represents selenium injected (SE), D1, D2, D3 represents scopolamine, and selenium injected (T) groups. The magnification is x10, x20, x40 left to right, respectively. Scale bar represents 200 μm in x10, 100 μm in x20, 50 μm in x40. Arrows indicate amyloid plaques.

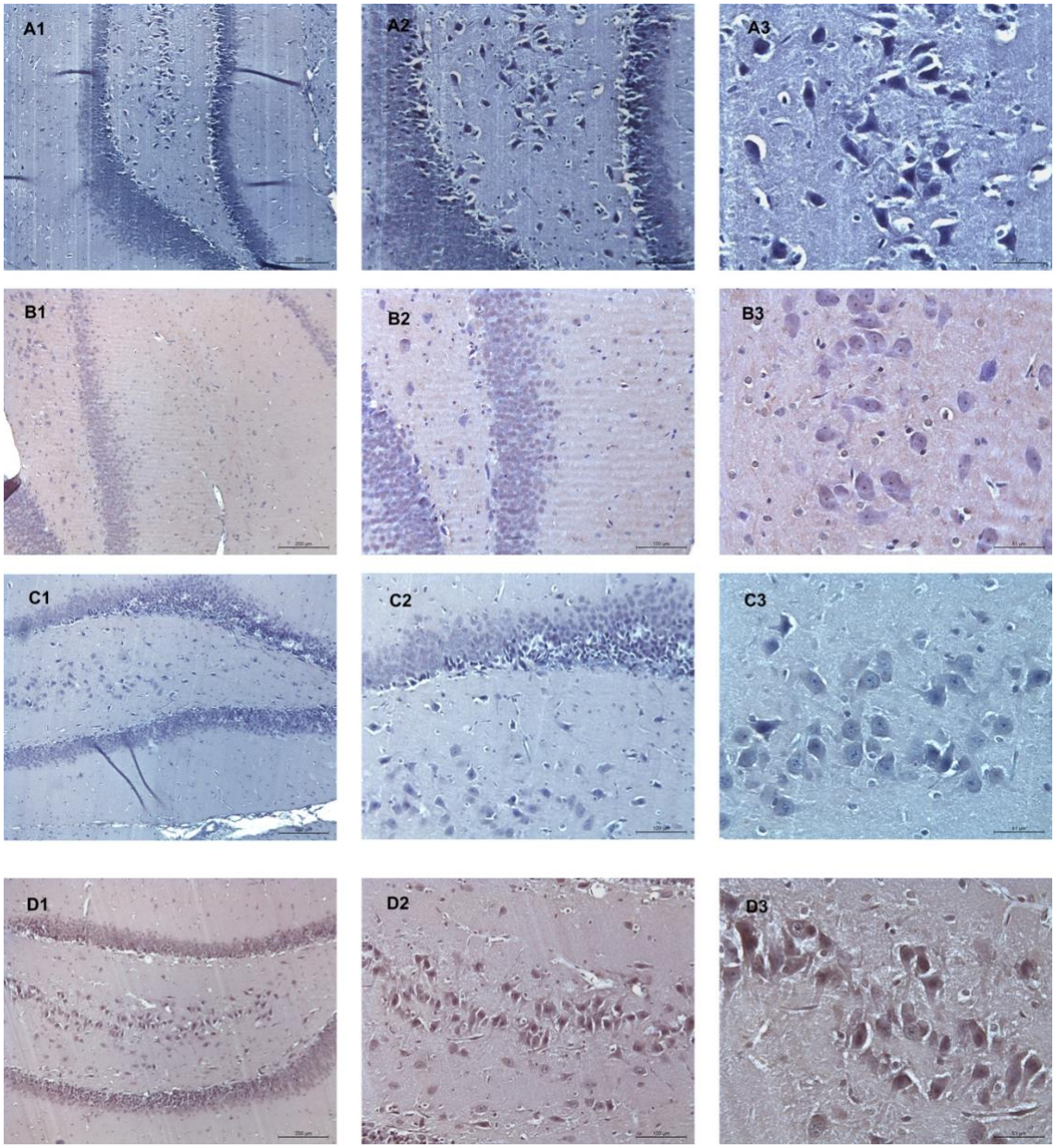

Figure 4.2.5.3. Photomicrographs demonstrate Amyloid beta immunoreactivity in hippocampus.
A1, A2, A3 represents Saline treated control group (C), B1, B2, B3 scopolamine injected (SC), C1, C2, C3 represents selenium injected (SE), D1, D2, D3 represents scopolamine, and selenium injected (T) groups. The magnification is x10, x20, x40 left to right, respectively. Scale bar represents 200 μm in x10, 100 μm in x20, 50 μm in x40. Arrowheads indicates neurofibrillary tangles while arrows indicate amyloid plaques.

Table 4.2.5.1. Cerebral Cortex Amyloid Beta Immunostaining H-score

Cerebral Cortex Amyloid Beta H-Score				
Tukey's multiple comparisons test	Mean 1	Mean 2	Mean Diff	P Value
Control vs. Scopolamine	28,26	42,74	-14,48	<0,0001
Control vs. Selenium	28,26	29,42	-1,16	0,8878
Control vs. Scopolamine+Selenium	28,26	32,92	-4,66	0,0472
Scopolamine vs. Selenium	42,74	29,42	13,32	<0,0001
Scopolamine vs. Scopolamine+Selenium	42,74	32,92	9,82	<0,0001
Selenium vs. Scopolamine+Selenium	29,42	32,92	-3,50	0,1734

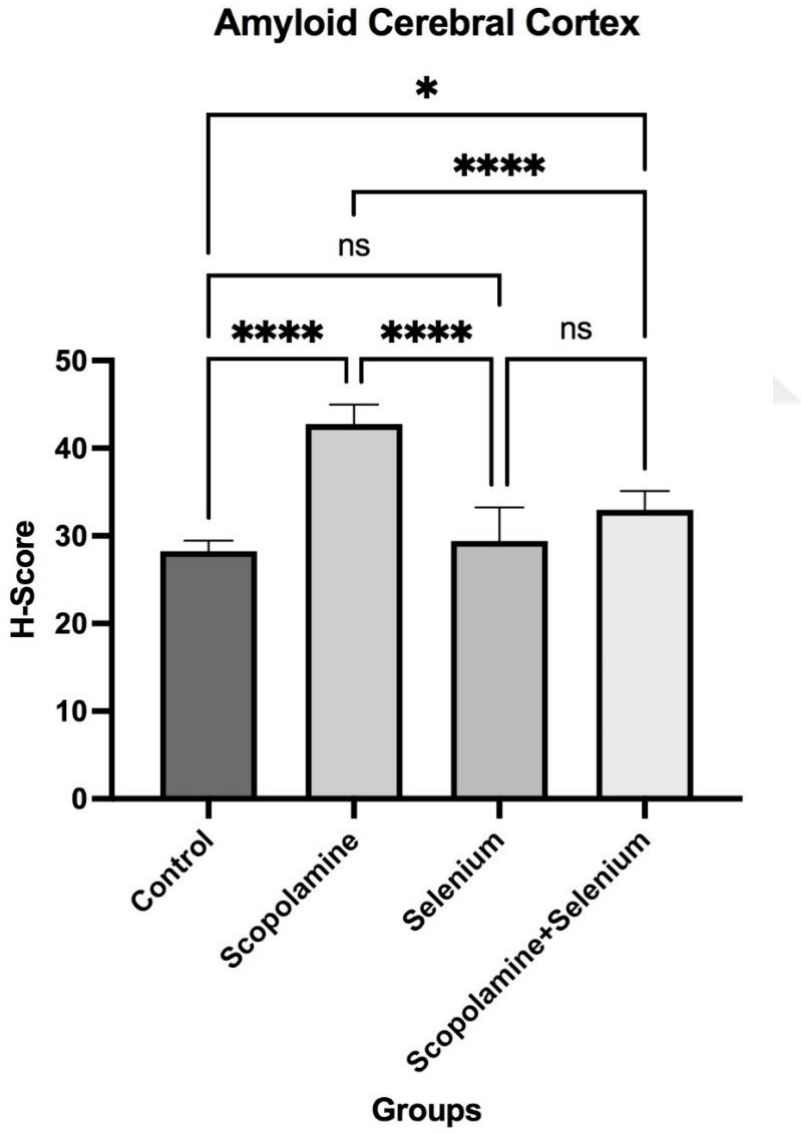

Figure 4.2.5.4. Graph of Amyloid Beta H-score Cerebral Cortex(P<0.05)

When looked at the H-Score graphs for Amyloid, Group Sc is higher than the H-Scores of Group C, Group Se and Group T in cerebral cortex region ($p<0,0001$, $p<0,0001$, $p<0,0001$ respectively). H-Score for Amyloid beta of Group T is lower than the H-Scores of Groups Se and Group C in cerebral cortex region ($p>0.05$), $p=0,04272$ respectively) according to Tukey's multiple comparisons test.

.

Table 4.2.5.2 Hippocampus Amyloid Beta Immunostaining H-score

Hippocampus Amyloid Beta H-Score				
Tukey's multiple comparisons test	Mean 1	Mean 2	Mean Diff	P Value
Control vs. Scopolamine	26,76	43,83	-17,07	<0,0001
Control vs. Selenium	26,76	27,90	-1,14	0,8900
Control vs. Scopolamine+Selenium	26,76	34,10	-7,34	0,0015
Scopolamine vs. Selenium	43,83	27,90	15,93	<0,0001
Scopolamine vs. Scopolamine+Selenium	43,83	34,10	9,73	<0,0001
Selenium vs. Scopolamine+Selenium	27,90	34,10	-6,20	0,0065

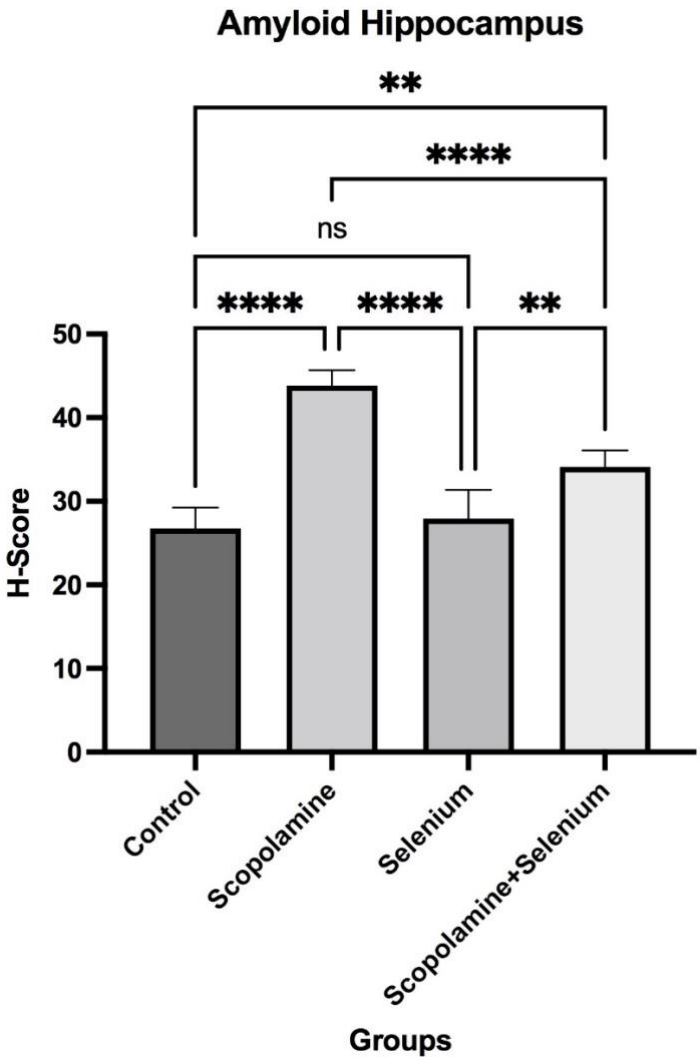

Figure 4.2.5.5. Graph of Amyloid Beta H-score Hippocampus(P<0.05)

When looked at the H-Score graphs for Amyloid, Group Sc is higher than the H-Scores of Group C, Group Se and Group T in hippocampus region (p<0,0001, p<0,0001, p<0,0001 respectively) .H-Score for Amyloid Beta for hippocampus of Group T is higher than the H-Scores of Group C and Group Se (p=0,0015, 0,0065 respectively) according to Tukey's multiple comparisons test.

5.DISCUSSION

One of the most frequent neurodegenerative disorders is Alzheimer's disease (AD). As a result of various pathological alterations such as the production of amyloid plaques and tau hyperphosphorylation, neurons in affected regions gradually die (37,81)

Scopolamine is a neurotoxin that replicates the effects of Alzheimer's when applied properly, making it one of the most common neurotoxins used to simulate Alzheimer's disease(9,10,56,57).

Besides that, one of the compounds being researched to avoid inflammation in Alzheimer's disease is selenium (56,60,82–84) . In the scopolamine-induced Alzheimer's Disease model, the aim of this study is to examine how selenium (14) affects morphological alterations in the hippocampus and cerebral cortex neurons. In the scopolamine-induced AD rat model, selenium is thought to reduce degenerative effects in neurons.

First, locomotor activity tests were conducted for every group before decapitation of animals in order to determine cognitive states of rats. As a result, the distance travelled by animals, stereotypic activity ($p<0.001$), ambulatory activity ($p<0.01$), horizontal activity ($p<0.0001$), vertical activity($p<0.001$) is the lowest in Sc group compared to C group which indicates that the scopolamine leads to a cognitive loss in this study as expected (55,57,58). Since the cerebral cortex includes the region responsible for motor activities, intense loss of neurons may be the reason for these results. Furthermore, animals in T group increased in stereotypic activity ($p<0.05$) and ambulatory activity ($p<0.05$) compared to Sc group when treated with Selenium. On the other hand, horizontal activity, distance travelled by the animals and vertical activity also increased in T group compared to Sc group but there was no statistical significance calculated. Selenium might have shown a preventive effect instead of curing it, only regressing the Alzheimer's Model. In the summary, selenium administration in scopolamine model might improve cognitive conditions(57,84). Nevertheless, more studies must be conducted to determine selenium's exact effects on cognitive impairment.

Second of all, Amyloid plaques and neurofibrillary tangles were observed in SC and T group sections in compared to C and SE groups in Hematoxylin Eosin, Cresyl Violet, Silver stained sections. These abnormalities were observed most densely in SC group (58,85–87) whereas they were rarely seen in T group as expected (67,88,89) . On

the other hand, no abnormalities were observed in C and SE groups. Therefore, it can be said that amyloid plaques and neurofibrillary tangles can be observed with specific histological staining's in scopolamine model and selenium administration in this model can reduce their density in cerebral cortex and hippocampus (17,87,90). In Hematoxylin&Eosin, Cresyl Violet and Silver stained sections there was no distinguished density difference between hippocampus and cerebral cortex in SC and T groups. It can be said that scopolamine can cause homogeneous amyloid plaq and neurofibrillary tangle distribution in the brain regions.

Next, three immunohistochemical staining were performed and their H-score was calculated. VEGF, iNOS and amyloid Beta immunohistochemical staining were analyzed by calculating H-score.

VEGF is an important growth factor for blood vessel growth, and it contributes to neurogenesis promotion, glial growth, and neuroprotection processes (78,79,91) . H-Score graphs of VEGF cerebral cortex and VEGF hippocampus are alike considering the comparisons of each group within their own region i.e., Sc Group has the highest H-Score for VEGF, Group C has the lowest H-Score for VEGF, T Group has the second highest H-Score for VEGF and Se Group has the third highest H-Score for VEGF for both regions. However, H-Scores for VEGF of cerebral cortex are overall lower than the H-Scores for VEGF of hippocampus for all four groups. It may be explained by hippocampus requires more neurogeneration or neuroprotection than the cerebral cortex (91) . As previously stated, C Group has a lower H-Score for VEGF than Group Sc, Group Se and Group T in cerebral cortex region ($p<0,0001$, ns, 0,0009 respectively). Likewise, H-Score for VEGF of C Group is also lower than Group Sc, Group Se and Group T in hippocampus region as well ($p<0,0001$, ns, $p<0,0001$ respectively). In a study conducted in 2019 (92) , VEGF was shown to increase the permeability of the blood-brain barrier, therefore it was suggested to advance Alzheimer's pathology. Since scopolamine is a substance that causes inflammation, vascularization for prophylactic purposes may have increased and the amount of vegf may have increased. Both cerebral cortex and hippocampus region have responded well to selenium treatment, which can be seen when comparing Sc Groups and T Groups within their own regions. H-Score for VEGF of Group T is slightly lower than H-Score for VEGF of Group Sc in both cerebral cortex and hippocampus region ($p=0,0041$, ns respectively) (93) . Moreover, H-Score for VEGF

of Group Sc in cerebral cortex region is considerably higher than the H-Score for VEGF of Group Se with a p value smaller than 0,0001 according to Tukey's multiple comparisons test. H-Score for VEGF of Group Se is also significantly smaller than the H-Score for VEGF of Group Sc in hippocampus region with a p value of 0,0003. Even though there is no statistical significance according to Tukey's multiple comparisons test between the H-Scores of Groups Se and Group T in cerebral cortex region, still the H-Score of Group Se is lightly lower than the H-Score of Group T. The comparison of the H-Scores of Groups Se and Group T in hippocampus region is also very much alike which means Group Se has a lower H-Score than Group T, with only difference being that there is also a statistical significance with a p value of 0,0027. As the result of VEGF H-score calculations, no major difference was observed between the groups. The duration or dose of selenium may be the cause of this result.

Inducible Nitric Oxide Synthase iNOS can be found in aging brain because of its effects on balance between damage and repair of brain (5,76,77,94) . When comparing the H-Scores of cerebral cortex iNOS, it can be seen that Sc Group and T Group have a higher H-Score for iNOS than Group C, whereas Se Group has a slightly lower H-Score for iNOS ($p<0,0001$, $p=0,0005$, ns respectively). The situation is similar regarding the H-Scores of hippocampus iNOS with the only difference being that Se Group has a slightly higher H-Score level than C Group, though there is no statistical significance according to Tukey's multiple comparisons test. H-Scores for iNOS immunochemistry in hippocampus region of Sc Group and T Group are again higher than C Group ($p<0,0001$, $p=0,0031$ respectively). Both regions' Sc Group has a higher H-Score for iNOS than Se Group ($p<0,0001$ for both regions) (85). Scopolomine may have lead to this result because it creates conditions that cause inflammation. Expectedly, T Group has a lower H-Score for iNOS immunochemistry than Sc Group for both cerebral cortex and hippocampus which indicates a positive outcome for the selenium administration ($p=0,0248$, $p=0,0099$ respectively) (95,96) . H-Score for iNOS of Group Sc in cerebral cortex region is relatively higher than the H-Score for iNOS of Group Se which means selenium treatment and scopolamine injections worked ideally as anticipated($p<0,0001$). Correspondingly, Sc Group in hippocampus region has a higher H-Score for iNOS immunochemistry than the Se Group of hippocampus ($p<0,0001$). Considering that selenium reduces oxidative stress by controlling NFKB activity and thus regulates

inflammation, it may be explained the decrease in the test group. In conclusion, there was a significant difference between the scopolamine and control groups in iNOS immunohistochemistry staining. It can be interpreted as scopolamine can cause neuroinflammation and selenium can help to reduce neuroinflammation in cerebral cortex and hippocampus.

When looked at the H-Score graphs for Amyloid Beta in cerebral cortex and hippocampus regions, it can be observed that Sc Group has the highest H-Score, and Se Group has the lowest H-Score for both cerebral cortex and hippocampus regions. To be precise, H-Score for Amyloid Beta of Group Sc is higher than the H-Scores of Group C, Group Se and Group T in cerebral cortex region ($p<0,0001$, $p<0,0001$, $p<0,0001$ respectively). Likewise, Sc Group in hippocampus region has a higher H-Score for Amyloid Beta than C Group, Se Group and T Group ($p<0,0001$, $p<0,0001$, $p<0,0001$ respectively). When comparing the T Group with Se Group and Control Group, it is evident that H-Score for Amyloid beta of Group T is lower than the H-Scores of Groups Se and Group C in cerebral cortex region (ns, $p=0,04272$ respectively). However, as previously said, T Group has a lower H-Score than Sc group thus quantifying the positive effects of selenium treatment. Same positive outcome can be observed for hippocampus region as well, even though H-Score for Amyloid Beta of Group T is higher than the H-Scores of Group C and Group Se ($p=0,0015$, $0,0065$ respectively). Last but not least, there aren't any meaningful differences between the H-Scores for Amyloid Beta of Group Se and Group C both in cerebral cortex and hippocampus region, in addition to that, there were no statistical significance calculated between the H-Scores of these groups in both cerebral cortex and hippocampus regions according to Tukey's multiple comparisons test. By Amyloid Beta immunohistochemistry staining, intense amyloid plaque formation was detected in the scopolamine group and rare in the test group. In other words, while scopolamine can lead to formation of amyloid beta (1,4,9,97), selenium can reduce amyloid beta in cerebral cortex and hippocampus in this model (56,60,82,83). The decrasing amount of amyloid beta results can be explained by the ability of selenium to decrease gamma secretase and alpha secretase enzyme activities.

The apoptotic index was calculated with the TUNEL experiment, and the highest values were obtained in the scopolamine group, second highest in the test group, and the lowest in the control and selenium groups. When comparing the apoptotic index of

cerebral cortex, it can be said that Sc Group and T Group have a higher apoptotic index for than Group C (9,56,98,99) . The situation is similar regarding the apoptotic index of hippocampus. The apoptotic index of hippocampus region of Sc Group and T Group are again higher than C Group. Both regions' Sc Group has a higher the apoptotic index than Se Group. Expectedly, T Group has a lower the apoptotic index than Sc Group for both cerebral cortex and hippocampus which indicates a positive outcome for the selenium treatment. The apoptotic index of Group Sc in cerebral cortex region is relatively higher than the Group Se which means selenium treatment and scopolamine injections worked ideally as anticipated. Correspondingly, Sc Group in hippocampus region has a higher the apoptotic index than the Se Group of hippocampus. In conclusion, there was a significant difference between the scopolamine and control groups' apoptotic index (56,69,82,100). It can be interpreted as scopolamine can cause apoptosis due to neuroinflammation and selenium can help to reduce apoptosis due to neuroinflammation in cerebral cortex and hippocampus (82).

In conclusion, the result of this histological study is consistent with the results of Demirci et.al. physiological study (56). Scopolamine can be an alternative as Alzheimer's model for investigating the effects of selenium. Moreover, the result of this study indicates that selenium has promising effects on scopolamine Alzheimer model pathology, morphologically. Therefore, this study can be used as a guide to improve preventive studies of Alzheimer including selenium in the future.

6. REFERENCES

1. Perl DP. Neuropathology of Alzheimer ' s Disease. 2010;77(1):32–42.
2. Giacobini E, Gold G. Alzheimer disease therapy — moving from amyloid - β to tau. Nat Publ Gr [Internet]. 2013;1–10. Available from: http://dx.doi.org/10.1038/nrneurol.2013.223
3. Congdon EE, Sigurdsson EM. Tau-targeting therapies for. Nat Rev Neurol [Internet]. 2018; Available from: http://dx.doi.org/10.1038/s41582-018-0013-z
4. Harrington CR. The Molecular Pathology of Alzheimer's Disease. Neuroimaging Clin N Am [Internet]. 2012;22(1):11–22. Available from: http://dx.doi.org/10.1016/j.nic.2011.11.003
5. Glass CK, Saijo K, Winner B, Marchetto MC, Gage FH. Review Mechanisms Underlying Inflammation in Neurodegeneration. Cell [Internet]. 2010;140(6):918–34. Available from: http://dx.doi.org/10.1016/j.cell.2010.02.016
6. Huang Y, Mucke L. Alzheimer mechanisms and therapeutic strategies. Cell [Internet]. 2012;148(6):1204–22. Available from: http://dx.doi.org/10.1016/j.cell.2012.02.040
7. Thériault P, Elali A, Rivest S. The dynamics of monocytes and microglia in Alzheimer ' s disease. 2015;1–10.
8. Meraz-ríos MA, Toral-rios D, Franco-bocanegra D, Villeda-hernández J. Inflammatory process in Alzheimer ' s Disease. 2013;7(August):1–15.
9. Tang KS. The cellular and molecular processes associated with scopolamine-induced memory de fi cit : A model of Alzheimer ' s biomarkers. Life Sci [Internet]. 2019;233(April):116695. Available from: https://doi.org/10.1016/j.lfs.2019.116695
10. Ghasemi S, Moradzadeh M, Hosseini M, Sadeghnia HR. Beneficial effects of Urtica dioica on scopolamine- induced memory impairment in rats : protection against acetylcholinesterase activity and neuronal oxidative damage. Drug Chem Toxicol [Internet]. 2019;42(2):167–75. Available from: https://doi.org/10.1080/01480545.2018.1463238
11. Folch J, Ettcheto M, Petrov D, Abad S, Pedrós I, Marin M, et al. Review of the advances in treatment for Alzheimer disease: strategies for combating β-amyloid protein. Neurol (English Ed [Internet]. 2017; Available from: http://linkinghub.elsevier.com/retrieve/pii/S2173580817300639
12. Loef M, Schrauzer GN, Walach H, Office E, Oder F. Selenium and Alzheimer ' s Disease : A Systematic Review. 2011;26:81–104.
13. Varikasuvu SR. Brain Selenium in Alzheimer ' s Disease (BRAIN SEAD Study): a Systematic Review and Meta-Analysis. 2019;361–9.
14. Berr C, Arnaud J, Akbaraly TN. Selenium and cognitive impairment: a brief-review based on results from the EVA study. Biofactors. 2012;38(2):139–44.
15. Spinks AB, Wasiak J, Villanueva E V, Bernath V. Scopolamine (hyoscine) for preventing and treating motion sickness. Cochrane database Syst Rev. 2007 Jul;(3):CD002851.
16. Maurer K., Riederer P. BH. Morphology of cerebral cortex. In: Alzheimer's Disease Epidemiology, Neuropathology, Neurochemistry, and Clinics. wien: Springer, Vienna.; 1990.

17. Barkur RR, Bairy LK. Histological study on hippocampus, amygdala and cerebellum following low lead exposure during prenatal and postnatal brain development in rats. Toxicol Ind Health. 2016;32(6):1052–63.

18. Anand KS, Dhikav V. Review : Progress in Medicine (Update on advances in pathophysiology) Hippocampus in health and disease : An overview. 2012;15(4).
19. Vida I. Morphology of Hippocampal Neurons. 2010.
20. Gautam A. Nerve Cells. In 2017. p. 1–3.
21. Stahl SM. Structure and Function of Neurons ■. :1–10.
22. Stevens B. Glia : much more than the neuron ' s side-kick. :469–72.
23. Shichita T, Yoshimura A. Neuroimmunology. 2016;7:18–27.
24. Krause DL, Norbert M. Neuroinflammation , Microglia and Implications for Anti-Inflammatory Treatment in Alzheimer ' s Disease. 2010;2010.
25. Carter SF, Herholz K, Rosa-neto P, Pellerin L, Nordberg A. Astrocyte Biomarkers in Alzheimer ' s Disease. Trends Mol Med [Internet]. 2018;1–19. Available from: https://doi.org/10.1016/j.molmed.2018.11.006
26. Sweeney MD, Sagare AP, Zlokovic B V. Blood–brain barrier breakdown in Alzheimer disease and other neurodegenerative disorders. Nat Publ Gr [Internet]. 2018;14(3):133–50. Available from: http://dx.doi.org/10.1038/nrneurol.2017.188
27. Villabona-rueda A, Erice C, Pardo CA, Stins MF. The Evolving Concept of the Blood Brain Barrier (BBB): From a Single Static Barrier to a Heterogeneous and Dynamic Relay Center. 2019;13(September).
28. Tajes M, Ramos-fernández E, Weng-jiang X, Bosch-morató M, Guivernau B, Eraso-pichot A, et al. The blood-brain barrier : Structure , function and therapeutic approaches to cross it to cross it. 2014;7688.
29. Alzheimer's Association. 2017 Alzheimer's Disease Facts and Figures. Alzheimers Dement [Internet]. 2017;13:325–73. Available from: http://www.alz.org/documents_custom/2017-facts-and-figures.pdf
30. Patterson C, Feightner JW, Garcia A, Hsiung GYR, MacKnight C, Sadovnick AD. Diagnosis and treatment of dementia: 1. Risk assessment and primary prevention of Alzheimer disease. Cmaj. 2008;178(5):548–56.
31. Iqbal K, Liu F, Gong C. Tau and neurodegenerative disease: the story so far. 2015;1–14.
32. Fischer R, Maier O. Interrelation of Oxidative Stress and Inflammation in Neurodegenerative Disease: Role of TNF. Oxid Med Cell Longev. 2015;2015.
33. Mondragón-rodríguez S, Basurto-islas G, Lee H, Zhu X, Castellani RJ, Smith MA, et al. NIH Public Access. 2011;10(5):683–91.
34. Thompson PM. Pathologic Lesions in Neurodegenerative Diseases I . Introduction A . Neuropathologic Features [Internet]. 1st ed. Vol. 107, Molecular Biology of Neurodegenerative Diseases. Elsevier Inc.; 2012. 1–40 p. Available from: http://dx.doi.org/10.1016/B978-0-12-385883-2.00009-6
35. Zhou S, Yu G, Chi L, Zhu J, Zhang W, Zhang Y, et al. Neuroprotective effects of edaravone on cognitive deficit, oxidative stress and tau hyperphosphorylation induced by intracerebroventricular streptozotocin in rats. Neurotoxicology. 2013 Sep;38:136–45.

36. Mammana S, Fagone P, Cavalli E, Basile MS, Petralia MC, Nicoletti F, et al. The Role of Macrophages in Neuroinflammatory and Neurodegenerative Pathways of Alzheimer ' s Disease , Amyotrophic Lateral Sclerosis , and Multiple Sclerosis : Pathogenetic Cellular Effectors and Potential Therapeutic Targets. (Figure 1):1–20.
37. Kinney JW, Bemiller SM, Murtishaw AS, Leisgang AM, Salazar AM, Lamb BT. Inflammation as a central mechanism in Alzheimer ' s disease. Alzheimer's Dement Transl Res Clin Interv [Internet]. 2018;4:575–90. Available from: https://doi.org/10.1016/j.trci.2018.06.014
38. Drummond E, Wisniewski T. Alzheimer's disease: experimental models and reality. Acta Neuropathol. 2017 Feb;133(2):155–75.
39. Zheng-Bradley X, Rung J, Parkinson H, Brazma A. Large scale comparison of global gene expression patterns in human and mouse. Genome Biol [Internet]. 2010;11(12):R124. Available from: https://doi.org/10.1186/gb-2010-11-12-r124
40. Jucker M. The benefits and limitations of animal models for translational research in neurodegenerative diseases. Nat Med. 2010 Nov;16(11):1210–4.
41. Busche MA, Wegmann S, Dujardin S, Commins C, Schiantarelli J, Klickstein N, et al. effects , in Alzheimer models in vivo. Nat Neurosci [Internet]. 2019;22(January). Available from: http://dx.doi.org/10.1038/s41593-018-0289-8
42. Manuscript A. Transgenic Mouse Models of Alzheimer ' s Disease. 2010;77(1):69–81.
43. Nazem A, Sankowski R, Bacher M, Al-abed Y. Rodent models of neuroinflammation for Alzheimer ' s disease. ??? [Internet]. 2015;1–15. Available from: ???
44. Correia SC, Santos RX, Santos MS, Casadesus G, Lamanna JC, Perry G, et al. Mitochondrial abnormalities in a streptozotocin-induced rat model of sporadic Alzheimer's disease. Curr Alzheimer Res. 2013 May;10(4):406–19.
45. Newman M, Kretzschmar D, Khan I, Chen M, Verdile G, Lardelli M. Animal Models of Alzheimer's Disease. In: Animal Models for the Study of Human Disease: Second Edition. 2017. p. 1031–85.
46. Sil S, Raj A, Goutam G, Tusharkanti D, Ad C. Effects of Naproxen on Immune Responses in a Colchicine-Induced Rat Model of Alzheimer ' s Disease. 2014;304–21.
47. Kamat PK, Rai S, Nath C. NeuroToxicology Okadaic acid induced neurotoxicity : An emerging tool to study Alzheimer ' s disease pathology. Neurotoxicology [Internet]. 2013;37:163–72. Available from: http://dx.doi.org/10.1016/j.neuro.2013.05.002
48. Bubser M, Byun N, Wood MR, Jones CK. Muscarinic receptor pharmacology and circuitry for the modulation of cognition. Handb Exp Pharmacol. 2012;(208):121–66.
49. Lee HJ, Park MK, Seo YR. Pathogenic Mechanisms of Heavy Metal Induced-Alzheimer's Disease. Toxicol Environ Health Sci [Internet]. 2018;10(1):1–10. Available from: https://doi.org/10.1007/s13530-018-0340-x
50. Whitton PS. Inflammation as a causative factor in the aetiology of Parkinson's disease. Br J Pharmacol. 2007 Apr;150(8):963–76.

51. Altman DG, Bland JM. Statistics Notes The normal distribution. 1995;310(February):1995.

52. Kamat PK, Tota S, Shukla R, Ali S, Najmi AK, Nath C. Mitochondrial dysfunction: a crucial event in okadaic acid (ICV) induced memory impairment and apoptotic cell death in rat brain. Pharmacol Biochem Behav. 2011 Dec;100(2):311–9.
53. Blood T, Barrier B, Daneman R, Prat A. The Blood –Brain Barrier. 2015;1–23.
54. Renner UD, Oertel R, Kirch W. Pharmacokinetics and Pharmacodynamics in Clinical Use of Scopolamine. 2005;27(5):655–65.
55. Ebert U, Kirch W. Scopolamine model of dementia : electroencephalogram findings and cognitive performance. 1998;944–9.
56. Demirci K, Naz M, Övey İS, Balaban H. Selenium attenuates apoptosis , inflammation and oxidative stress in the blood and brain of aged rats with scopolamine-induced dementia. 2017;321–9.
57. Klinkenberg I, Blokland A. The validity of scopolamine as a pharmacological model for cognitive impairment: a review of animal behavioral studies. Neurosci Biobehav Rev. 2010 Jul;34(8):1307–50.
58. Zaki HF, Abd-el-fattah MA, Attia AS. Naringenin protects against scopolamine-induced dementia in rats. Bull Fac Pharmacy, Cairo Univ [Internet]. 2014;52(1):15–25. Available from: http://dx.doi.org/10.1016/j.bfopcu.2013.11.001
59. Mehdi Y, Hornick J-L, Istasse L, Dufrasne I. Selenium in the environment, metabolism and involvement in body functions. Molecules. 2013 Mar;18(3):3292–311.
60. Steinbrenner H, Sies H. Protection against reactive oxygen species by selenoproteins. Biochim Biophys Acta. 2009 Nov;1790(11):1478–85.
61. Gonca S. Selenium: a micronutrient essential for maintaining human health. Med Sci | Int Med J. 2013;2(3):649.
62. Perrone D, Monteiro M, Nunes J. The Chemistry of Selenium. In 2015.
63. Nakayama A, Hill KE, Austin LM, Motley AK, Burk RF. All Regions of Mouse Brain Are Dependent on Selenoprotein P for Maintenance of Selenium. J Nutr [Internet]. 2007;137(3):690–3. Available from: https://doi.org/10.1093/jn/137.3.690
64. Nazıroğlu M, Şenol N, Ghazizadeh V, Yürüker V. Neuroprotection Induced by N-acetylcysteine and Selenium Against Traumatic Brain Injury-Induced Apoptosis and Calcium Entry in Hippocampus of Rat. Cell Mol Neurobiol [Internet]. 2014;34(6):895–903. Available from: https://doi.org/10.1007/s10571-014-0069-2
65. Burk RF, Hill KE. Regulation of Selenium Metabolism and Transport. Annu Rev Nutr. 2015;35:109–34.
66. Conrad M, Kagan VE, Bayir H, Pagnussat GC, Head B, Traber MG, et al. Regulation of lipid peroxidation and ferroptosis in diverse species. Genes Dev. 2018 May;32(9–10):602–19.
67. Eersel J Van, Ke YD, Liu X, Delerue F, Kril JJ, Götz J, et al. Sodium selenate mitigates tau pathology , neurodegeneration , and functional de fi cits in Alzheimer ' s disease models. 2016;107(31).

68. Tung ying-tsen, Hsu W-M, Wang B-J, Wu S-Y, Yen C-T, Hu M-K, et al. Sodium selenite inhibits gamma-secretase activity through activation of ERK. Neurosci Lett. 2008;440:38–43.
69. Gisele A, Leme S, Cardoso BR. Selenium and Alzheimer ' s disease. 2020;739–48.
70. Kobayashi K, Shimizu N, Matsushita S, Murata T. The assessment of mouse spontaneous locomotor activity using motion picture. J Pharmacol Sci [Internet]. 2020;143(2):83–8. Available from: https://doi.org/10.1016/j.jphs.2020.02.003
71. Woods A, Wllis R. Laboratory Histopathology: A Complete Referenc. 1994. p. 8.1-18-8.1-19, 8.2-9-8.2:37-8.2:20.
72. Cardiff RD, Miller CH, Munn RJ. Manual hematoxylin and eosin staining of mouse tissue sections. Cold Spring Harb Protoc. 2014;2014(6):655–8.
73. Alvarez-Buylla A, Ling CY, Kirn JR. Cresyl violet: A red fluorescent Nissl stain. J Neurosci Methods. 1990;33(2–3):129–33.
74. Shafri, Mohd Affendi Jais Matjais AM, MD J, Kim MK, Ithnin H, Mohamed F. Effect of Haruan Traditional Extract Against Neurodegenerative Damage of Ketamine. Int J Pharm Pharm Sci. 2012;4(4):163–8.
75. Intorcia AJ, Filon JR, Hoffman B, Serrano GE, Sue LI, Beach TG. A Modification of the Bielschowsky Silver Stain for Alzheimer Neuritic Plaques: Suppression of Artifactual Staining by Pretreatment with Oxidizing Agents. bioRxiv. 2019;1–16.
76. Choi JY, Nam SA, Jin DC, Kim J, Cha JH. Expression and Cellular Localization of Inducible Nitric Oxide Synthase in Lipopolysaccharide-treated Rat Kidneys. J Histochem Cytochem. 2012;60(4):301–15.
77. Kleinert H, Forstermann U. Inducible nitric oxide synthase. xPharm Compr Pharmacol Ref. 2007;1–12.
78. Maae E, Nielsen M, Steffensen KD, Jakobsen EH, Jakobsen A, Sørensen FB. Estimation of immunohistochemical expression of VEGF in ductal carcinomas of the breast. J Histochem Cytochem. 2011;59(8):750–60.
79. Storkebaum E, Carmeliet P. VEGF: A critical player in neurodegeneration. J Clin Invest. 2004;113(1):14–8.
80. Garrity MM, Burgart LJ, Riehle DL, Hill EM, Sebo TJ, Witzig T. Identifying and quantifying apoptosis: Navigating technical pitfalls. Mod Pathol. 2003;16(4):389–94.
81. Newcombe EA, Camats-Perna J, Silva ML, Valmas N, Huat TJ, Medeiros R. Inflammation: the link between comorbidities, genetics, and Alzheimer's disease. J Neuroinflammation [Internet]. 2018;15(1):276. Available from: https://doi.org/10.1186/s12974-018-1313-3
82. Takemoto AS, Berry MJ, Bellinger FP. Role of selenoprotein P in Alzheimer's disease. Ethn Dis. 2010;20(1 SUPPL.1):1–7.
83. Ishrat T, Parveen K, Khan MM, Khuwaja G, Khan MB, Yousuf S, et al. Selenium prevents cognitive decline and oxidative damage in rat model of streptozotocin-induced experimental dementia of Alzheimer ' s type. Brain Res [Internet]. 2009;1281:117–27. Available from: http://dx.doi.org/10.1016/j.brainres.2009.04.010
84. Lakshmi BVS, Sudhakar M, Prakash KS. Protective Effect of Selenium Against Aluminum Chloride-Induced Alzheimer's Disease: Behavioral and Biochemical Alterations in Rats.

85. Yang L, Zhou R, Tong Y, Chen P, Shen Y, Miao S, et al. Neuroprotection by dihydrotestosterone in LPS-induced neuroinflammation. Neurobiol Dis. 2020;140.
86. Group NW, Akiyama H, Barger S, Barnum S, Bradt B, Bauer J, et al. NIH Public Access. Vol. 21. 2014. 383–421 p.

87. Baghel V, Tripathi M, Parida G, Gupta R, Yadav S, Kumar P, et al. In Vivo Assessment of Tau Deposition in Alzheimer Disease and Assessing Its Relationship to Regional Brain Glucose Metabolism and Cognition. Clin Nucl Med. 2019;44(11).
88. Özbal S, Erbil G, Koçdor H, Tuğyan K, Pekçetin Ç, Özoğul C. The effects of selenium against cerebral ischemia-reperfusion injury in rats. Neurosci Lett. 2008;438(3).
89. Ali AA, Abd El-Fattah AI, Abu-Elfotuh K, Elariny HA. Natural antioxidants enhance the power of physical and mental activities versus risk factors inducing progression of Alzheimer's disease in rats. Int Immunopharmacol. 2021;96.
90. Brat DJ. Normal Brain Histopathology. Pract Surg Neuropathol A Diagnostic Approach A Vol Pattern Recognit Ser. 2018 Jan 1;19–37.
91. Rosenstein JM, Krum JM, Ruhrberg C. Rosenstein_10_107. 2010;(June):107–14.
92. Moore AM, Mahoney ER, Dumitrescu L, De Jager PL, Koran MEI, Petyuk VA, et al. P3-138: APOE ε 4 -SPECIFIC ASSOCIATIONS OF VEGF GENE FAMILY EXPRESSION WITH COGNITIVE AGING AND ALZHEIMER'S DISEASE . Alzheimer's Dement. 2019;15.
93. Cardoso BR, Szymlek-Gay EA, Roberts BR, Formica M, Gianoudis J, O'connell S, et al. Selenium status is not associated with cognitive performance: A cross-sectional study in 154 older Australian adults. Nutrients. 2018;10(12).
94. Licinio J, Prolo P, McCann SM WM. Brain iNOS: current understanding and clinical implications. Mol Med Today. :225-32.
95. Varikasuvu SR, Prasad V S, Kothapalli J, Manne M. Brain Selenium in Alzheimer's Disease (BRAIN SEAD Study): a Systematic Review and Meta-Analysis. Biol Trace Elem Res. 2019;189(2).
96. Dursun E, Gezen-Ak D, Yilmazer S. A new mechanism for amyloid-β induction of iNOS: Vitamin D-VDR pathway disruption. J Alzheimer's Dis. 2013;36(3):459–74.
97. Hernández-Rodríguez M, Arciniega-Martínez IM, García-Marín ID, Correa-Basurto J, Rosales-Hernández MC. Chronic Administration of Scopolamine Increased GSK3βP9, Beta Secretase, Amyloid Beta, and Oxidative Stress in the Hippocampus of Wistar Rats. Mol Neurobiol. 2020;57(9).
98. Jahanshahi M, Nickmahzar EG, Babakordi F. The effect of Ginkgo biloba extract on scopolamine-induced apoptosis in the hippocampus of rats. Anat Sci Int. 2013;88(4):217–22.
99. Balaban H, Nazıroğlu M, Demirci K, Övey İS. The Protective Role of Selenium on Scopolamine-Induced Memory Impairment, Oxidative Stress, and Apoptosis in Aged Rats: The Involvement of TRPM2 and TRPV1 Channels. Mol Neurobiol. 2017;54(4).
100. Cardoso R, Roberts BR, Bush AI, Hare DJ. Selenium, selenoproteins and neurodegenerative diseases. 2015;1213–28.

7. APPENDICES

7.1. Ethical Approval Form

T.C. YEDİTEPE ÜNİVERSİTESİ
Hayvan Deneyleri Yerel Etik Kurulu (HADYEK)

ETİK KURUL KARARI

Protokol No	Toplantı Tarihi	Toplantı Sayısı	Karar No	Proje Yürütücüsü
2021-027	03.06.2021	2021/06	2021/06-1	Dr. Öğr. Üyesi Alev Cumbul

'Selenyumun Scopolaminle Oluşturulan Alzheimer Tipi Demans Sıçan Modelinde Hipokampüs ve Serebral Korteksdeki Morfolojik Değişiklikler Üzerine Etkisinin Histolojik Olarak İncelenmesi' isimli proje oy birliğiyle etik açıdan uygun görülmüştür.

Hayvan Türü / Irkı	Toplam Hayvan Sayısı	Hayvanın Cinsiyeti
Sıçan / Spraque Dawley	24	Erkek

Görevi	Adı Soyadı	Katılım Durumu
Başkan	Prof. Dr. Bayram YILMAZ	
Başkan Vekili	Prof. Dr. Erdem YEŞİLADA	
Üye	Dr. Veteriner Hekim Engin SÜMER	
Üye	Prof. Dr. M. Ece GENÇ	Katılmadı
Üye	Prof. Dr. Rukset ATTAR	
Üye	Prof. Dr. Gamze TORUN KÖSE	
Üye	Doç. Dr. Ediz DENİZ	Katılmadı
Üye	Doç. Dr. Aylin YABA UÇAR	
Üye	Doç. Dr. Burcu GEMİCİ BAŞOL	
Üye	Hakan GÖKSEL	
Üye	Ahmet ŞENKARDEŞLER	

7.2. CURRICULUM VITAE

Kişisel Bilgiler

Adı	Dilara	**Soyadı**	Baban

Öğrenim Durumu

Derece	Alan	Mezun Olduğu Kurumun Adı	Mezuniyet Yılı
Yüksek Lisans	Histoloji ve Embriyoloji	**Yeditepe Üniversitesi**	-
Lisans	Genetik ve Biyomühendislik	**Yeditepe Üniversitesi**	2018
Lise	-	**İstek Belde Fen Lisesi**	2013

Başarılmış birden fazla sınav varsa(KPDS, ÜDS, TOEFL; EELTS vs), tüm sonuçlar yazılmalıdır

Bildiği Yabancı Dilleri	Yabancı Dil Sınav Notu (#)
İngilizce	IELTS: 6.5
Almanca	-

İş Deneyimi (Sondan geçmişe doğru sıralayın)

Görevi	Kurum	Süre (Yıl - Yıl)
-	-	-
-	-	-

Bilgisayar Bilgisi

Program	Kullanma becerisi
Microsoft Office Programları	Çok iyi
SPSS	Orta
Matlab	Zayıf

*****Çok iyi, iyi, orta, zayıf olarak değerlendirin

Bilimsel Çalışmaları

SCI, SSCI, AHCI indekslerine giren dergilerde yayınlanan makaleler

of Sodium Pentaborate Pentahydrate Ameliorates Lipid Accumulation and Pathological Damage Caused by High Fat Diet Induced Obesity in BALB/c Mice' article at Journal of Trace Elements in Medicine and Biology,2021

Diğer dergilerde yayınlanan makaleler

-
-

Uluslararası bilimsel toplantılarda sunulan ve bildiri kitabında (*Proceedings*) basılan bildiriler

Electron Microscopy Congress'19
-

Hakemli konferans/sempozyumların bildiri kitaplarında yer alan yayınlar

-
-

Diğer (Görev Aldığı Projeler/Sertifikaları/Ödülleri)

Stem cell and Tissue Engineering Course Certificate, Istinye University, Istanbul Turkey,2019
Participation Certificate for Electron Microscopy Congress, Edirne Turkey, 2019
Certificate of Animal Use in Experimental research by Animal Research Ethics Committee of Yeditepe University,2015